Universidade de Trás-os-Montes e Alto Douro

New Tissue-engineered Matrix for Periodontal Regeneration Based on a Biodegradable Material Combined with Canine Adipose-derived Stem Cells

PhD Dissertation in Veterinary Sciences

João Filipe Martins Freire Requicha

Supervisors:

Professor Carlos Alberto Antunes Viegas

Professor Manuela Estima Gomes

Doctor Fernando Muñoz Guzón

Vila Real, 2013

The research described in this Thesis was financially supported by the Portuguese Foundation for Science and Technology (FCT) under the João Filipe Requicha’s PhD scholarship (SFRH/BD/44143/2008) and the project MIT/ECE/0047/2009, and by the European Union's Seventh Framework Programme (FP7/2007-2013) under grant agreement n° REGPOT-CT2012-316331-POLARIS.

I declare that the contents of this Thesis are my own work and that they have not been presented to any University other than the University of Trás-os-Montes and Alto Douro.

To my Family and Friends

“The universe cannot be read until we have learned the language and become familiar with the characters in which it is written”

(Galileo Galilei)

Acknowledgements

A clear sign that a cycle is being fulfilled is when we look behind and remember the people who contributed to it. This work is not the result of only one person’s efforts, but the product of many contributions in different circumstances.

I will start by thanking the University of Trás-os-Montes e Alto Douro (UTAD), in the person of Rector Fontaínhas Fernandes, for authorizing and giving conditions to execute part of this work.

I acknowledge my supervisor, Professor Carlos Alberto Viegas, the great mentor of this journey, for never letting me forget that the practice of Veterinary Medicine and the Research are not opposites, but allies in the search of better animal care. To him, a fraternal and friendly compliment.

To my co-supervisor Professor Manuela Estima Gomes, all my appreciation for the constant words of encouragement which have contributed to my scientific maturity within a multidisciplinary group. Thus, science does not end here.

I thank Professor Rui Reis for hosting me in the 3B's Research Group of the University of Minho where I was able to extend my background into a broader spectrum of knowledge.

To Doctor Fernando Muñoz Guzón I thank him for all the support in the Laboratory of Bone Research of the Veterinary Faculty of Lugo and for his advice on how to conduct preclinical studies. A special word to Doctor Monica Peña for her help with the histology.

I am grateful to have shared one of Doctor Isabel Leonor’s lines of research and for her confidence in the success of this work.

To Professor Fidel San Román, I thank him for his kindness and knowledge transmitted during the Posgraduation in Veterinary Dentistry in Madrid.

To Carlos Albuquerque for the great friendship and collaboration in this work. To my 2001’s friends, Açoriano, Ana Cristina, Filipe, Lixa, Mário, Raq and Sara, and to the newest batch, Alexandra, Ana Jacinto, Cris, Juliana, Marta, Raquel and Sónia, a word of great affection.

To João Rodrigues, I am thankful for the good mood and valuable opinions from one who shares the taste for Veterinary Dentistry. It was also a good experience to have worked with Francisco Morinha, Teresa Teigão and Tiago Moura.

I acknowledge Professor Isabel Dias for her friendship and constant willingness to help me. To Professor Jorge Azevedo for the statistical analysis of the experimental results. I thank Professor Maria dos Anjos Pires for have received me at the UTAD`s Laboratory of Histology and Anatomical Pathology and to D. Lígia Lourenço for her technical contribution.

Colleagues and friends from the Veterinary Teaching Hospital of the UTAD and from the 3B's Research Group, an embrace for your camaraderie and for the moments of healthy entertainment.

A word to Doctor Tommaso Rada for welcoming me in the daily routine of cell cultures. I thank Shantesh Hede for his dedication to this work and for his kindness. To Márcia Rodrigues and Albino Martins for the knowledgeable opinions. A special word to Ana Dias, and Ana Catarina, and to Ana Rodrigues, Maria Susano, Luis Mendes, Silvia Mihaila, Pedro Babo, Dianinha, Ana Gonçalves, Praveen, Wojtech, and to the Management Team and the Support and Administration Staff.

To my Celeirós' housemate Pedro Carvalho, thank you for the moments of nonsense philosophy and for understanding how I idealize Science. A transatlantic kiss to Alessandra and a hug to Helena and Zé.

To the Brites family, a very kind and grateful word for making Tourinhas my second home for more than a decade.

To my Family, my parents, brother, grandmother and uncles, I merely say that this was the result of you being my Family.

To all friends and colleagues who, in one way or another, have been with me, I express my sincere gratitude.

Abstract

New tissue-engineered matrix for periodontal regeneration based on a biodegradable material combined with canine adipose-derived stem cells

Periodontium is the organ which involves and sustains the tooth and it is constituted by the alveolar bone which forms the dental alveolus, the cementum which surrounds the tooth root, the periodontal ligament, which connects them and form a joint, and the gingiva.

Periodontitis is an inflammatory pathology highly prevalent in both dogs and humans that, when not treated, can lead to tooth exfoliation and also to life threatening systemic implications due to the blood dispersion of inflammatory mediators and pathogenic microorganisms.

The routine clinical therapies currently used to treat periodontal defects are often ineffective. Tissue Engineering has emerged as a valuable alternative approach aiming to regenerate *ad integrum* the architecture and the biological function of the damaged tissue by providing the repair site with a suitable supportive biomaterial seeded with stem cells.

Mesenchymal stem cells from oral and dental origin have the ability to regenerate the periodontium; however, harvesting cells from these sites implies significant local tissue morbidity and low cell yield, as compared to non-oral sources, such as the adipose tissue. Adipose-derived stem cells (ASCs) hold a great potential in cell based therapies for their easiness of harvesting with low morbidity, generating high yields of cells with capacity to differentiate into several lineages.

The main goal of this Thesis was to develop a new Tissue Engineering approach for the treatment of periodontal defects, based on an innovative biodegradable supportive matrix combined with ASCs. As the dog is the most relevant animal model to study human periodontal disease and, simultaneously, an important subject in Veterinary Medicine, we envisioned to validate this Tissue Engineering strategy in a canine model prior to the translation of this strategy for human application. With this in mind, the work aimed to achieve the following distinct objectives:

- Optimize harvesting and isolation of canine ASCs (cASCs) from different anatomical regions and characterize their stemness and osteogenic potential at different passages;

- Evaluate the response to the implantation of cASCs in a healthy mice subcutaneous model;
- Develop and characterize a double layer biodegradable scaffold meeting the requirements to achieve different functionalities, targeting regeneration of periodontal defects;
- Evaluate the potential of the developed double layer scaffold for Tissue Engineering by culturing it with cASCs,
- Assess the *in vivo* functionality of the scaffold for bone regeneration, using a rat mandibular defect model.

In order to achieve the proposed objectives, in a first stage, canine adipose tissue samples were harvested from two different anatomical sites, namely subcutaneous and omental adipose tissue, and the isolation of cASCs was optimized. The stemness and the osteogenic differentiation potential of these cells were analyzed along passages using real time RT-PCR and staining procedures. Subsequently, the same stem cells were xenotransplanted (into a mouse model) in order to evaluate the response of the xenogenic host against the cASCs.

Concomitantly, a double layer scaffold made of a blend of starch and poly (ε-caprolactone) was designed, comprising a 3D fiber mesh functionalized with silanol groups to promote osteogenesis and a solvent casting membrane aiming to act as a barrier against the migration of gingival epithelium into the periodontal defect. The obtained scaffolds were extensively characterized regarding their mechanical properties, degradation behaviour and effectiveness of the functionalization. Ultimately, the scaffolds were seeded/cultured with cASCs to assess the *in vitro* functionality of the obtained constructs.

Finally, to assess the ability of the developed scaffold to promote bone regeneration, these were implanted in a circular critical size defected induced in rat mandible, and the formation of new bone was quantified after 8 weeks of implantation.

In general, the stemness and osteogenic differentiation potential of the cASCs was found to decrease along increasing passages. Additionally, it was shown that the anatomical origin of the adipose tissue has a significant effect in the osteogenic differentiation ability of these cells. After the injection of cASCs in a xenogenic host (mouse), it was proved that no significant local immunogenic response was detected against them.

The physicochemical characterization of the newly developed double layer scaffold showed that this matrix presents a morphology, surface composition, degradation behaviour and

mechanical properties suitable for assisting periodontal regeneration. The biological studies with cASCs revealed the potential of both layers to allow cellular adhesion and proliferation, and also to promote the osteogenic differentiation on the functionalized fiber mesh.

In the induced mandibular defect, the functionalized scaffold with silanol groups was shown to enhance higher new bone formation in comparison to a collagen commercial membrane and to empty defects. Moreover, the membrane layer was observed to avoid the epithelial and connective tissue ingrowth, which is one of the main requirements for guided tissue regeneration.

In summary, this work demonstrated that the canine adipose tissue provides an alternative source of stem cells with the ability to differentiate into different cellular lineages and which do not induce an *in vivo* inflammatory response in the xenogeneic host. These findings together with the observed potential of the developed scaffold to accommodate the proliferation and differentiation of the cultured cASCs and to enhance *in vivo* bone regeneration allows to propose this tissue-engineered matrix for periodontal regeneration as an alternative to the techniques currently used in the dentistry field, both in human and in veterinary medical practice.

Keywords: Periodontium, Periodontal regeneration, Tissue Engineering, Biomaterials, Adipose-derived stem cells, Dog, Animal models

Resumo

Nova matriz de engenharia de tecidos para regeneração periodontal baseada num material biodegradável combinado com células estaminais derivadas do tecido adiposo canino

O periodonto é o órgão que envolve e sustenta o dente, sendo constituído pelo osso alveolar que forma o alvéolo dentário, o cemento que envolve a raiz do dente, o ligamento periodontal que estabelece a ligação entre os dois tecidos anteriores formando uma articulação e a gengiva.

A periodontite é uma doença inflamatória de elevada prevalência em cães e seres humanos e que, quando não tratada, pode conduzir à esfoliação dentária e colocar em risco a vida do doente devido às manifestações sistémicas decorrentes pela dispersão sanguínea de mediadores inflamatórios e microrganismos patogénicos.

Os tratamentos que atualmente se usam para tratar esta patologia revelam-se muitas vezes ineficazes. A Engenharia de Tecidos emergiu, recentemente, como uma potencial terapia alternativa. Esta abordagem consiste no fornecimento de um biomaterial de suporte semeado com células estaminais que visa a regeneração *ad integrum* da arquitetura e da função biológica do tecido afetado.

As células estaminais mesenquimatosas de origem oral e dentária têm a capacidade de regenerar os tecidos periodontais. No entanto, as células provenientes destes locais pressupõem uma morbilidade significativa associada ao local da colheita e possuem um baixo rendimento celular em comparação com fontes não-orais, como por exemplo o tecido adiposo.

As células estaminais derivadas do tecido adiposo (ASCs) possuem um grande potencial de aplicação em terapias celulares devido à sua facilidade de colheita e baixa morbidade associada, ao alto rendimento de células isoladas e à capacidade demonstrada para se diferenciarem em inúmeras linhagens celulares.

O principal objetivo da presente Tese consistiu no desenvolvimento de uma nova abordagem de Engenharia de Tecidos para o tratamento de defeitos periodontais com base numa matriz biodegradável combinada com ASCs.

Partindo do conhecimento de que o cão é o modelo animal mais relevante para estudar a doença periodontal em humanos, pretende validar-se esta estratégia de Engenharia de Tecidos em modelo canino antes da aplicação translacional para a Medicina Humana, sem descuidar nunca que esta doença assume também grande importância na Medicina Veterinária. Tendo isto em consideração, o trabalho desenvolvido nesta Tese teve como principais objetivos:

- Otimizar a colheita e o isolamento de ASCs caninas (cASCs) provenientes de diferentes regiões anatómicas e caracterizar a sua estaminalidade e o seu potencial osteogénico em diferentes passagens;
- Avaliar a resposta à implantação de cASCs em modelo subcutâneo de murganho saudável;
- Desenvolver e caracterizar um material de suporte (*scaffold)* biodegradável de dupla camada que vise a regeneração de defeitos periodontais;
- Avaliar o potencial *in vitro* do *scaffold* de dupla camada desenvolvido para uso em Engenharia de Tecidos através da sua cultura com cASCs;
- Avaliar a funcionalidade *in vivo* do *scaffold* para a regeneração óssea, utilizando um modelo de defeito mandibular em rato.

A fim de alcançar os objetivos propostos, numa primeira etapa, as amostras de tecido adiposo canino foram colhidas a partir de duas localizações anatómicas diferentes, a saber, tecido subcutâneo e tecido omental, e o isolamento das cASCs foi posteriormente otimizado. A estaminalidade destas células e o potencial de diferenciação osteogénica foram analisadas ao longo das diferentes passagens através de RT-PCR em tempo real e histologia. Posteriormente, as mesmas cASCs foram xenotransplantadas em murganho, a fim de avaliar a resposta xenogénica do hospedeiro contra as mesmas.

Concomitantemente, desenvolveu-se um *scaffold* composto por uma mistura de amido e poli-ε-caprolactona e compreendendo duas camadas: uma malha tridimensional de fibras (*“fiber mesh*”) funcionalizadas com grupos silanol para promover a osteogénese ao nível do osso alveolar, e uma membrana obtida por evaporação de solvente com o intuito de atuar como barreira contra a migração de epitélio gengival para o interior do defeito periodontal.

Os *scaffolds* obtidos foram extensivamente caracterizados quanto às suas propriedades mecânicas, ao comportamento de degradação e à eficácia da técnica de funcionalização. De seguida, os *scaffolds* foram semeados com cASCs a fim de avaliar a funcionalidade *in vitro* das construções obtidas.

Como forma de avaliar a capacidade dos *scaffolds* desenvolvidos para promover a regeneração óssea, estes foram implantados num defeito circular de tamanho crítico induzido na mandíbula do rato, e a formação de novo osso foi determinada após oito semanas de implantação.

Em geral, a estaminalidade e o potencial de diferenciação osteogénica das cASCs decresceu ao longo de passagens. Além disso, demonstrou-se também que a origem anatómica do tecido adiposo tem um efeito significativo nas duas características analisadas. Após a injeção de cASCs num hospedeiro xenogénico (murganho), não foi observada nenhuma resposta inflamatória local exuberante contra as mesmas.

A caracterização físico-química do *scaffold* desenvolvido demostrou que esta matriz apresenta uma morfologia, composição da superfície, comportamento de degradação e propriedades mecânicas adequadas para auxiliar a regeneração periodontal. Os estudos biológicos com cASCs revelaram o potencial que ambas as camadas têm de permitir a adesão e proliferação celular, bem como de promover a diferenciação osteogénica na malha funcionalizada.

Nos defeitos mandibulares experimentais, o *scaffold* funcionalizado com grupos silanol induziu uma maior formação de osso novo em comparação com a membrana comercial de colagénio e com os defeitos vazios. Além disso, a face composta pela membrana evitou o crescimento do tecido epitelial e conjuntivo para o interior do defeito, o qual é um dos requisitos para o sucesso da regeneração guiada de tecidos.

Em resumo, este trabalho demonstrou que o tecido adiposo canino fornece uma fonte alternativa de células estaminais com capacidade de diferenciação osteogénica e que estas não induzem uma resposta inflamatória exuberante no hospedeiro xenogénico. Estes resultados, juntamente com o potencial observado do *scaffold* desenvolvido para acomodar a proliferação e diferenciação das cASCs cultivadas e para promover a regeneração de osso *in vivo*, permite propor esta construção como uma alternativa às técnicas atualmente utilizadas na regeneração periodontal, tanto no homem como no cão.

Palavras-chave: Periodonto, Regeneração periodontal, Engenharia de Tecidos, Biomateriais, Células estaminais derivadas do tecido adiposo, Cão, Modelos animais

Table of Contents

Acknowledgements vii

Abstract ix

Resumo xiii

Table of Contents xvii

Index of Tables xxvi

Index of Figures xxvii

Abbreviations List xxxi

Short *Curriculum vitae* xxxv

List of Publications xxxvii

Section I - General Introduction 1

Chapter I - Periodontal tissue engineering strategies based on non-oral stem cells 3

Abstract 3

1. Introduction 5
2. Perspective on the current periodontal therapies 6
3. Tissue Engineering 7
4. Bone marrow stem cells 9
5. Adipose-derived stem cells 13
6. Embryonic stem cells 14
7. Induced pluripotent stem (iPS) cells 14
8. Periosteal progenitor cells 15
9. Conclusion 15
10. Acknowledgements 15

11.References 16

Section II* - *Detailed description of experimental Materials and Methodologies 25

Chapter II - Materials and Methods 27

1. Canine adipose-derived stem cells (cASCs): harvesting of source tissue, isolation, expansion and differentiation...27

1.1. Harvesting of the canine adipose tissue...28

1.1.1. Animal enrolment 28

1.1.2. Anaesthesia 28

1.1.3. Surgical procedure 28

1.1.4. Adipose tissue storing 29

1.2.Isolation of the canine ASCs...29

1.3.Expansion of canine ASCs 30

1.4.Differentiation of the canine ASCs 30

1.4.1. Osteogenic differentiation of the canine ASCs 30

1.4.2. Chondrogenic differentiation of canine ASCs 31

1.5.Characterization of the canine ASCs 31

1.5.1. Gene expression analysis 31

1.5.2. Cytology 35

2. Subcutaneous implantation of the canine ASCs in healthy mice.................................36

2.1.Preparation of the canine ASCs suspension..36

2.2.Study animals...36

2.3.Subcutaneous injection of the canine ASCs 37

2.4.Euthanasia and explants collection...37

2.5.Preparation of the canine ASCs’ cytoblocks 37

2.6.Hematoxylin and eosin 37

2.7.Immunohistochemistry 37

3. Development of a double layer scaffold for periodontal regeneration 39

3.1.Description of the raw material – Blend of starch and poly (ε-caprolactone) 39

3.2.Production of the SPCL solvent casting membranes 40

3.3.Production of the SPCL wet-spun fiber meshes 40

3.4.Production of the SPCL double layer scaffolds 41

3.5.Characterization of the morphology and structure of the developed scaffolds..........42

3.5.1. Scanning electron microscopy..42

3.5.2. Micro-computed tomography..42

3.6.Characterization of the surface chemical composition 42

3.7.Characterization of the degradation behaviour..43

3.7.1. Water uptake and weight loss 43

3.7.2. Assessment of the morphology of samples after degradation..........................43

3.7.3. α-Amylase activity 43

3.7.4. Calcium and silicon concentration of the degradation solutions.......................44

3.8.Characterization of the mechanical behaviour 44

4. Seeding/culturing of the canine ASCs onto the materials 44

4.1.Seeding/culturing onto solvent casting membranes 45

4.2.Seeding/culturing onto wet-spun fiber meshes..45

4.3.Characterization of the canine ASCs-material constructs 45

4.3.1. Scanning electron microscopy..45

4.3.2. Cellular metabolic activity 46

4.3.3. Cellular proliferation 46

4.3.4. Alkaline phosphatase activity 46

4.3.5. Gene expression analysis of the osteoblastic markers 47

4.3.6. Histology – Donath technique..47

4.3.7. Lévai Laczkó staining 48

5. *In vivo* evaluation of the double layer scaffold in a rat mandibular defect....................49

5.1. Study animals 49

5.2. Experimental design 49

5.3. Surgical procedure 50

5.4. Postoperative care..51

5.5. Euthanasia and explants collection...52

5.6. Histology..52

5.7. Histomorphometric analysis...52

6. Statistical analysis..53

7. References..54

Section III** - **New tissue-engineered matrix for periodontal regeneration based on a biodegradable material combined with canine adipose-derived stem cells 59

Chapter III - **Effect of anatomical origin and cell passage number on the stemness and osteogenic differentiation potential of canine adipose-derived stem cells** 61

Abstract 61

1. Introduction 63

2. Materials and Methods..64

2.1. Harvesting of canine adipose tissue 64

2.2. Isolation and expansion of canine ASCs..65

2.3. Canine ASCs expansion and differentiation..65

    - 2.3.1. Osteogenic differentiation 65
    - 2.3.2. Chondrogenic differentiation 65
  - 2.4. Canine ASCs characterization 66
    - 2.4.1. Gene expression analysis of MSCs markers 66
    - 2.4.2. Canine ASCs osteogenic potential assessment 67
    - 2.4.3. Canine ASCs chondrogenic potential assessment 68
  - 2.5. Statistical analysis 68
- 3. Results 69
  - 3.1. Effect of the passage number in the undifferentiated canine ASCs 69
  - 3.2. Effect of the anatomical site in the undifferentiated canine ASCs 70
  - 3.3. Osteogenic differentiation assessment 71
  - 3.4. Chondrogenic differentiation assessment 73
- 4. Discussion 74
- 5. Acknowledgments 79
- 6. References 80

Chapter IV - Evaluation of the response to the implantation of canine adipose-derived stem cells in a healthy mice subcutaneous model 87

- Abstract 87
- 1. Introduction 89
- 2. Materials and Methods 90
  - 2.1. Surgical harvesting of the canine adipose tissue 90
  - 2.2. Isolation and expansion of the canine ASCs 90
  - 2.3. Preparation of the canine ASCs suspension 90
  - 2.4. Study animals 90

2.5.Subcutaneous injection of the canine ASCs 91

2.6.Euthanasia and explants collection..91

2.7.Preparation of the canine ASCs' cytoblocks 91

2.8.Hematoxylin and eosin 92

2.9.Immunohistochemistry..92

3. Results..93

3.1.Histology of the explants..93

3.2.Immunohistochemistry of the explants..94

4. Discussion..95

5. Conclusion 97

6. Acknowledgments..97

7. References..98

Chapter V - Design and characterization of a biodegradable double layer scaffold aimed at periodontal tissue engineering applications..103

Abstract 103

1. Introduction 105

2. Materials and methods..106

2.1.Production of the materials 106

2.2.Morphology characterization..108

2.2.1. Scanning electron microscopy..108

2.2.2. Micro-computed tomography..108

2.3.Fourier transform attenuated total reflectance infrared spectroscopy....................108

2.4.Degradation behaviour 109

2.4.1. Water uptake and weight loss 109

2.4.2. Morphology after degradation......109

2.4.3. α-Amylase activity......110

2.4.4. Calcium and silicon concentration of the degradation solutions......110

2.5. Mechanical behaviour......110

2.6. Culturing of canine adipose-derived stem cells......110

2.6.1. Scanning electron microscopy......111

2.6.2. dsDNA quantification......111

2.6.3. Real time RT-PCR analysis......111

2.7. Statistical analysis......112

3. Results......112

3.1. Morphology characterization......112

3.2. Fourier transform attenuated total reflectance infrared spectroscopy......113

3.3. Degradation behaviour......114

3.3.1. Water uptake and weight loss......114

3.3.2. Morphology after degradation......114

3.3.3. α-Amylase activity......116

3.3.4. Calcium and silicon concentration of the degradation solutions......117

3.4. Mechanical behaviour......117

3.5. Culturing of canine ASCs......118

4. Discussion......119

5. Conclusion......123

6. Acknowledgements......123

7. References......124

Chapter VI - A tissue engineering approach for periodontal regeneration based on a biodegradable double layer scaffold and adipose-derived stem cells 131

Abstract 131

1. Introduction 133

2. Materials and Methods 134

   2.1. Preparation of the materials 134

   2.2. Seeding/culturing of the canine ASCs onto materials 135

   2.3. Characterization of the membranes/fiber meshes cultured with canine ASCs 136

      2.3.1. Cellular morphology 136

      Scanning electron microscopy 136

      Histology – Donath technique 137

      2.3.2. Cellular metabolic activity 137

      2.3.3. Cellular proliferation 137

      2.3.4. Osteogenic differentiation of the canine ASCs on the wet-spun fiber meshes 138

      Alkaline phosphatase activity 138

      Gene expression of specific osteogenic markers 138

   2.4. Statistical analysis 139

3. Results 140

   3.1. Cellular morphology 140

   3.2. Cellular metabolic activity – MTS assay 142

   3.3. Cellular proliferation – dsDNA assay 142

   3.4. Osteogenic differentiation assessment 143

4. Discussion 145

5. Conclusion 148

6. Acknowledgments 148

7. References......149

Chapter VII - **Evaluation of a starch-based double layer scaffold for bone regeneration in a rat model**......153

Abstract......153

1. Introduction......155

2. Materials and Methods......156

2.1. Production of the materials......156

2.2. Animals......156

2.3. Surgical procedure......157

2.4. Histology......157

2.5. Statistical analysis......158

3. Results......158

3.1. Histology......158

3.2. Bone histomorphometry......159

4. Discussion......160

5. Conclusion......162

6. Acknowledgments......162

7. References......164

Section III - ***Final Conclusions***......167

Chapter VIII - **Final Conclusions**......169

Index of Tables

Chapter I – Periodontal tissue engineering strategies based on non-oral stem cells

Table 1. 1 – Summary table describing tissue engineered approaches for periodontal regeneration based on the use of BMSCs 12

Table 1. 2 – Summary table describing tissue engineered approaches for periodontal regeneration based on the use of ASCs 14

Chapter II – Materials and Methods

Table 2. 1 – Primer sequences for targeted cDNAs 34

Table 2. 2 – Characteristics of the antibodies used in this study 38

Table 2. 3 – Summary of the components of the double layer scaffold which were developed and characterized 41

Chapter III – Effect of anatomical origin and cell passage number on the stemness and osteogenic differentiation potential of canine adipose-derived stem cells

Table 3. 1 – Primer sequences for targeted cDNAs 68

Chapter IV – Evaluation of the response to the implantation of canine adipose-derived stem cells in a healthy mice subcutaneous model

Table 4. 1 – Characteristics of the antibodies used in this study 92

Chapter V – Design and characterization of a biodegradable double layer scaffold aimed at periodontal tissue engineering applications

Table 5. 1 – Mechanical properties of the SPCL-DLS and SPCL-DLS-Si 118

Chapter VI – A tissue engineering approach for periodontal regeneration based on a biodegradable double layer scaffold and adipose-derived stem cells

Table 6. 1 – Primer sequences for targeted cDNAs 139

Index of Figures

Chapter I – Periodontal tissue engineering strategies based on non-oral stem cells

Figure 1. 1 – Schematic representation of the dental and periodontal anatomy 5

Figure 1. 2 – Periodontal disease aspect in humans. A: healthy gingiva; B: gingivitis; C: periodontitis 5

Figure 1. 3 – Schematic image of the several stem cells sources for application in periodontal regeneration 8

Chapter II – Materials and Methods

Figure 2. 1 – Schematic representation of the rat mandible 50

Figure 2. 2 – Surgical procedure to induce the defect and implant the material 51

Chapter III – Effect of anatomical origin and cell passage number on the stemness and osteogenic differentiation potential of canine adipose-derived stem cells

Figure 3. 1 – Representative light microscopy images of cASCs obtained by enzymatic digestion from different anatomical sites, namely subcutaneous and omental, cultured in basal medium 69

Figure 3. 2 – Real time RT-PCR analysis of various MSCs genes, namely *CD73*, *CD90* and *CD105*, in canine ASCs cultured in basal medium..70

Figure 3. 3 – Light microscopy images of cASCs cultured in osteogenic conditions, stained with Alizarin Red...71

Figure 3. 4 – Real time RT-PCR analysis results of the various osteoblastic genes, namely *COLIA1*, *RUNX2* and *Osteocalcin*, in cASCs, obtained cultured in osteogenic conditions....72

Figure 3. 5 – Representative light microscopy images of subcutaneous cASCs cultured in chondrogenic conditions stained with Toluidine Blue, Safranin O, Alcian Blue and H&E 74

Chapter IV – Evaluation of the response to the implantation of canine adipose-derived stem cells in a healthy mice subcutaneous model

Figure 4. 1 – Histological images of the observed clusters on the dermis and the cASCs' cytoblock stained with H&E and immunostained against keratin, vimentin and CD44...........94

Chapter V – Design and characterization of a biodegradable double layer scaffold aimed at periodontal tissue engineering applications

Figure 5. 1 – Schematic representation of the developed double layer scaffold comprising the membrane and the fiber mesh. Schematic picture of the implantation of the double layer scaffold in a periodontal defect. Table summarizing the components of the double layer scaffold that were developed and characterized 107

Figure 5. 2 – SEM micrographs of the SPCL-M, SPCL-WS and SPCL-WS-Si. At the right, the micro-CT image of the double layer scaffold and the FTIR-ATR spectrum of the SPCL-WS and SPCL-WS-Si 113

Figure 5. 3 – SEM micrographs and degradation profile in terms of water uptake and weight loss of the SPCL-DLS and SPCL-DLS-Si 115

Figure 5. 4 – Cumulative release of reducing sugars as function of degradation time of SPCL-DLS and SPCL-DLS-Si 116

Figure 5. 5 – Cumulative release of calcium and silicon as function of degradation time of SPCL-DLS-Si 117

Figure 5. 6 – Canine ASCs proliferation in the SPCL-M, SPCL-WS and SPCL-WS-Si cultured in basal medium..118

Figure 5. 7 – Osteocalcin gene expression in cASCs cultured onto SPCL-WS and SPCL-WS-Si in basal and osteogenic medium 119

Chapter VI – A tissue engineering approach for periodontal regeneration based on a biodegradable double layer scaffold and adipose-derived stem cells

Figure 6. 1 – Schematic representation of the envisioned tissue engineering strategy based on the use of a double layer scaffold with two different target functionalities to culture the harvested/isolated canine ASCs. Description of the different components 135

Figure 6. 2 – SEM micrographs of SPCL-P and SPCL-NP cultured with cASCs in basal medium, and SPCL-WS and SPCL-WS-Si cultured with cASCs in both basal medium and osteogenic medium 141

Figure 6. 3 – Optical microscopy images of cASCs cultured onto the SPCL-WS and SPCL-WS-Si in basal and in osteogenic medium (Lévai Laczkó staining) 141

Figure 6. 4 – cASCs metabolic activity and proliferation upon culturing onto the SPCL-NP and SPCL-P membranes in basal medium, and culturing onto the SPCL-WS and SPCL-WS-Si in basal and osteogenic medium 142

Figure 6. 5 – Alkaline phosphatase activity of the cASCs cultured onto the SPCL-WS and SPCL-WS-Si in basal and osteogenic medium 143

Figure 6. 6 – Real time RT-PCR analysis of osteoblastic genes, namely *COLIA1*, *RUNX2* and *Osteocalcin*, in cASCs cultured onto the SPCL-WS and SPCL-WS-Si in basal and osteogenic medium 144

Chapter VII – Evaluation of a starch-based double layer scaffold for bone regeneration in a rat model

Figure 7. 1 – Representative images of the mandibular defect without scaffold (empty) and filled with collagen, SPCL and SPCL-Si scaffolds (Lévai Laczkó staining)..........................159

Figure 7. 2 – Box plot of the percentage of new bone formation in empty defects, collagen, SPCL and SPCL-Si after 8 weeks of implantation 160

Abbreviations List

A

ALP – Alkaline phosphatase

ANOVA – Analysis of variance

ASCs – Adipose-derived stem cells

αMEM – Alpha Minimum Essential Medium Eagle

B

BMSCs – Bone marrow stem cells

BM – Basal medium

BMP – Bone morphogenetic protein

C

cASCs – Canine adipose-derived stem cells

CD – Cluster of differentiation

cDNA – Complementary DNA

CO_2 – Carbon dioxide

COLIA1 – Collagen type I alpha 1

CT – Computed tomography

D

DGAV – Direção-Geral de Alimentação e Veterinária

DLS – Double layer scaffold

DMEM – Dulbecco’s Minimum Essential Medium Eagle

DNA – Deoxyribonucleic acid

DPSCs – Dental pulp stem cells

dsDNA – Double strain DNA

DNS – Dinitrosalicyclic acid

E

ESCs – Embryonic stem cells

F

FBS – Fetal bovine serum

FCT – Portuguese Foundation for Science and Technology

FELASA – Federation for Laboratory Animal Science Associations

FGF – Fibroblast growth factor

FTRI-ATR – Fourier transform infrared spectroscopy with attenuated total reflectance

G

GAPDH – Glyceraldehyde-3-phosphate dehydrogenase

GTR – Guided tissue regeneration

H

HA – Hydroxyapatite

H&E – Hematoxylin and Eosin

I

IGF – Insulin growth factor

IHC – Immunohistochemistry

ITS – Insulin-Transferrin-Selenium

M

mCT – Micro-computed tomography

mRNA – Messenger RNA

MSCs – Mesenchymal stem cells

MTS – 3- (4,5-dimethylthiazol-2-yl)-5- (3-carboxymethoxyphenyl)-2- (4-sulfophenyl)-2H-tetrazolium

O

OD – Optical density

OM – Osteogenic medium

Om – Omental

P

P – Passage

PBS – Phosphate buffer saline

PCL – Polycaprolactone

PD – Periodontal disease

PDGF – Platelet derived growth factor

PDL – Periodontal ligament

PDLSCs – Periodontal ligament stem cells

PLA – Polylactic acid

PGLA – Poly (lactic-co-glycolic acid)

PRP – Platelet rich plasma

PTFE – Polytetrafluoroethylene

R

RNA – Ribonucleic acid

RT-PCR – Reserve transcription combined with polymerase chain reaction

ROI – Region of interest

RUNX2 – Runt-related transcription factor 2

S

Sc – Subcutaneous

SEM – Scanning electron microscopy

SPCL – Blend of starch and poly (ε-caprolactone)

SPCL-M – SPCL membrane

SPCL-NP – SPCL non-patterned membrane

SPCL-P – SPCL patterned membrane

SPCL-WS – SPCL wet-spun fiber mesh non-functionalized with silanol groups

SPCL-WS-Si – SPCL wet-spun fiber mesh functionalized with silanol groups

SPCL-DLS – SPCL double layer scaffold comprising a membrane and a wet-spun fiber mesh non-functionalized with silanol groups

SPCL-DLS-Si – SPCL double layer scaffold comprising a membrane and a wet-spun fiber mesh functionalized with silanol groups

T

TCP – Tricalcium phosphate

TE – Tissue Engineering

TGF – Transforming growth factor

W

WS – Wet-spun fiber mesh

Short *Curriculum vitae*

João Filipe Requicha was born on the 6th October 1983, in Viseu, Portugal and he obtained the degree in Veterinary Medicine in 2007 by the University of Trás-os-Montes e Alto Douro (UTAD; Vila Real, Portugal).

After graduation, he worked as a clinical practitioner in small animal medicine in a private veterinary clinic and in the Veterinary Teaching Hospital of the UTAD, and collaborated in the lecturing of subjects, such as Veterinary Anatomy and Veterinary Dentistry and Small Animal Internal Medicine. During that period, he developed his interest, knowledge and skills in Veterinary Dentistry.

In 2008 he was awarded with a Portuguese Science Foundation (FCT) PhD scholarship and started his PhD program in Veterinary Sciences at the University of Trás-os-Montes e Alto Douro, under the supervision of Carlos A. Viegas, in collaboration with the 3B's Research Group of the University of Minho (Guimarães, Portugal), under the supervision of Manuela E. Gomes. He spent some periods during his PhD in the Doctor Fernando Muñoz's Laboratory of Bone Research of the Veterinary Faculty of the University of Santiago de Compostela (Lugo, Spain).

Meanwhile, in 2011 he also completed a Master's degree in Veterinary Medicine by the University of Trás-os-Montes e Alto Douro with a thesis focused on the canine oral cavity neoplasia, and the Post graduation in Veterinary Dentistry and Maxillofacial Surgery of the University Complutense of Madrid (Spain).

In 2013 obtained the accreditation as Researcher-Coordinator on Animal Experimentation, issued by the *Direção-Geral de Alimentação e Veterinária* (*DGAV*, the Portuguese Veterinary Authority), after attending the Laboratory Animal Science course by Federation for Laboratory Animal Science Associations (FELASA).

João Requicha is an active member of several scientific organizations such as the Tissue Engineering and Regenerative Medicine International Society – European Chapter (TERMIS-EU), the Portuguese Society for Stem Cells and Cell Therapies (SPCE-TC) and the European Veterinary Dentistry Society (EVDS). He is also a founder member of the Portuguese Society of Veterinary and Experimental Dentistry being, at the present moment, a board member.

João Requicha has been also involved in the preparation of research projects proposals submitted to national (FCT) and European entities (EC 7th Framework Program), as well as in the organization of national and international scientific meetings, such as the 1st Iberian Congress of Veterinary Dentistry in 2010 (Vila Real), the XXXVIII Congress of the European Society for Artificial Organs in 2011 (Porto, Portugal), the 21st European Congress of Veterinary Dentistry in 2012 (Lisbon, Portugal) and the TermStem Congress in 2012 (Guimarães, Portugal). He has reviewed manuscripts for international scientific journals in the field of Tissue Engineering and Regenerative Medicine.

As a result of his research work, João F. Requicha has attended to some of the most relevant national and international conferences in his research field, presenting 6 oral communications and 4 poster presentations. He is the first author of 3 accepted papers in international refereed journals and 3 submitted papers for publication.

List of Publications

The work performed under the scope of this PhD Thesis resulted in the publications listed below.

International Refereed Journals

- **Requicha JF**, Moura T, Muñoz F, Leonor IB, Martins T, Gomes ME, Reis RL, Viegas CA. *Evaluation of a starch-based double layer scaffold for bone regeneration in a rat model*. Submitted
- **Requicha JF**, Carvalho PP, Pires MA, Dias I, Gomes ME, Reis RL, Viegas CA. *Evaluation of the response to the implantation of canine adipose-derived stem cells in a healthy mice subcutaneous model*. Submitted
- **Requicha JF**, Viegas CA, Leonor IB, Reis RL, Gomes ME. *A tissue engineering approach for periodontal regeneration based on a biodegradable double layer scaffold and adipose-derived stem cells*. Submitted
- **Requicha JF**, Viegas CA, Hede S, Leonor IB, Reis RL, Gomes ME. *Design and characterization of a biodegradable double layer scaffold aimed at periodontal tissue engineering applications*. Journal of Tissue Engineering and Regenerative Medicine. doi: 10.1002/term.1816
- **Requicha JF**, Viegas CA, Muñoz F, Reis RL, Gomes ME. *Non-oral stem cells on periodontal regeneration strategies*. The Anatomical Record. doi: 10.1002/ar.22797
- **Requicha JF**, Viegas CA, Albuquerque CM, Azevedo JM, Reis RL, Gomes ME. 2012. *Effect of anatomical origin and cell passage number on the stemness and osteogenic differentiation potential of canine adipose-derived stem cells*. Stem Cell Reviews and Reports, 8 (4): 1211-1222

Non-indexed International Refereed Journal

- **JF Requicha**, ME Gomes, IR Dias, RL Reis, CA Viegas. 2013. *Ingeniería de tejidos aplicada a la regeneración periodontal*. Selecciones Veterinarias - Argentina, 1 (1): 43-50

Communications in National and International Conferences

Oral communications

- **Requicha JF**, Leonor IB, Muñoz F, Moura T, Carvalho P, Anjos M, Azevedo J, Reis RL, Gomes ME, Viegas CA. *Development of a new approach to the periodontal regeneration*. 101st FDI Annual World Dental Congress, Istanbul, Turkey; 28-31 August 2013.
- **Requicha JF**, Moura T, Leonor IB, Muñoz F, Gomes ME, Reis RL, Viegas CA. *Assessment of a scaffold for periodontal regeneration in a rodent model*. XXII European Congress of Veterinary Dentistry and XII World Veterinary Dental Congress. Prague, Czech Republic; 23-26 May 2013
- **Requicha JF**, Viegas CA, Albuquerque CM, Azevedo JM, Reis RL, Gomes ME. *Canine adipose stem cells: the influence of the anatomy and passaging on the stemness and osteogenic differentiation potential*. Term Stem 2012. Guimarães, Portugal; 9-12 October 2012
- **Requicha JF**, Leonor IB, Viegas CA, Reis RL, Gomes ME. *Tissue engineered constructs for periodontal regeneration based on adipose stem cells and a newly designed polymeric scaffold*. XXXVIII Congress of the European Society for Artificial Organs (ESAO 2011) and IV Biennial Congress of the International Federation on Artificial Organs (IFAO 2011). Oporto, Portugal; 9-12 October 2011
- **Requicha JF**, Leonor IB, Albuquerque C, Gomes ME, Reis RL, Viegas CA. *New biodegradable membrane for periodontal tissue engineering*. XX European Congress of Veterinary Dentistry. Chalkidiki, Greece; 1-3 September 2011
- **Requicha JF**, Leonor IB, Viegas CA, Reis RL, Gomes ME. *Biodegradable double layer scaffold for periodontal engineering*. European Chapter of the Tissue Engineering and Regenerative Medicine International Society (TERMIS) 2011 Annual Meeting. Granada, Spain; 7-10 June 2011

Poster presentations

- **Requicha JF**, Leonor IB, Muñoz F, Moura T, Azevedo J, Viegas CA, Reis RL Gomes ME. A novel tissue engineering concept targeting the regeneration of periodontal defects. European Chapter of the Tissue Engineering and Regenerative Medicine International Society (TERMIS) 2013 Annual Meeting, Istanbul, Turkey, June 2013.

- **Requicha JF**, Leonor IB, Muñoz F, Moura T, Azevedo JM, Gomes ME, Reis RL, Viegas CA. Tissue engineered scaffold for periodontal regeneration: laboratorial and preclinical characterization. I Simpósio Inter-Universitário de Investigação em Medicina Dentária. Coimbra, Portugal, March 2013
- **Requicha JF**, Leonor IB, Muñoz F, Moura T, Azevedo JM, Gomes ME, Reis RL, Viegas CA. *In vitro* and *in vivo* assessment of an innovative double layer scaffold for periodontal tissue engineering. II 3B's-ICVS Associate Laboratory Meeting. Braga, Portugal; May 2012
- **Requicha JF**, Hede S, Leonor IB, Viegas CA, Reis RL, Gomes ME. Characterization of canine adipose derived stem cells and its potential in periodontal tissue engineering applications. The 6th Annual International Meeting of the SPCE-TC, Cantanhede, Portugal, April 2011

Section I

General Introduction

Chapter I

Periodontal tissue engineering strategies based on non-oral stem cells

Abstract

Periodontal Disease is an inflammatory disease which constitutes an important health problem in humans, due to its enormous prevalence and life threatening implications on systemic health. Routine standard periodontal treatments include gingival flaps, root planning, application of growth/differentiation factors or filler materials and guided tissue regeneration. However, these treatments have come short on achieving regeneration *ad integrum* of the periodontium, mainly due to the presence of tissues from different embryonic origins and their complex interactions along the regenerative process.

Tissue Engineering (TE) aims to regenerate damaged tissue by providing the repair site with a suitable scaffold seeded with sufficient undifferentiated cells and thus constitutes a valuable alternative to current therapies for the treatment of periodontal defects. Stem cells from oral and dental origin are known to have potential to regenerate these tissues. Nevertheless, harvesting cells from these sites implies a significant local tissue morbidity and low cell yield, as compared to other anatomical sources of adult multipotent stem cells. This manuscript reviews studies describing the use of non-oral stem cells in Tissue Engineering strategies, highlighting the importance and potential of these alternative stem cells sources in the development of advanced therapies for periodontal regeneration.

---

*This Chapter is based on the following publication:

Requicha JF, Viegas CA, Muñoz F, Reis RL, Gomes ME. Non-oral stem cells on periodontal regeneration strategies. The Anatomical Record. doi: 10.1002/ar.22797

1. Introduction

Periodontium is an organ constituted by various tissues namely the alveolar bone, which forms the dental alveolus, the cementum which surrounds the root, the periodontal ligament (PDL) which is sustained by the bone and the cementum, bonding them, and finally the gingiva, which involves all the tissues above (1, 2) (Fig. 1.1).

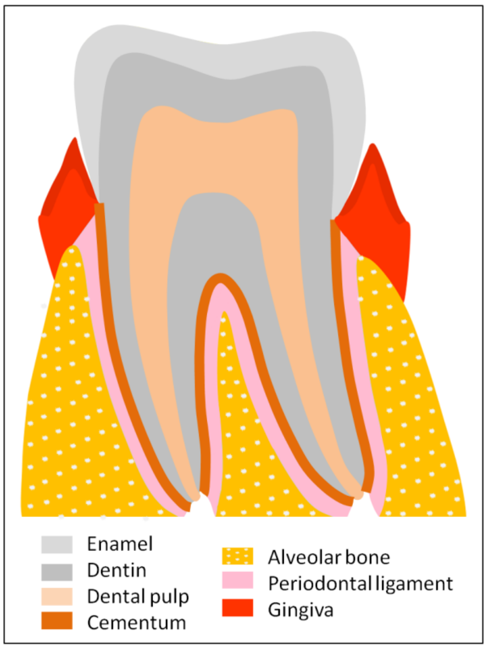

Figure 1. 1 – Schematic representation of the dental and periodontal anatomy.

The periodontium is often affected by the Periodontal Disease (PD), an inflammatory disease which includes two different inflammatory stages: an initial form called gingivitis and an advanced form called periodontitis (Fig. 1.2), which usually progresses with bone resorption, cementum necrosis and gingival recession or hyperplasia. Ultimately, when left untreated, it leads to the formation of a periodontal pocket with permanent loss of tooth support, and consequently increasing mobility and teeth loss (3-5).

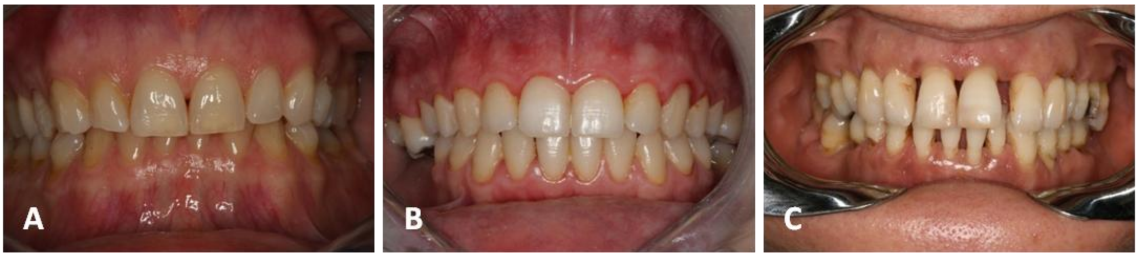

Figure 1. 2 – Periodontal disease aspect in humans. A: healthy gingiva; B: gingivitis; C: periodontitis.

Periodontal disease has a multifactorial aetiology involving microbial, behavioural (absence of oral hygiene and diet), local (malocclusions and overcrowding), systemic (immunodeficiency, infections, metabolic disease and nutritional disturbances) and genetic factors (6-8). The PD is an important health problem in Medicine, due to its enormous prevalence and life threatening implications on systemic health. It has been reported a correlation between PD and preterm birth, low weight at birth and neonatal morbidity, diabetes, respiratory, osteoarticular and cardiovascular diseases (4). Chronic periodontitis affects about 30% of the adult population and 7-13% of them have the severe form of the disease (9).

Periodontal regeneration consists of a complex and orchestrated sequence of biological events at a molecular and cellular level, accomplishing success when the following goals are met: formation of new cementum in the radicular surface, restoration of the alveolar crest till the cementum-enamel junction, reestablishment of the junctional epithelium and formation of a dense set of periodontal ligament fibers obliquely oriented assuring its functionality (1, 10, 11). This phenomenon involves the pool of progenitor cells present in the periodontium, clustered near the periodontal ligament blood vessels, which form the fibroblasts, osteoblasts, and cementoblasts (2) helped by progenitor cells existent in the bone endosteal spaces which migrate to the PDL (12).

2. Perspective on the current periodontal therapies

The main aims of the current periodontal therapies include the infection control and the re-establishment of a periodontal tissue apparatus. As the dental plaque is the primary cause of PD, their removal from the tooth crown, gingival sulcus and root surfaces is essential for the prevention and/or control of periodontal disease. Plaque removal can be accomplished by a combination of home care procedures that include mechanical and chemical plaque reduction techniques. In order to control the microbial population, clindamycin hydrochloride, amoxicillin/clavulanate and metronidazole seem to be particularly effective systemic antimicrobials. Locally delivered antimicrobials (perioceutics), such as doxycycline gel, can be applied to teeth that have been cleaned and polished (6, 7, 13).

However, when the disease progresses, advanced periodontal surgery becomes necessary. To treat patients with deep pockets and bone loss, mucogingival surgery (flap exposure), open curettage (5, 10) and the root conditioning with demineralizing agents (5, 10, 11, 14) are required. In order to stimulate the periodontal regeneration, the clinicians sometimes inject into the defects cocktails of growth factors, such as enamel matrix derivatives (EMD) or platelet-rich plasma (PRP) (15, 16) or specific growth/differentiation factors (e.g. PDGF, IGF-1, BMP-2 and BMP-7) (5, 11). In some cases, depending on the dimensions of the defect and the degree of osteolysis and/or tooth root exposition, it is advised the application of filler materials such as autografts, allografts and alloplastic materials (most frequently, hydroxyapatite-HA and tricalcium phosphate-TCP) (5, 10, 14) and/or guided tissue regeneration (GTR) membranes.

GTR techniques were firstly proposed in the 80s (11, 14) and have the objective to guide selectively the cell proliferation in different compartments, namely the alveolar bone, cementum and PDL, using ePTFE, PLA, PGLA or collagen membranes as a physical barrier (10, 13, 17). In fact, this was one of the first techniques which considered the physiopathology of the periodontal regeneration, avoiding some of the major drawbacks reported for the other existing therapies, namely, the gingival epithelium and connective tissue expansion, ankylosis and radicular resorption phenomenon and the difficulty to avoid the collapse of the periodontal defect (1, 5, 11, 17). However, none of these procedures, even when used in combination (for example, simultaneous application of filler materials with GTR membranes) have revealed enough efficacy to achieve full periodontal regeneration.

3. Tissue Engineering

Recently, Tissue Engineering (TE) and other cell based therapies have emerged as an alternative approach for the regeneration of several tissues damaged by disease or trauma, including the periodontium. TE involves the use of a support material – membrane or scaffold – where cells are seeded and cultured in order to obtain hybrid materials which can induce the regeneration of the target tissue.

Several materials have been proposed to be used in TE, mostly biodegradable polymers of synthetic and natural origin (17-19) aimed at acting as a support for cells and new tissue ingrowth until complete regeneration of the tissue defect is accomplished (11, 18, 20, 21). Tissue engineering approaches usually rely on the use of adult mesenchymal stem cells (MSCs) (Fig. 1.3), that have the capacity to differentiate in various types of cells, as for example, osteoblasts, chondroblasts, adipocytes, cardiomyocytes, neuronal cells or periodontal ligament cells (10, 22, 23).

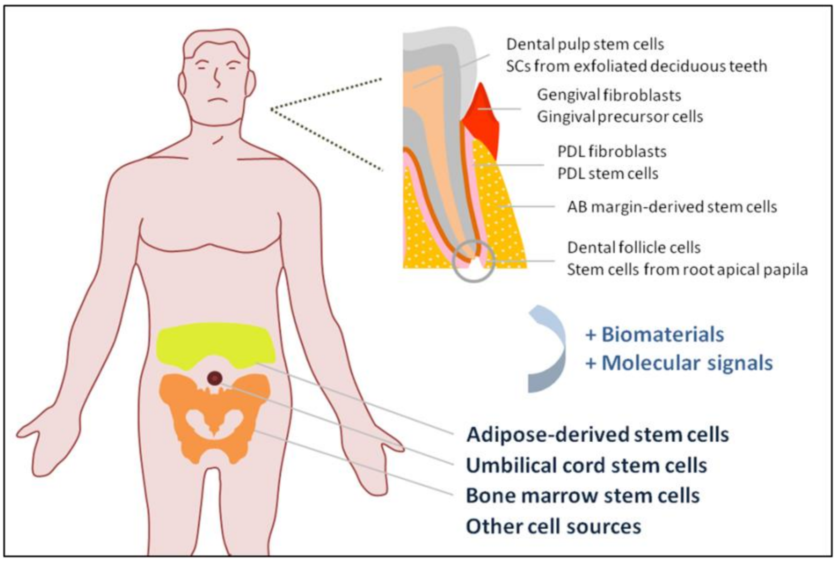
Dental pulp stem cells
SCs from exfoliated deciduous teeth
Gengival fibroblasts
Gingival precursor cells
PDL fibroblasts
PDL stem cells
AB margin-derived stem cells
Dental follicle cells
Stem cells from root apical papila
+ Biomaterials
+ Molecular signals
Adipose-derived stem cells
Umbilical cord stem cells
Bone marrow stem cells
Other cell sources

Figure 1. 3 – Schematic image of the several stem cells sources for application in periodontal regeneration.

Periodontium is a highly specialized and complex organ and is derived from the dental follicle and the neural crest cells. These cells constitute a multipotent cell population in vertebrates and participate in the embryonic development of most dental tissues including the gingiva, the dental follicle, the periodontal ligament and the alveolar bone (24, 25).

From the embryonary dental structures, Gronthos and colleagues identified for the first time, in 2000, the dental pulp stem cells (DPSCs) (26). Stem cells have also been isolated from human exfoliated deciduous teeth (SHEDs) (27). In the periodontal ligament have been described the PDL fibroblasts (28) and the PDL stem cells (PDLSCs) (29), which are the most studied cell source from periodontal origin. From the gingiva, it is possible to obtain distinct cell populations, such as the gingival fibroblasts and gingival precursor cells (30, 31). Other undifferentiated dental stem cells have been referred in the literature along the years, namely, the dental follicle cells (DFCs) (32), the stem cells from the apical papilla (SCAP) (33) and the cementum-derived cells (CDCs) (34). Regarding the osseous component of the periodontium, McCulloch *et al*. proposed, in 1987, that paravascular cells from the endosteal spaces of alveolar bone communicate with the PDL and may contribute to its cell populations (12). Recently, undifferentiated stem cells were isolated from the alveolar bone margin (35).

However, the development of new strategies for periodontal regeneration requires significant amounts of cells with regenerative potential to have therapeutic efficacy, combined or not with a biodegradable supportive matrices. Furthermore, autologous approaches are usually preferred for safety reasons and, for this purpose, it is very important to collect these cells without sacrifice of the tissues that are intended to regenerate, namely, the periodontium or even the teeth. Thus, it is of utmost relevance to consider the use of adult MSCs from other origins. Among those cells, the bone marrow stem cells and the adipose-derived stem cells assume an important role in the present and future research in this field. Therefore, this review will focus on the application of undifferentiated stem cells from non-dental and non-periodontal origin in Tissue Engineering approaches targeting the regeneration of periodontal defects.

4. Bone marrow stem cells

Bone marrow stem cells (BMSCs) were firstly identified in 1968 (36) and since then they have been extensively studied, being considered the gold standard in cell-base therapies and other regenerative medicine approaches. In 2009, Kramer *et al*. after inject male DiI-labeled BMSCs into a female rat periodontal pocket, observed for the first time that these cells obtain PDL morphology and PDL protein markers *in vivo* over a 6-week period (37).

Along the years, as described below, different Tissue Engineering approaches combining distinct types of supportive matrices (gels or scaffolds) with undifferentiated BMSCs were developed and assessed in pre-clinical models, as summarized in the Table 1.1.

One of the first reports on the use of BMSC in periodontal regeneration therapies refers to a study by Kawaguchi and colleagues (2004) that proposed the auto-transplantation of canine BMSCs on an atelocollagen gel into dog furcation defects. It was observed that cementum with extrinsic fibers was formed along almost denuded root surfaces (38), providing one of the first data on periodontal regeneration in a superior animal model with resemblances to human. In a subsequent study, the same researchers transplanted BMSCs labeled with green fluorescence proteins (GFP), using the same gel and experimental model, and identified cementoblasts, osteoblasts, osteocytes and fibroblast derived from those cells, concluding that they participate effectively in the periodontal regeneration (39). This data was corroborated by Wei *et al*. who used BMSCs labeled with bromodeoxyuridine (BrdU) mixed with alginate gel in the same model (40) and observed new bone, PDL, cementum and blood vessels formation and expression of typical surface markers of osteoblasts and fibroblasts.

Another approach (41) described the implantation of BMSCs engineered to express BMP-2 in a pluronic F-127 hydrogel into rabbit periodontal defects where it was demonstrated that this growth/differentiation factor enhances the regeneration of periodontal tissues comparing to the use of cells or polymeric gel alone (41).

A distinct study reported the use of goat BMSCs seeded onto a PLG scaffold that was fitted around a titanium fixture immediately after tooth removal. The results showed the formation of new bone and periodontal tissue-like bundles of fibers extending from the periphery of the wound toward the surface of implant, suggesting that BMSCs-PLG construct promoted osteointegration (42). In the same year, Zhang and his team implanted a tooth/bone construct seeded with BMSCs into mandible defects in swines and observed the formation of small tooth-like structures consisting of organized dentin, enamel, pulp, cementum, periodontal ligament resembling Sharpey’s fibers and alveolar bone (43).

Rat BMSCs (GFP+) have also been loaded into gelatin microbeads and transplanted into a surgically created rat periodontal defect (44). After three weeks of implantation, it was found higher evidence of bone, cementum and PDL regeneration in defects filled with microbeads-BMSCs than in empty defects or defects filled with the beads alone.

Recently, a study performed by Tsumanuma and colleagues compared the performance of BMSCs with PDLSCs and alveolar periosteal cells (APCs), when applied as cell sheets in a biodegradable polymer membrane for periodontal regeneration. The obtained histological data showed that the alveolar bone regeneration ratio was higher when using the PDLSCs, as well as the cementum thickness and the quality of PDL fibers orientation (45). Moreover, Wei and his team (2012) reported that the formation of human PDLSCs sheets was promoted by vitamin C induction and extrapolated this finding to both human BMSCs and UCSCs by culturing them with 20 mg/ml of vitamin C (46). Recently, several molecular factors have been proposed to promote the regenerative mechanism of the periodontium, for example, the platelet-rich plasma (15), the enamel matrix derivatives (EMD) (47, 48) or other specific growth/differentiation factors (e.g. PDGF, IGF-1, BMP-2 and BMP-7) (5, 49-51). For examples, Assunção *et al*. evaluated the effect of platelet-poor plasma (PPP), calcium chloride-activated platelet-rich plasma (PRP/Ca), calcium chloride- and thrombin-activated PRP (PRP/Thr/Ca), as well as BMSCs with PRP/Ca (BMSCs/PRP/Ca) on the healing of replanted dog teeth. The obtained outcomes suggest that thrombin activation is more effective in the healing, and that the use PRP/Ca with BMSCs show advantages in comparison to PRP/Ca alone (52). A study comparing the use BMSCs plus PRP and PRP or autogenous cortical bone alone concluded that no differences were observed between the treatments (53).

Zhou *et al*. described a study in which canine BMSCs modified by osteoprogesterin gene were seeded onto a PLGA scaffold and implanted in an autologous periodontal defect, leading to enhanced formation of new alveolar bone and cementum as well as new connective tissue, as compared to the controls (without cells and material). This study shows that gene therapy utilizing osteoprogesterin may be used as an adjuvant in periodontal TE therapies/strategies (54).

In the same year, it was reported the use of a collagen membrane as a vehicle for canine BMSCs transfected with BMP-7, revealing higher bone formation and new cementum length upon implantation in a canine furcation defect, comparing to the material with non-transfected cells (49). Chung *et al*. engineered these cells with BMP-2 and obtained promising results in terms of periodontal regeneration (51). Bone marrow stem cells transfected with human β-FGF have also shown to accelerate significantly the periodontal regeneration in dog class III furcation defects (55).

A work focused on using either human BMSCs or PDLFs seeded onto bone ceramic particles with EMD in a subcutaneous mice model, revealed no differences between the two cell sources in terms of ectopic bone formation. In contrast, a large amount of bone/cementum-like tissue and PDL-like fibrous tissue was found when used implants containing PDLFs, as compared to those based on BMSCs (48).

Another comparative study demonstrated that co-cultured human PDLSCs and BMSCs subsequently combined with an osteoinduced ceramic bovine bone led to the formation of a neovascularized ectopic cementum/PDL-like complex resembling the physiologic PDL Sharpey’s fibers (56) in a subcutaneous mice model.

Apart of the effect of molecular stimuli on the cells behaviour, other stimuli has been studied, as recently referred by Cmielova *et al*. who concluded that BMSCs, as well as PDLSCs, respond to ionizing radiation by induction of senescence without affect viability (57).

Bone marrow stem cells have also been proposed in several strategies for regenerate the alveolar bone, a particular component of the periodontium, combined with different materials, namely β-TCP (58), HA/TCP (59) and fluorohydroxyapatite (60), nano-hydroxyapatite block scaffolds (61), chitosan-gelatin scaffold (62) and fibrin glue (63), or even combined with PRP for improve the osteointegration of hydroxyapatite-coated dental implants (64).

Table 1. 1 – Summary table describing tissue engineered approaches for periodontal regeneration based on the use of BMSCs.

Animal origin	Source	Material	Molecular signal	Animal model	Experimental defect	Implantation time	Reference
Canine (2y, Beagle)	Iliac crest	Atelocollagen (2% type I collagen) gel		Canine (autologous)	Class III furcation defect	4 weeks	Kawaguchi et al., 2004
Canine (12-20m, Beagle)	Iliac crest	Atelocollagen (2% type I collagen) gel		Canine	Class III furcation defect	4 weeks	Hasegawa et al., 2006
Rabbits (adult, New Zealand)	Iliac crest	Pluronic F 127 gel	Cells expressing BMP-2	Rabbits (autologous)	Periodontal defect	6 weeks	Chen et al., 2008
Goat (6m-3.5y)	Femur	PLG scaffold			Canine fresh extraction socket	10 days and 4 weeks	Marei et al., 2009
Canine (6-10m, Beagle)	Tibia	Calcium alginate gel	Cells transfected with human bFGF	Canine	Class III furcation defect	6 weeks	Tan et al., 2009
Pig (3.6m, female, Yucatan mini pigs)	Iliac crest	PLGA 3D scaffold		Pig (autologous)	Alveolar bone defect	12 and 20 weeks	Zhang et al., 2009
Canine (adult, Beagle)	Femur	Collagen membranes		Canine (autologous)	Periodontal defect	8 weeks	Li et al., 2009
Canine (adult, Beagle)	Tibia	Calcium alginate gel		Canine (autologous)	Class III furcation defect	6 weeks	Wei et al., 2010
Rat (8w, male, Sprague-Dawley)		Microcarrier gelatin bead		Rat (allogenic)	Periodontal defect	3 weeks	Yang et al., 2010
Canine (adult, Beagle)		Collagen membrane	Cells transfected with BMP-7	Canine (autologous)	Class II furcation defect	12 weeks	(Li et al., 2010
Canine (adult, Beagle)		PLGA scaffold	Cells expressing osteoprogesterin	Canine (autologous)	One-wall defect	6 weeks	Zhou et al., 2010
Canine (adult, Beagle, male)	Iliac crest	PGA membrane		Canine (autologous)	One-wall defect	8 weeks	Tsumanuma et al., 2011
Canine (12-18m, mongrel)	Iliac crest		PPP and PRP		Extracted incisors replantation	120 days	Assunção et al., 2011
Canine (adult, Beagle, male)	Iliac crest	Pluronic F 127 gel	Cells transfected with BMP-2	Canine (autologous)	Periodontal defect	8 weeks	Chung et al., 2011
Human	Femur	Bone ceramic particles	EMD	Mouse (6w, NOD/SCID)	Subcutaneous implantation	6-8 weeks	Mrozik et al., 2012
Canine (adult, mongrel)	Iliac crest	PRP		Canine (autologous)	Class II furcation defect	8 weeks	Simsek et al., 2012

5. Adipose-derived stem cells

Adipose-derived stem cells (ASCs) were firstly identified in 2001 by Zuk (65) and since then they have been the focus of many studies on regenerative medicine (66, 67). In fact, the adipose tissue exhibits several attractive advantages over other stem cells sources such as the bone marrow, mainly due to its wide availability (68), the relative simplicity of the harvesting procedures (69, 70) and their great differentiation potential (22, 71). In fact, it is possible to obtain a large quantity of cells without causing high morbidity in the harvesting site, as for example, from 1 g of adipose tissue it can be isolated about 5,000 stem cells, whereas the yield from BMSCs is 100-1,000 cells/ml of bone marrow (72). Therefore, ASCs are considered a very attractive stem cell type for the development of new Tissue Engineering and other cell-based therapies, including for periodontal regeneration. Table 1.2 summarizes recent studies focusing on the use of ASCs in periodontal TE strategies.

The use of ASCs in periodontal regeneration strategies was reported for the first time in 2008 (15). In the referred study, rat ASCs were mixed with PRP and implanted into periodontal defects induced in rats. After 2 and 4 weeks of implantation, a small amount of regenerated alveolar bone was observed. Moreover, 8 weeks after implantation, it was observed the formation of a PDL-like structure along with alveolar bone (15).

Hung *et al*. (2011) demonstrated that implants composed of collagen gels with either rabbit ASCs or rabbit DPSCs, were able to promote the growth of self-assembled new teeth in adult rabbit extraction sockets with high success rate. Furthermore, rabbit ASCs demonstrated a higher growth rate and a better senescence resistance in culture, when compared to rabbit DPSCs (73).

An interesting *in vitro* study by Wen *et al*. described the potential of ASCs for periodontal regeneration showing that when incubated in dentin non-collagenous proteins and dental follicle cell conditioned medium adopted flat, cuboidal or polygonal shapes, features typical of a cementoblast-like morphology. Additionally, under these conditions, cells showed *in vitro* mineralization ability, ALP activity and expression of bone sialoprotein, type I collagen, osteonectin and osteocalcin characteristic of cementoblasts (74).

Table 1. 2 – Summary table describing tissue engineered approaches for periodontal regeneration based on the use of ASCs.

Animal origin	**Source**	**Material**	**Molecular signal**	**Animal model**	**Experimental defect**	**Implant. time**	**Ref.**
Rat (10w, male, Wistar)	Inguinal region		PRP	Rat	Periodontal fenestration defect	2, 4 and 8 weeks	Tobita *et al*., 2008
Rabbit (2-6m female, New Zealand)	Abdomen	Porcine collagen I gel	BMP-2	Rabbit (auto-logous)	Incisors extraction socket	12 weeks	Hung *et al*., 2011

6. Embryonic stem cells

Embryonic stem cells (ESCs) are derived from the inner cell mass of blastocysts and are pluripotent stem cells capable of differentiating into almost all kinds of cells of the adult body (75).

Only a few studies have addressed the potential use of ESCs in periodontal regeneration. Inanç and colleagues (2007) characterized the osteogenic differentiation potential of human embryonic stem cells (hESCs) under the inductive influence of human PDL fibroblast monolayers (76). The same authors have also achieved with success the differentiation of hESCs (HUES-9) into periodontal ligament fibroblastic progenitors (76, 77). A study on the differentiation capacity of hESCs toward the periodontal compartment cells and their relationship with tooth root surfaces *in vitro*, demonstrated that hESCs differentiation is influenced by tooth structures (extracted tooth root slices), PDLFs, and osteogenic medium, resulting in increased propensity toward mesenchymal lineage commitment, and formation of soft-hard tissue relationship in close contact areas (78). These reports suggest that human ESCs may be considered an important cell source for periodontal Tissue Engineering applications.

7. Induced pluripotent stem (iPS) cells

The reprogramming of somatic cells into induced pluripotent stem (iPS) cells by forced expression of a small number of defined factors (e.g., Oct3/4, Sox2, Klf4 and c-Myc) (79, 80) has great potential for tissue-specific regenerative therapies, avoiding ethical issues surrounding the use of ESCs and problems with rejection following implantation of non-autologous cells.

So far, the only study on iPS cells focusing in periodontal regeneration showed that iPS cells combined with EMD were found to provide a valuable tool for periodontal Tissue Engineering by promoting the formation of new cementum, alveolar bone, and normal periodontal ligament when applied in an apatite-coated silk fibroin scaffold into a mouse periodontal defect (81).

8. Periosteal progenitor cells

The cultured periosteum was also considered as a suitable cell source for periodontal regeneration because it has the capacity to differentiate into an osteoblastic lineage and expresses periodontal tissue-related genes (82, 83). Mizuno *et al*. (2006) grafted autologous cultured cell membrane derived from periosteum into a class III furcation defect in dogs. Three months after the surgery, periodontal regeneration containing alveolar bone, cementum and periodontal ligament-like connective tissue was observed (84). In 2008, Yamamiya *et al*. showed that cultured periosteum combined with PRP and hydroxyapatite induced clinical improvements in human periodontal infrabony defects regeneration (85).

9. Conclusion

Great advances concerning the use of undifferentiated stem cells in regenerative medicine approaches have been done in the last decade. The regeneration of the periodontium is known to be challenging to the clinicians. Thus, the development of new therapies based on cells and/or tissue engineered scaffolds opened a new era of the periodontal regeneration. The stem cells from dental and oral origin were the firsts to be proposed for this aim, nevertheless, adult mesenchymal stem cells, namely, those from bone marrow and adipose tissue, have revealed promising characteristics to fulfill the regeneration of periodontal damages. Among the stem cells from adult origin, the adipose-derived stem cells assume a particular interest in terms of clinical application, regarding their easiness of harvesting, expansion and differentiation in several cellular lineages. Thus, in the near future it is expected that many efforts on the development of new Tissue Engineering strategies based in this cell source will be proposed for the regeneration of bone and periodontal damages.

10. Acknowledgements

João Filipe Requicha acknowledges the support from the Portuguese Foundation for Science and Technology (FCT) for his PhD scholarship (SFRH/BD/44143/2008). Figure 2's photographs were a courtesy of Orlando Martins (DDS, MSc; University of Coimbra, Portugal).

11. References

1. Polimeni G, Xiropaidis AV, Wikesjo UME. Biology and principles of periodontal wound healing/regeneration. Periodontology 2000. 2006;41:30-47.

2. Melcher AH. On the repair potential of periodontal tissues. J Periodontol. 1976;47 (5):256-60.

3. Albuquerque C, Morinha F, Requicha J, Martins T, Dias I, Guedes-Pinto H, *et al*. Canine periodontitis the dog as an important model for periodontal studies. Vet J. 2012;191 (3):299-305.

4. Kuo L-C, Polson AM, Kang T. Associations between periodontal diseases and systemic diseases: A review of the inter-relationships and interactions with diabetes, respiratory diseases, cardiovascular diseases and osteoporosis. Public Health. 2008;122 (4):417-33.

5. Bosshardt DD, Sculean A. Does periodontal tissue regeneration really work? Periodontology 2000. 2009;51:208-19.

6. Stabholz A, Soskolne WA, Shapira L. Genetic and environmental risk factors for chronic periodontitis and aggressive periodontitis. Periodontology 2000. 2010;53:138-53.

7. Pihlstrom BL, Michalowicz BS, Johnson NW. Periodontal diseases. Lancet. 2005;366 (9499):1809-20.

8. Tatakis DN, Kumar PS. Etiology and Pathogenesis of Periodontal Diseases. Dental clinics of North America. 2005;49 (3):491-516.

9. Nares S. The genetic relationship to periodontal disease. Periodontology 2000. 2003;32:36-49.

10. Lin NH, Gronthos S, Bartold PM. Stem cells and periodontal regeneration. Australian Dental Journal. 2008;53 (2):108-21.

11. Bartold PM, McCulloch CAG, Narayanan AS, Pitaru S. Tissue engineering: a new paradigm for periodontal regeneration based on molecular and cell biology. Periodontology 2000. 2000;24:253-69.

12. McCulloch CA, Nemeth E, Lowenberg B, Melcher AH. Paravascular cells in endosteal spaces of alveolar bone contribute to periodontal ligament cell populations. Anat Rec. 1987;219 (3):233-42.

13. Chen FM, Jin Y. Periodontal tissue engineering and regeneration: current approaches and expanding opportunities. Tissue Engineering Part B-Reviews. 2010;16 (2):219-55.

14. Wikesjo UME, Nilveus R. Periodontal repair in dogs: Healing patterns in large circumferential periodontal defects. Journal of Clinical Periodontology. 1991;18 (1):49-59.

15. Tobita M, Uysal AC, Ogawa R, Hyakusoku H, Mizuno H. Periodontal tissue regeneration with adipose-derived stem cells. Tissue Engineering Part A. 2008;14 (6):945-53.

16. Viegas CAA, Dias MIR, Azevedo J, Ferreira A, San Román F, Cabrita AMS. A utilização de plasma rico em plaquetas (PRP) na regeneração do osso longo e do osso alveolar. Estudos experimentais num modelo de regeneração de defeito ósseo cortical na ovelha (*Ovies aries*) e num modelo de defeito ósseo periodontal em cão Beagle (*Canis familiaris*). Revista Portuguesa de Ciências Veterinárias 2006;101 (559-560):193-213.

17. Wikesjo UME, Lim WH, Thomson RC, Hardwick WR. Periodontal repair in dogs: gingival tissue occlusion, a critical requirement for GTR? Journal of Clinical Periodontology. 2003;30 (7):655-64.

18. Salgado AJ, Coutinho OP, Reis RL. Bone tissue engineering: State of the art and future trends. Macromolecular Bioscience. 2004;4 (8):743-65.

19. Rai B, Ho KH, Lei Y, Si-Hoe KM, Teo CMJ, bin Yacob K, *et al*. Polycaprolactone-20% tricalcium phosphate scaffolds in combination with platelet-rich plasma for the treatment of critical-sized defects of the mandible: A pilot study. Journal of Oral and Maxillofacial Surgery. 2007;65 (11):2195-205.

20. Gomes ME, Azevedo HS, Moreira AR, Ella V, Kellomaki M, Reis RL. Starch-poly (epsilon-caprolactone) and starch-poly (lactic acid) fibre-mesh scaffolds for bone tissue engineering applications: structure, mechanical properties and degradation behaviour. Journal of Tissue Engineering and Regenerative Medicine. 2008;2 (5):243-52.

21. Martins AM, Pham QP, Malafaya PB, Sousa RA, Gomes ME, Raphael RM, *et al*. The Role of Lipase and alpha-Amylase in the Degradation of Starch/Poly (epsilon-Caprolactone)

Fiber Meshes and the Osteogenic Differentiation of Cultured Marrow Stromal Cells. Tissue Engineering Part A. 2009;15 (2):295-305.

22. Requicha JF, Viegas CA, Albuquerque CM, Azevedo JM, Reis RL, Gomes ME. Effect of Anatomical Origin and Cell Passage Number on the Stemness and Osteogenic Differentiation Potential of Canine Adipose-Derived Stem Cells. Stem Cell Rev. 2012.

23. Caplan AI. Mesenchymal Stem-Cells. Journal of Orthopaedic Research. 1991;9 (5):641-50.

24. Coura GS, Garcez RC, de Aguiar CBNM, Alvarez-Silva M, Magini RS, Trentin AG. Human periodontal ligament: a niche of neural crest stem cells. Journal of Periodontal Research. 2008;43 (5):531-6.

25. Tapadia MD, Cordero DR, Helms JA. It's all in your head: new insights into craniofacial development and deformation. Journal of Anatomy. 2005;207 (5):461-77.

26. Gronthos S, Mankani M, Brahim J, Robey PG, Shi S. Postnatal human dental pulp stem cells (DPSCs) in vitro and in vivo. Proceedings of the National Academy of Sciences of the United States of America. 2000;97 (25):13625-30.

27. Miura M, Gronthos S, Zhao M, Lu B, Fisher LW, Robey PG, *et al*. SHED - Stem cells from human exfoliated deciduous teeth. Journal of Dental Research. 2003;82:B305-B.

28. Murakami Y, Kojima T, Nagasawa T, Kobayashi H, Ishikawa I. Novel isolation of alkaline phosphatase-positive subpopulation from periodontal ligament fibroblasts. J Periodontol. 2003;74 (6):780-6.

29. Seo BM, Miura M, Gronthos S, Bartold PM, Batouli S, Brahim J, *et al*. Investigation of multipotent postnatal stem cells from human periodontal ligament. Lancet. 2004;364 (9429):149-55.

30. Schor SL, Ellis I, Irwin CR, Banyard J, Seneviratne K, Dolman C, *et al*. Subpopulations of fetal-like gingival fibroblasts: characterisation and potential significance for wound healing and the progression of periodontal disease. Oral Dis. 1996;2 (2):155-66.

31. Phipps RP, Borrello MA, Blieden TM. Fibroblast heterogeneity in the periodontium and other tissues. Journal of Periodontal Research. 1997;32 (1):159-65.

32. Morsczeck C, Gotz W, Schierholz J, Zellhofer F, Kuhn U, Mohl C, *et al*. Isolation of precursor cells (PCs) from human dental follicle of wisdom teeth. Matrix Biology. 2005;24 (2):155-65.

33. Sonoyama W, Liu Y, Yamaza T, Tuan RS, Wang S, Shi S, *et al*. Characterization of the Apical Papilla and Its Residing Stem Cells from Human Immature Permanent Teeth: A Pilot Study. Journal of Endodontics. 2008;34 (2):166-71.

34. Grzesik WJ, Cheng H, Oh JS, Kuznetsov SA, Mankani MH, Uzawa K, *et al*. Cementum-forming cells are phenotypically distinct from bone-forming cells. Journal of Bone and Mineral Research. 2000;15 (1):52-9.

35. El-Sayed KM, Paris S, Becker S, Kassem N, Ungefroren H, Fandrich F, *et al*. Isolation and characterization of multipotent postnatal stem/progenitor cells from human alveolar bone proper. J Craniomaxillofac Surg. 2012.

36. Friedens AJ, Petrakov KV, Kuroleso AI, Frolova GP. Heterotopic Transplants of Bone Marrow - Analysis of Precursor Cells for Osteogenic and Hematopoietic Tissues. Transplantation. 1968;6 (2):230-&.

37. Kramer PR, Kramer SF, Puri J, Grogan D, Guan G. Multipotent adult progenitor cells acquire periodontal ligament characteristics in vivo. Stem Cells Dev. 2009;18 (1):67-75.

38. Kawaguchi H, Hirachi A, Hasegawa N, Iwata T, Hamaguchi H, Shiba H, *et al*. Enhancement of periodontal tissue regeneration by transplantation of bone marrow mesenchymal stem cells. Journal of Periodontology. 2004;75 (9):1281-7.

39. Hasegawa N, Kawaguchi H, Hirachi A, Takeda K, Mizuno N, Nishimura M, *et al*. Behavior of transplanted bone marrow-derived mesenchymal stem cells in periodontal defects. J Periodontol. 2006;77 (6):1003-7.

40. Wei N, Gong P, Liao DP, Yang XM, Li XY, Liu YR, *et al*. Auto-transplanted mesenchymal stromal cell fate in periodontal tissue of beagle dogs. Cytotherapy. 2010;12 (4):514-21.

41. Chen YL, Chen PT, Jeng LB, Huang CS, Yang LC, Chung HY, *et al*. Periodontal regeneration using ex vivo autologous stem cells engineered to express the BMP-2 gene: an alternative to alveolaplasty. Gene Therapy. 2008;15 (22):1469-77.

42. Marei MK, Saad MM, El-Ashwah AM, Ei-Backly RM, Al-Khodary MA. Experimental formation of periodontal structure around titanium implants utilizing bone marrow mesenchymal stem cells: a pilot study. J Oral Implantol. 2009;35 (3):106-29.

43. Zhang WB, Abukawa H, Troulis MJ, Kaban LB, Vacanti JP, Yelick PC. Tissue engineered hybrid tooth-bone constructs. Methods. 2009;47 (2):122-8.

44. Yang Y, Rossi FMV, Putnins EE. Periodontal regeneration using engineered bone marrow mesenchymal stromal cells. Biomaterials. 2010;31 (33):8574-82.

45. Tsumanuma Y, Iwata T, Washio K, Yoshida T, Yamada A, Takagi R, *et al*. Comparison of different tissue-derived stem cell sheets for periodontal regeneration in a canine 1-wall defect model. Biomaterials. 2011;32 (25):5819-25.

46. Wei FL, Qu CY, Song TL, Ding G, Fan ZP, Liu DY, *et al*. Vitamin C treatment promotes mesenchymal stem cell sheet formation and tissue regeneration by elevating telomerase activity. Journal of Cellular Physiology. 2012;227 (9):3216-24.

47. Saito A, Saito E, Yoshimura Y, Takahashi D, Handa R, Honma Y, *et al*. Attachment Formation After Transplantation of Teeth Cultured With Enamel Matrix Derivative in Dogs. Journal of Periodontology. 2011;82 (10):1462-8.

48. Mrozik KM, Gronthos S, Menicanin D, Marino V, Bartold PM. Effect of coating Straumann Bone Ceramic with Emdogain on mesenchymal stromal cell hard tissue formation. Clin Oral Investig. 2012;16 (3):867-78.

49. Li YF, Yan FH, Zhong Q, Zhao X. [Effect of hBMP-7 gene modified bone marrow stromal cells on periodontal tissue regeneration]. Zhonghua Yi Xue Za Zhi. 2010;90 (20):1427-30.

50. Ripamonti U, Parak R, Petit JC. Induction of cementogenesis and periodontal ligament regeneration by recombinant human transforming growth factor-beta3 in Matrigel with rectus abdominis responding cells. J Periodontal Res. 2009;44 (1):81-7.

51. Chung VH-Y, Chen AY-L, Kwan C-C, Chen PK-T, Chang SC-N. Mandibular Alveolar Bony Defect Repair Using Bone Morphogenetic Protein 2-Expressing Autologous Mesenchymal Stem Cells. Journal of Craniofacial Surgery. 2011;22 (2):450-4 10.1097/SCS.0b013e3182077de9.

52. Assunção LRD, Colenci R, do-Amaral CCF, Sonoda CK, Bomfim SRM, Okamoto R, *et al*. Periodontal Tissue Engineering After Tooth Replantation. Journal of Periodontology. 2011;82 (5):758-66.

53. Simsek SB, Keles GC, Baris S, Cetinkaya BO. Comparison of mesenchymal stem cells and autogenous cortical bone graft in the treatment of class II furcation defects in dogs. Clin Oral Investig. 2012;16 (1):251-8.

54. Zhou W, Zhao CH, Mei LX. Effect of the compound of poly lactic-co-glycolic acid and bone marrow stromal cells modified by osteoprotegerin gene on the periodontal regeneration in Beagle dog periodontal defects. West China Journal of Stomatology. 2010;28 (3):324-9.

55. Tan Z, Zhao Q, Gong P, Wu Y, Wei N, Yuan Q, *et al*. Research on promoting periodontal regeneration with human basic fibroblast growth factor-modified bone marrow mesenchymal stromal cell gene therapy. Cytotherapy. 2009;11 (3):317-25.

56. Xie H, Liu H. A novel mixed-type stem cell pellet for cementum/periodontal ligament-like complex. J Periodontol. 2012;83 (6):805-15.

57. Cmielova J, Havelek R, Soukup T, Jiroutova A, Visek B, Suchanek J, *et al*. Gamma radiation induces senescence in human adult mesenchymal stem cells from bone marrow and periodontal ligaments. International Journal of Radiation Biology. 2012;88 (5):393-404.

58. Neamat A, Gawish A, Gamal-Eldeen AM. beta-Tricalcium phosphate promotes cell proliferation, osteogenesis and bone regeneration in intrabony defects in dogs. Arch Oral Biol. 2009;54 (12):1083-90.

59. Kim SH, Kim KH, Seo BM, Koo KT, Kim TI, Seol YJ, *et al*. Alveolar Bone Regeneration by Transplantation of Periodontal Ligament Stem Cells and Bone Marrow Stem Cells in a Canine Peri-Implant Defect Model: A Pilot Study. Journal of Periodontology. 2009;80 (11):1815-23.

60. Pieri F, Lucarelli E, Corinaldesi G, Fini M, Aldini NN, Giardino R, *et al*. Effect of Mesenchymal Stem Cells and Platelet-Rich Plasma on the Healing of Standardized Bone Defects in the Alveolar Ridge: A Comparative Histomorphometric Study in Minipigs. Journal of Oral and Maxillofacial Surgery. 2009;67 (2):265-72.

61. Lee JS, Park WY, Cha JK, Jung UW, Kim CS, Lee YK, *et al*. Periodontal tissue reaction to customized nano-hydroxyapatite block scaffold in one-wall intrabony defect: a histologic study in dogs. J Periodontal Implant Sci. 2012;42 (2):50-8.

62. Miranda SC, Silva GA, Mendes RM, Abreu FA, Caliari MV, Alves JB, *et al*. Mesenchymal stem cells associated with porous chitosan-gelatin scaffold: a potential strategy for alveolar bone regeneration. J Biomed Mater Res A. 2012;100 (10):2775-86.

63. Zhang L, Wang P, Mei S, Li C, Cai C, Ding Y. In vivo alveolar bone regeneration by bone marrow stem cells/fibrin glue composition. Arch Oral Biol. 2012;57 (3):238-44.

64. Yamada Y, Nakamura S, Ito K, Sugito T, Yoshimi R, Nagasaka T, *et al*. A Feasibility of Useful Cell-Based Therapy by Bone Regeneration with Deciduous Tooth Stem Cells, Dental Pulp Stem Cells, or Bone-Marrow-Derived Mesenchymal Stem Cells for Clinical Study Using Tissue Engineering Technology. Tissue Engineering Part A. 2010;16 (6):1891-900.

65. Zuk PA, Zhu M, Mizuno H, Huang J, Futrell JW, Katz AJ, *et al*. Multilineage cells from human adipose tissue: implications for cell-based therapies. Tissue Eng. 2001;7 (2):211-28.

66. Gimble JM, Nuttall ME. Bone and fat: old questions, new insights. Endocrine. 2004;23 (2-3):183-8.

67. Li HX, Luo X, Liu RX, Yang YJ, Yang GS. Roles of Wnt/beta-catenin signaling in adipogenic differentiation potential of adipose-derived mesenchymal stem cells. Mol Cell Endocrinol. 2008;291 (1-2):116-24.

68. Iverson RE, Pao VS. MOC-PS (SM) CME Article: Liposuction. Plastic and Reconstructive Surgery. 2008;121 (4):1-11.

69. Rada T, Reis RL, Gomes ME. Adipose tissue-derived stem cells and their application in bone and cartilage tissue engineering. Tissue Engineering Part B-Reviews. 2009;15 (2):113-25.

70. Zuk PA, Zhu M, Mizuno H, Huang J, Futrell JW, Katz AJ, *et al*. Multilineage cells from human adipose tissue: Implications for cell-based therapies. Tissue Engineering. 2001;7 (2):211-28.

71. Fraser JK, Wulur I, Alfonso Z, Hedrick MH. Fat tissue: an underappreciated source of stem cells for biotechnology. Trends Biotechnol. 2006;24 (4):150-4.

72. Strem BM, Hicok KC, Zhu M, Wulur I, Alfonso Z, Schreiber RE, *et al*. Multipotential differentiation of adipose tissue-derived stem cells. Keio J Med. 2005;54 (3):132-41.

73. Hung CN, Mar K, Chang HC, Chiang YL, Hu HY, Lai CC, *et al*. A comparison between adipose tissue and dental pulp as sources of MSCs for tooth regeneration. Biomaterials. 2011;32 (29):6995-7005.

74. Wen X, Nie X, Zhang L, Liu L, Deng M. Adipose tissue-deprived stem cells acquire cementoblast features treated with dental follicle cell conditioned medium containing dentin non-collagenous proteins in vitro. Biochem Biophys Res Commun. 2011;409 (3):583-9.

75. Thomson JA, Itskovitz-Eldor J, Shapiro SS, Waknitz MA, Swiergiel JJ, Marshall VS, *et al*. Embryonic Stem Cell Lines Derived from Human Blastocysts. Science. 1998;282 (5391):1145-7.

76. Inanc B, Elcin AE, Elcin YM. Effect of osteogenic induction on the in vitro differentiation of human embryonic stem cells cocultured with periodontal ligament fibroblasts. Artificial Organs. 2007;31 (11):792-800.

77. Inanç B, Elçin AE, Ünsal E, Balos K, Parlar A, Elçin YM. Differentiation of Human Embryonic Stem Cells on Periodontal Ligament Fibroblasts In Vitro. Artificial Organs. 2008;32 (2):100-9.

78. Inanc B, Elcin AE, Elcin YM. In vitro differentiation and attachment of human embryonic stem cells on periodontal tooth root surfaces. Tissue Eng Part A. 2009;15 (11):3427-35.

79. Yu J, Vodyanik MA, Smuga-Otto K, Antosiewicz-Bourget J, Frane JL, Tian S, *et al*. Induced Pluripotent Stem Cell Lines Derived from Human Somatic Cells. Science. 2007;318 (5858):1917-20.

80. Takahashi K, Yamanaka S. Induction of pluripotent stem cells from mouse embryonic and adult fibroblast cultures by defined factors. Cell. 2006;126 (4):663-76.

81. Duan XJ, Tu QS, Zhang J, Ye JH, Sommer C, Mostoslavsky G, *et al*. Application of Induced Pluripotent Stem (iPS) Cells in Periodontal Tissue Regeneration. Journal of Cellular Physiology. 2011;226 (1):150-7.

82. Breitbart AS, Grande DA, Kessler R, Ryaby JT, Fitzsimmons RJ, Grant RT. Tissue engineered bone repair of calvarial defects using-cultured periosteal cells. Plastic and Reconstructive Surgery. 1998;101 (3):567-74.

83. Horiuchi K, Amizuka N, Takeshita S, Takamatsu H, Katsuura M, Ozawa H, *et al*. Identification and characterization of a novel protein, periostin, with restricted expression to periosteum and periodontal ligament and increased expression by transforming growth factor beta. J Bone Miner Res. 1999;14 (7):1239-49.

84. Mizuno H, Hata K, Kojima K, Bonassar LJ, Vacanti CA, Ueda M. A novel approach to regenerating periodontal tissue by grafting autologous cultured periosteum. Tissue Eng. 2006;12 (5):1227-335.

85. Yamamiya K, Okuda K, Kawase T, Hata K-i, Wolff LF, Yoshie H. Tissue-Engineered Cultured Periosteum Used With Platelet-Rich Plasma and Hydroxyapatite in Treating Human Osseous Defects. Journal of Periodontology. 2008;79 (5):811-8.

Section II

Detailed description of experimental Materials and Methodologies

Chapter II

Materials and Methods

This Chapter provides a general overview and detailed information on all the techniques used and biological assays performed under the scope of this Thesis. Although described in the Materials and Methods section of each experimental work, herein the objective is to contextualize and justify the selection of materials and methodologies applied throughout the thesis and complement information provided in each chapter.

1. Canine adipose-derived stem cells (cASCs): harvesting of source tissue, isolation, expansion and differentiation

The adipose-derived stem cells (ASCs) have gained importance in the last years, mainly due to the wide availability of the adipose tissue, enabling to collect larger quantities and due to the easiness of its harvesting procedures, minimizing site morbidity (1, 2). Furthermore, ASCs have the potential to differentiate into several mesoderm lineages, which justifies the increasing interest of using these cells in distinct cell-based therapies. Therefore, the Chapter III describes the harvesting, culturing and characterization of ASCs from canine origin.

The rationale for selecting canine ASCs (cASCs) was mainly based on the fact that dog is considered as the most suitable model for research in Periodontology, because of the natural occurrence of periodontal disease in this specie, that resembles the pathophysiological mechanisms of the disease in humans, and also due to the similarities in terms of histological and microbiological characteristics of the periodontium (3, 4). As disadvantageous of the model, it can be highlighted the different dental anatomy presented by humans and the higher bone turnover rate (5).

Although the dog model is the paradigm for the research in periodontal regeneration, it raises ethical and social issues, and thus should be reserved for the last phase of validation before human application (3, 5). For that reason, on the scope of this Thesis, small rodent models were further used in order to assess the behaviour of the studied cells (Chapter IV) and the developed biomaterials (Chapter VII) prior to future studies in canine preclinical models.

Subsequently, cASCs were used in Chapters V and VI to seed/culture onto the materials developed in the scope of this Thesis envisioning their application in periodontal regeneration. These studies were aimed at assessing the biological behaviour of the newly developed scaffolds, but also to assess the *in vitro* functionality of a hybrid matrix composed of the scaffold and the cells targeting periodontal tissue engineering applications.

1.1. Harvesting of the canine adipose tissue

1.1.1. Animal enrolment

The adipose tissue samples were collected from six adult dogs, between 1 and 5 years of age, from both genders (3 males, 3 females) and in good general health status, and subject of convenience surgery in the Veterinary Hospital of the University of Trás-os-Montes e Alto Douro, with previous informed consent of the owners.

1.1.2. Anaesthesia

The dogs were sedated by an intramuscular administration of 0.2 mg/kg IM butorphanol tartrate (Torbugesic 1%; Fort Dodge, the Netherlands), which is a synthetic opioid partial agonist, and 30 µg/kg IM acepromazine maleate (Vetranquil; CEVA Sante Animal, France), a phenothiazine derivative. Anaesthesia was achieved by an intravenous administration of 0.25 mg/kg IV diazepam (Diazepam MG; Labesfal, Portugal), a benzodizepine, 4 mg/kg IV ketamine (Imalgene 1000; Merial, France), a dissociative, and 4 mg/kg IV propofol (Lipuro 2%; Braun, Germany), an alkyphenol derivative, and was maintained with an inhalant general anesthetic agent, namely 1% isoflurane (IsoFlo; Abbott Animal Health, USA) administered in oxygen through an endotracheal tube (6).

1.1.3. Surgical procedure

After anesthetized, the animals were placed in dorsal recumbence and it was made a careful tricothomy and asepsis of the ventral abdomen from the xiphoid to the pubis with 0.1% iodopovidone (Ectodine, Portugal). Briefly, a 4-8 cm incision was made just caudal to the umbilicus in the cranial third of the caudal abdomen through skin and subcutaneous tissue to expose the linea alba (7). At this moment, samples of adipose tissue were collected from the abdominal subcutaneous region for further use in the following experimental sections.

Then, while the *linea alba* was grasped tenting it outward, a stab incision was made into the abdominal cavity. The incision was extended cranial and caudally with Mayo scissors and the abdominal wall was elevated by grasping the *linea* or external rectus sheath with thumb forceps (7). After identifying the great omentum, samples of adipose tissue were collected from that organ for further use.

After accomplished the convenience surgery, the *linea alba* was closed with simple interrupted sutures or a simple continuous suture pattern, by using strong, 2/0 or 3/0 absorbable suture material, such us polyglyconate (Monosyn; BBraun, Portugal) or polyglycolic acid (Safil; BBraun, Portugal). The subcutaneous tissue was closed with a simple continuous pattern of absorbable suture material and, then, the skin was sutured with simple interrupted appositional pattern using a nonabsorbable suture material, such us silk (Silkan, Braun) (7).

1.1.4. Adipose tissue storing

All the adipose tissue samples (abdominal subcutaneous and omental) collected from the animals enrolled in this study were placed into sterile containers with PBS (Phosphate Buffer Solution; Sigma Aldrich, Germany) with 10% antibiotic/antimycotic (Fluka, UK), refrigerated at 4 ºC and transported to the laboratory to be processed.

1.2. Isolation of the canine ASCs

All the adipose tissue samples were processed within 12 hours upon harvesting. The cASCs were isolated by an enzymatic isolation method, which was previously optimized for human ASCs and described in several reports including from the 3B's Research Group (2, 8, 9). This method was used to obtain the cASCs used in Chapters III to VI of this Thesis.

Briefly, the adipose tissue samples were washed with PBS containing 10% antibiotics/antimycotic and minced into small fragments using a scissor. The fragments were digested with a solution of 0.1% collagenase type IA (Sigma Aldrich, Germany) in PBS at 37 ºC under shacking at 200 rpm for 40 min (10 mL/10 cm^{-3} tissue). This collagenase is purified from the fermentation of *Clostridium histolyticum* bacteria and contains collagenase, non-specific proteases, clostripain, neutral protease and aminopeptidase which act together to break down the connective tissue.

Collagenase was inactivated with an equal volume of culture medium containing 10% FBS (Fetal Bovine Serum; Invitrogen, USA). The digested tissue was filtered with a 100 µm nylon mesh and centrifuged at 1250 rpm for 5 min at 20 °C and the supernatant removed.

The obtained cells were resuspended in culture medium (basal medium, BM) composed of DMEM (Dulbecco's Minimum Essential Medium Eagle; Sigma Aldrich, Germany), 10% FBS, sodium bicarbonate (Sigma Aldrich, Germany) and 1% antibiotic/antimycotic and then seeded in 25 cm^2 culture flasks.

After 48 hours, the cells were rinsed with PBS and the medium was changed to remove non-adherent cells, such as hematopoietic cells or dead cells. The adherence of cells to the plastic culture flask is one of the criteria of being considered mesenchymal stem cells (MSCs) as stated in the last consensus of the International Society of Cellular Therapy (10).

1.3. Expansion of canine ASCs

The cells were (11, 12) cultured in plastic adherent culture 150 cm^2 T-flasks, using basal medium, which was changed three times a week until reaching a confluence of around 80%. At each passage (P), 10 µL of cell suspension were collected and mixed with 10 µL of Trypan Blue (Alfagene, Portugal) in order to assess cell viability and the total nucleated cells counts determined using a hematocytometer before being used in the further differentiation studies. Along the different passages, the cultured cASCs, both from subcutaneous and omental origin, were collected for gene expression analysis in order to evaluate the effect of the passaging and the effect of the anatomical origin in their stemness and osteogenic potential (Chapter III).

1.4. Differentiation of the canine ASCs

The multilineage differentiation potential is another important criteria to characterize the MSCs (10). Thus, in Chapter III was assessed the osteogenic and chondrogenic differentiation potential of the cASCs after culturing in previously established conditions. In the same study, it was also evaluated the effect of passaging and the effect of the anatomical origin of the tissue in the osteogenic differentiation of the cASCs.

1.4.1. Osteogenic differentiation of the canine ASCs

Canine ASCs, at passage P1, P2, P3 and P4, were seeded at a density of 5×10^4 cells per culture flask (75 cm^2 T-flask), and further cultured for 14, 21, 28 and 35 days in osteogenic medium (OM) composed of αMEM (Alpha Minimum Essential Medium Eagle; Sigma Aldrich, Germany) supplemented with 10% FBS, sodium bicarbonate, 1% antibiotic/antimycotic, ascorbic acid (Sigma, USA), 10^{-8} M dexamethasone (Sigma, USA) and 10 mM β-glycerophosphate (Sigma, USA); the culture medium was changed twice a week.

The osteogenic medium used in this work included the ascorbic acid (vitamin C), which is essential for collagen synthesis and secretion; the β-glycerophosphate that provides an inorganic source of phosphate needed for the mineralization process; and the dexamethasone that has a role in enhancement of alkaline phosphatase activity and the mineralization process (13, 14).

1.4.2. Chondrogenic differentiation of canine ASCs

Canine ASCs (about 5×10^5 cells), at P1, P2, P3 and P4, were resuspended in chondrogenic medium (CM) and centrifuged at 800 G for 5 min, in order to obtain cell pellets. Pellets were cultured in the same medium for up to 21 days at 37 ºC and 5% CO_2, in 15 mL falcon tubes.

Chondrogenic medium was composed of DMEM supplemented with 5% FBS, sodium bicarbonate, 1% antibiotic/antimycotic, 1 mM dexamethasone, 17 mM ascorbic acid, 10 ng/mL TGF-β1 (human transforming growth factor-β1; eBioscience, USA), 10% Insulin-Transferrin-Selenium (ITS) (Sigma, USA), 35 mM L-proline (Sigma, USA) and 0.1 M sodium pyruvate (Sigma, USA) and was changed twice a week.

The TGF-β1 is known to provide an appropriate external signal for chondrogenesis stimulating cartilage-specific proteoglycan production (15); ITS supplement provides a rich source of recombinant human insulin, human transferrin and sodium selenite; L-proline, which is essential for the collagen type II synthesis (16); Sodium pyruvate is an additional source of energy for the differentiation process due to its role in the glycolysis.

1.5. Characterization of the canine ASCs

Cultured cASCs from the different passages, culturing conditions and culturing periods were collected for further evaluation of their stemness and for their capacity to differentiate into the chondrogenic and osteogenic lineages. This characterization was carried out by the gene expression analysis by real time RT-PCR, and by cytology assessing the production of mineralized matrix (cASCs in osteogenic medium) and cartilage matrix (cASCs in chondrogenic medium).

1.5.1. Gene expression analysis

Reserve transcription combined with real time polymerase chain reaction (Real time RT-PCR) has proven to be a powerful method to quantify gene expression. There are two different methods of analyzing data from quantitative PCR, the absolute quantification and the relative quantification (17).

In Chapter III was evaluated the relative gene expression of three MSCs markers (*CD73*, *CD90* and *CD105*) on the undifferentiated cASCs, and the relative gene expression of the three specific osteoblast markers (*Collagen type I alpha 1*, *Runt-related transcription factor 2* and *Osteocalcin*) on the cASCs cultured in osteogenic medium.

The same gene expression analysis of the osteoblast markers by real time RT-PCR was performed on the cASCs cultured on biomaterials, both in basal and in osteogenic medium, as described in Chapters V and VI.

Typical markers of the mesenchymal stem cells

The clusters of differentiation CD73, CD90 and CD105 are the widely accepted as main positive markers of the mesenchymal stem cells (MSCs) (10), which are described below in terms of molecular characteristics:

- CD73 or Ecto-5'-nucleotidase is a glycoprotein located in the plasma membrane as an ectoenzyme (18);
- CD90 or Thy-1 is a cell adhesion molecule and the smallest member of the immunoglobulin superfamily. CD90 is also known as thymocyte differentiation antigen-1 based on its presence on mouse thymocytes (19);
- CD105 or Endoglin is a type I integral membrane homodimer protein found on vascular endothelial cells and syncytiotrophoblasts of placenta. This protein is a component of the transforming growth factor-β receptor complex (20).

The fact that it is difficult to find in the market specific antibodies for cells of canine origin, was the main reason to select real time RT-PCR analysis and not flow cytometry or other immune-based assays, for the assessment of the MSCs and osteoblasts markers.

Specific osteoblast markers

In literature, several osteogenic markers have been used to characterize the osteogenic differentiation potential of MSCs, such as the Collagen I alpha 1 (COLIA1), the Runt-related transcription factor 2 (RUNX2) and the Osteocalcin, among others:

- Collagen type I is the most abundant type collagen in body, namely in bone, cornea, dermis and tendon. *COLIA1* gene produces the pro-alpha-1 chain, which is combined with another pro-alpha-1 chain and a pro-alpha-2 chain to make a molecule of type I procollagen. Once these molecules are processed, they cross-link resulting in the formation of very strong mature type I collagen fibers (21);
- Runt-related transcription factor 2 (RUNX2) is a transcription factor which binds osteoblast-specific factor 2 in the promoter to initiate mesenchymal condensations, enhancing the osteogenesis in an immature stage, and afterwards needs to be suppressed to form mature bone (22, 23). *RUNX2* gene regulates pre-osteoblasts

and is required for the expression of non-collagenous proteins, such as Bone sialoprotein and Osteocalcin (24);

- Osteocalcin is the most abundant osteoblast-specific non-collagenous protein and is involved with the binding of calcium and hydroxyapatite. The Osteocalcin and the Bone sialoprotein play a crucial role in bone formation and bone turnover (24).

Isolation of mRNA

In Chapter III, the cASCs were detached using trypsin (Alfagene, Portugal) and 1×10^6 cells of each culturing condition (cASCs at P0, P1, P2, P3, P4 in basal medium and cASCs at P1, P2, P3, P4 in osteogenic medium both from subcutaneous and omental origin) were retrieved and kept in 800 µL of TRIzol Reagent (Invitrogen, USA). The mRNA was extracted with TRIzol following the procedure provide by the supplier. Briefly, after an incubation of 5 min, additional 160 µL of chloroform (Sigma Aldrich, Germany) were added and the samples were then incubated for 15 min at 4 °C and centrifuged at the same temperature and 13000 rpm for 15 min. After the centrifugation, the aqueous part was collected and an equal part of isopropanol (VWR, USA) was added. After an incubation of 2 hours at -20 °C, the samples were washed in ethanol (Panreac, Spain), centrifuged at 4 °C and 9000 rpm for 5 min and resuspended in 12 µL of RNase/DNase free water (Gibco, UK).

Synthesis of cDNA

Previous to this step, the mRNA content was quantified in all samples using a NanoDrop ND1000 Spectrophotometer (NanoDrop Technologies, USA).

For the cDNA synthesis, it were used the samples with a 260/280 ratio between 1.7 and 2.0. The cDNA synthesis was performed in the Mastercycler real time PCR equipment (Eppendorf, USA) using the iScript cDNA Synthesis Kit (Quanta Biosciences, USA) and an initial amount of mRNA of 2 µg and a total volume of 20 µL RNase free water (Gibco, UK) was used as a negative control.

Real time RT-PCR analysis

After the synthesis of the cDNA, real time PCR analysis was carried in the Mastercycler real time PCR equipment (Eppendorf, USA) using the PerfeCta Sybr-Green FastMix (Quanta Biosciences, USA) to analyze the relative expression of the MSCs and osteoblast genes in each sample, using *GAPDH* as housekeeping gene. The primers were previously designed using the Primer 3 Plus v0.4.0 (MWG Biotech, Germany) (Table 2.1).

The amplification protocol included an initial denaturation at 95 ºC for 2 min, followed by 45 cycles of denaturation at 95 ºC for 15 sec, specific annealing temperature (Ta) indicated in Table 2.1 for 30 sec and extension at 72 ºC for 1 min. The fluorescence signal was captured at the end of each cycle. Finally, melting curves were obtained using the thermal conditions of 95 ºC at 15 sec followed by cooling to 55 ºC and then sequential temperature increments of 0.5 ºC at each 15 sec (20 cycles) with temperature ranging from 55 ºC to 95 ºC, with fluorescence measurements in all intervals.

Table 2. 1 – Primer sequences for targeted cDNAs.

Primer	**RefSeqID**	**Product length (bp)**	**5′-3′ sequence (F, forward; R, reverse)**	**Ta (ºC)**
CD73	ENSCAFT00000004810	191	F: ATCCTGCCGCTTTAAGGAAT R: GTACAGCAGCCAGGTTCTCC	57.1
CD90	ENSCAFT00000019082	214	F: CGTGATCTATGGCACTGTGG R: GCCCTCACACTTGACCAGTT	56.8
CD105	ENSCAFT00000032002	161	F: AGGAGTCAACACCACGGAAC R: GATTGCAGAAGGACGGTGAT	56.6
COL1A1	ENSCAFT00000026953	170	F: ATGCCATCAAGGTTTTCTGC R: CTGGCCACCATACTCGAACT	57.4
Osteocalcin	ENSCAFT00000026668	166	F: GATCGTGGAAGAAGGCAAAG R: AGCCTCTGCCAGTTGTCTGT	59.4
RUNX2	ENSCAFT00000020482	148	F: CAGACCAGCAGCACTCCATA R: CAGCGTCAACACCATCATTC	58.4
GAPDH	NM_001003142.1	238	F: CCAGAACATCATCCCTGCTT R: GACCACCTGGTCCTCAGTGT	59.3

Delta Delta Ct method, according to Livak (2011) (25), was performed using the results corresponding to cASCs at P0 as calibrator of data obtained from cASCs at P1, P2, P3 and P4, when analyzed the MSCs genes; and using the data corresponding to cASCs cultured in basal medium at the respective passage as calibrator of the results obtained for cASCs cultured in osteogenic medium, when analyzed the osteoblasts genes.

1.5.2. Cytology

Alizarin Red

Alizarin Red (1,2-dihydroxyanthraquinone) is an organic compound used to identify calcium-rich deposits (26). Before staining, cASCs cultured in osteogenic medium for 14, 21, 28 and 35 days, were fixed with 4% phosphate-buffered formalin (Sigma Aldrich, Germany) and washed with PBS and then with distilled water.

The cells were stained with a 2% Alizarin Red solution (Merk, Germany) in distilled water with a pH of 4.1-4.3, for 10 min, and finally washed with distilled water. Stained cells were observed under an optical microscope (Axivert 40 CFL; Zeiss; Germany) and photographed using the camera Axio Cam MRm (Zeiss, Germany).

Specific cartilage matrix stainings

After 21 days of culture in chondrogenic medium, cASCs pellets were fixed with 4% phosphate-buffered formalin, washed with PBS, embedded in paraffin using a spin tissue processor (Microm STP120-2, Thermo Scientific, USA) and cut into sections of 3 µm using a microtome (Microm HM355S, Thermo Scientific, USA). After deparaffinization, sections were stained with hematoxylin (Sigma, USA) and eosin (Inopat, Portugal) (H&E) for 5 min in order to identify the nucleus in blue and the cytoplasm in pink, respectively.

Cartilage-like matrix deposition was assessed by staining the samples sections with 1% Toluidine Blue (Sigma, USA) for 3 min, which is cationic dye frequently used for the detection of mucin, cartilage and mast cells, from orange to red; 0.1% Safranin Orange (Sigma, USA) for 5 min, which stains blue the nucleic acids and purple the polysaccharides; and 1% Alcian Blue (Sigma, USA) for 30 min, that is used to detect acid mucosubstances and acetic mucins colouring by blue.

The stained sections were subsequently rinsed with distilled water and dehydrated in a series of ethanol-water solutions with increasing ethanol concentration (30%, 50%, 70%, 90% and 100% v/v) finishing with xylene (Thermo Scientific, Germany) before mounting using Entelan (Merck, Germany). Afterwards, the slides were observed under an optical microscope (Axivert 40 CFL; Zeiss; Germany), and photographed using the camera Axio Cam MRm (Zeiss, Germany).

2. Subcutaneous implantation of the canine ASCs in healthy mice

In Chapter IV, the cASCs were subcutaneously implanted in mice in order to assess the response of the xenogenic tissue against these cells and also to optimize the identification of these cells in the host tissue by immunohistochemistry analysis. This study aimed at contributing to the characterization of this subcutaneous mouse model as an alternative to study cASCs aimed at being used in cell based regenerative medicine therapies in canine veterinary medicine. Furthermore, as previously explained, dog is a very important animal model for assessing therapies with potential to treat several problems in human medicine, such as periodontal disease; Nevertheless, it is important to establish models that can minimize the use of dogs in experimental research as it raises additional ethical issues.

2.1. Preparation of the canine ASCs suspension

The cASCs were isolated from canine adipose tissue by enzymatic digestion method and expanded, as previously described, up to passage 2 until reach the necessary number of cells. These cells were then resuspended in phosphate buffer solution (PBS; Sigma Aldrich, Germany), obtaining a cellular suspension with a concentration of 1×10^{7} cells ml^{-1} to be subsequently injected in the mice.

From the same culture, a cellular suspension of 2×10^{6} cASCs per ml was also obtained, washed with PBS and fixed in 4% phosphate-buffered formalin for further cytology and immunostaining assays.

2.2. Study animals

Thirty five immunocompetent 10 weeks old Hsd:CD1 (ICR), outbred and SPF male mice (Harlan Laboratories, Spain) were used in this protocol. The housing care and experimental protocol was performed according to the national guidelines, after approval by the National Ethical Committee for Laboratory Animals and conducted in accordance with Portuguese legislation (Portaria 1005/92) and international standards on animal welfare as defined by the European Directive 2010/63/EU.

The animals were housed in groups of five individuals, fed *ad libitum* with maintenance diet for mice (4RF21/C diet, Mucedola, Italy) and autoclaved water, and bedded in corn cob (Scobis Due, Mucedola, Italy) with suitable environment enrichment and with a day/night cycle of 14/10 hours.

2.3. Subcutaneous injection of the canine ASCs

The animals were placed in dorsal recumbence for subcutaneous injection in the abdominal right flank with 100 µL of suspension containing 1 × 10^7 cells ml-1 by using a 1 mL syringe with a 26 G needle.

2.4. Euthanasia and explants collection

All animals were euthanized by an intravenous injection of sodium pentobarbital (Eutasil, CEVA, France). A group of five animals injected with PBS with no cells (time 0) were considered the negative control. Throughout the following 28 days, the remaining six experimental groups (n=5) were sacrificed at 12 hours, and 1, 3, 7, 21 and 28 days after injection.

The abdominal skin and adjacent muscle, around the site of injection, were collected with a safety margin of 1 cm, in order to assess the local response against the xenotransplanted cASCs.

The organs, namely, mesenteric and inguinal lymph nodes, liver, kidney, lung, heart, spleen, brain, and intestine were also collected, in order to evaluate the presence of cASCs at distance and also the host response against these cells. All samples were fixed in 4% phosphate-buffered formalin (Inopat, Portugal) during 24 hours.

2.5. Preparation of the canine ASCs' cytoblocks

A cellular culture suspension of 2 × 10^6 cASCs ml^{-1} was fixed in 4% phosphate-buffered formalin and centrifuged in the Shandon CytoSpin 3 centrifuge (Thermo Scientific, USA) to a proper cassette.

2.6. Hematoxylin and eosin

Explants retrieved from mice and the cASCs' cytoblock were processed in an automatic tissue processor Shandon Hypercenter XP (ThermoFisher Scientific, USA) and embedded in paraffin. Paraffin blocks were cut at 3 µm to silane-coated slides and stained by routine with hematoxylin and eosin (H&E) and mounting with Entelan (Merck, Germany).

2.7. Immunohistochemistry

Indirect avidin-biotin immunohistochemistry (IHC) was performed using mouse monoclonal anti-human antibodies to Vimentin, (clone V9, Leica Biosystems, UK) and to Keratin (clone

AE1/AE3, Dako, USA), and rat monoclonal anti-human CD44 (clone 8E2F3, Santa Cruz Biotechnology, Germany) (Table 2.2).

Table 2. 2 – Characteristics of the antibodies used in this study.

	Vimentin	**Cytokeratin**	**CD44**
Type	Monoclonal	Monoclonal	Monoclonal
Host	Mouse	Mouse	Rat
Immunogen	Porcine eye lens	Human epidermal callus	Mouse spontaneous myeloid leukemia
Reactivity	Anti-human	Anti-human	Anti-mouse, human, canine, feline and equine
Clone	V9	AE1/AE3	IM7
Isotype	IgG1	IgG1 kappa	IgG2 beta
Dilution	1:100	1:400	1:100
Antigen recovery	Sodium citrate, 90 ºC, 20 min		
Incubation	Room temperature, 4 hours	Room temperature, 4 hours	4 ºC, overnight

Antigen retrieval was performed in a water bath at 96 ºC for 20 min, in citrate buffer (pH=6). The slides were washed with PBS and endogenous peroxidase was blocked with 3% hydrogen peroxide (Sigma, Germany) at room temperature for 30 min.

RTU Vectastain Universal Elite ABC Kit (Vector PK-7200, UK) in combination with the Mouse-on-Mouse (MOM) Basic Kit (Vector BMK-2202, UK) was used for antibody incubation, according to the instructions of the manufacturers.

The use of the MOM kit aimed at block the endogenous mouse's immunoglobulins in order to reduce the background and the cross reactivity of the used antibodies (vimentin, CD44 and keratin). This protocol was essential to avoid the detection of these antibodies in the host tissue, ensuring that they only react against the xenotransplanted cASCs allowing to identify these cells in the tissue explants.

Briefly, non-specific binding of primary antibodies was blocked using a horse serum for 40 min, and the mice's immunoglobulins blocked for 1 hour. Then, after the incubation with the primary antibody, tissue sections were incubated with biotinylated antibody for 20 min, followed by incubation with streptavidin-peroxidase for 20 min.

After washing with PBS, antibody detection was revealed using the peroxidase substrate kit DAB (Vector SK-4100, UK). Slides were washed in water for 5 min and then counterstained with Gill's hematoxylin (Sigma, Germany) for nuclear contrast.

The sections of the cASCs' cytoblock were submitted to the same procedure and used as positive control of the immunohistochemistry. The sections were observed under a light microscope (E600 Nikon Instruments, UK) and the images were obtained using the digital camera Nikon DXM200.

3. Development of a double layer scaffold for periodontal regeneration

Aiming at contribute with a new alternative to the current therapies for periodontal regeneration it was proposed a new scaffold designed to address both the regeneration of the alveolar bone and promote the formation of a functional periodontal ligament (PDL).

This construct consists in a double layer scaffold made of a blend of starch and poly (ε-caprolactone) (SPCL), comprehending a biodegradable membrane which acts in the guided regeneration of the PDL, and a tridimensional fiber mesh with osteoconductive properties. The production of the fiber mesh and further combination with the cellular impermeable membrane is obtained through a one-step processing procedure, thus, discarding the need of other chemical and physical steps.

Regarding its potential to translate to human or veterinary dentistry, this construct is protected under the scope of a Patent submitted to *Instituto Nacional da Propriedade Intelectual* (*INPI*) with the submission number 20131000056257 and, at the present moment, subject of formal examination.

3.1. Description of the raw material – Blend of starch and poly (ε-caprolactone)

The material used for the production of the double layer scaffolds that were developed and characterized under the scope of this Thesis, namely in the Chapters V, VI and VII, was a blend of 30% starch and 70% poly (ε-caprolactone) (PCL) (SPCL) in weight from Novamont (Italy).

The starch is the major polysaccharide constituent of photosynthetic tissues and of many storage organs in plants (27). It consists of a mixture of linear and branched amylose and branched amylopectin. Starch is naturally produced in the form of semicristalline granules with different size and composition depending upon the source (28, 29).

PCL is an aliphatic linear polyester prepared by either ring-opening polymerization of ε-caprolactone using a variety of anionic, cationic and co-ordination catalysts or via free radical ring-opening polymerization of 2-methylene-1-3-dioxepane. PCL is a hydrophobic and semicrystalline polymer (28, 30). After the 90s PCL earned great interest in biomaterials' research due to its advantageous rheological and viscoelastic properties (30) which allow the easy manufacturation into a large range of scaffolds obtained by different processing techniques.

The SPCL polymeric blend has already been used to produce different tridimensional structures with different physicochemical characteristics using distinct technologies, namely electrospinning (31, 32), fiber bonding (33), wet-spinning (34), rapid prototyping (32), injection molding (35) or supercritical phase inversion (36).

The potential of this material for Tissue Engineering use was already assessed by culturing with human osteoblast-like cells (SaOs-2) (37), bovine articular chondrocytes (38), rat bone marrow stem cells (BMSCs) (39), goat BMSCs (33), and human ASCs (40), among others.

The biodegradability (41, 42), the processing versatility and the distinct mechanical behaviours and morphologies of the developed matrices, as well as the *in vivo* biocompatibility of the SPCL (43), clearly demonstrated the potential of this material in several applications in Tissue Engineering and Regenerative Medicine field and were the main reason for selecting SPCL for the studies present in the Chapters V, VI and VII of this Thesis.

3.2. Production of the SPCL solvent casting membranes

The SPCL membranes were obtained by a solvent casting method. For this purpose, SPCL granules were dissolved in chloroform (Sigma-Aldrich, Germany) at a concentration of 20 wt%. At room temperature, 3 mL of the polymeric solution was casted onto a 5 cm diameter patterned Teflon mold for the patterned surface membranes (SPCL-P or SPCL-M), or onto non-patterned Teflon mold for the non-patterned surface membranes (SPCL-NP) in order to assess the effect of patterning in the cellular adhesion and proliferation. Membranes were dried in a hood and then cut into discs samples of 6 mm of diameter.

3.3. Production of the SPCL wet-spun fiber meshes

Wet-spinning was used to produce the SPCL fiber meshes. The same SPCL solution used to produce the membranes was loaded into a 5 mL plastic syringe with a metallic needle (21 G×1.5"). The syringe was connected to a programmable syringe pump (KD Scientific, World Precision Instruments, UK) to inject the polymer solution at a controlled pumping rate of 5 mL per hour to allow the formation of the fiber mesh directly into the coagulation bath. The wet-spun fiber mesh structure was formed during the process by the random movement of the coagulation bath. Two different coagulation baths were used: methanol (Vaz Pereira, Portugal) as control (SPCL-WS), and calcium silicate solution $Si(OC_2H_5)_4/H_2O/C_2H_5OH/HCl/CaCl_2$ with a molar ratio of 1.0/4.0/4.0/0.014/0.20 to incorporate the silanol groups in the polymeric fibers, as described in previous works (SPCL-WS-Si) (34, 40, 44). Using methanol, SPCL-WS were dried at room temperature overnight in order to remove any remaining solvent. In the case of using calcium silicate solution, the SPCL-WS-Si were dried in an oven at 60 °C for 24 hours.

3.4. Production of the SPCL double layer scaffolds

After the preparation of each layer, as described above, several different methodologies were tested to assemble the two different layers, namely producing the fiber mesh directly onto the membrane layer, attaching the two components upon heating, or placing a dried fiber mesh on the membrane layer while its drying. The optimized procedure allowing to maintain the integrity of each layer consisted in combining the two layers together by dropping chloroform onto the top side of the solvent casting membranes allowing it to become slightly soften and then, by applying a certain pressure the fiber mesh, were attached. The combined layers were dried in a hood and cut into discs with 6 mm of diameter.

The Table 2.3 describes the composition of each developed layers, including the solvent casting membranes, the wet-spun fiber meshes and the double layer scaffolds, further referred and characterized in the Section III of this Thesis.

Table 2. 3 – Summary of the components of the double layer scaffold which were developed and characterized.

Layers	Description	Abbreviation
SPCL solvent casting membrane	Non-patterned membrane	SPCL-NP
	Patterned membrane	SPCL-M or SPCL-P
SPCL wet-spun fiber mesh	Non-functionalized with silanol groups	SPCL-WS
	Functionalized with silanol groups	SPCL-WS-Si
SPCL double layer scaffold	Patterned membrane plus wet-spun fiber mesh non-functionalized with silanol groups	SPCL-DLS
	Patterned membrane plus wet-spun fiber mesh functionalized with silanol groups	SPCL-DLS-Si

The developed double layer scaffolds were characterized in terms of the physicochemical characteristics, in Chapter V, and the potential to serve as a matrix for cASCs, in Chapter VI; and were also evaluated their potential to enhance bone formation in a rat mandibular model (Chapter VII).

3.5. Characterization of the morphology and structure of the developed scaffolds

3.5.1. Scanning electron microscopy

The surface morphology and topography changes after degradation of the developed materials were analyzed, in Chapter V, by scanning electron microscopy (SEM) performed using a Hitachi SU-70 UHR Schottky (Hitachi, Japan). Three samples of each material in study were analyzed, and prior to any SEM observations, all the materials were sputter-coated with gold by ion sputtering (Polaron SC502, Fisons Instruments, UK).

3.5.2. Micro-computed tomography

In Chapter V, micro-computed tomography (mCT) was performed to evaluate the morphology and porous structure of the SPCL-DLS and SPCL-DLS-Si and the assembling of the two different layers. Micro-CT was carried out using a high-resolution micro-CT Skyscan 1072 scanner (Skyscan, Kontich, Belgium). X-ray scans were performed in triplicate using a resolution of pixel size of 8.7 µm and integration time of 1.9 sec. The X-ray source was set at 49 keV of energy and 122 µA of current. Approximately 400 projections were acquired over a rotation range of 180º with a rotation step of 0.45º. Data sets were reconstructed using standardized cone-beam reconstruction software (NRecon v1.4.3, SkyScan). Representative data sets of 200 slices were segmented into binary images with a dynamic threshold of 37 to 120 to identify the organic and inorganic phases. This data were used to build 3D models (CTAnalyser, v 1.5.1.5, SkyScan).

3.6. Characterization of the surface chemical composition

In Chapter V, Fourier Transform Attenuated Total Reflectance Infrared Spectroscopy (FTRI-ATR) was used to confirm if the polymeric fibers were effectively functionalized with the silanol functional groups, during the protocol of wet-spinning using the calcium-silicate precipitation bath. The SPCL-WS and SPCL-WS-Si were analyzed in an IRPrestige 21 (Shimadzu, Japan). Spectra were collected at 4 cm^{-1} resolution using 60 scans in the spectral range 4400-800 cm^{-1}. For each sample, three individual measurements were performed.

3.7. Characterization of the degradation behaviour

3.7.1. Water uptake and weight loss

In Chapter V, was simulated the *in vivo* degradation of the polymeric scaffolds by incubating SPCL-DLS and SPCL-DLS-Si in different enzymatic solutions at physiological conditions (pH 7.4, 37 ºC), namely in amylase and in lipase to study their effect on starch and PCL hydrolysis, respectively. These two enzymes are found in healthy dogs' serum at concentration in the range of 373-1503 U/L and 90-527 U/L, respectively (45). The rationale of using dog reference values is based on the fact that dog is the final preclinical model in which is intended to assess these biomaterials, before clinical human application. Pre-weighed samples were individually immersed in 2.5 mL of four different solutions: (i) phosphate-buffered saline (PBS, 0.01 M, pH 7.4; Sigma-Aldrich, Germany), (ii) PBS solution containing 400 U/L α-amylase from *Bacillus* sp. (Sigma-Aldrich, Germany), (iii) PBS solution containing 500 U/L lipase from *Pseudomonas* sp. (Sigma-Aldrich, Germany), and (iv) PBS containing lipase and amylase at the same concentrations (50:50 vol%). A control, in PBS only, was also performed. All the prepared solutions were sterilized using a 0.2 µm syringe filter and kept at 4 ºC until further usage. The samples were incubated at 37 ºC for 1, 3, 7, 14, 21 and 28 days, and the solutions were changed weekly.

At the end of each degradation period, the samples were removed from the solution and placed between two filter papers, to remove excess of liquid, and immediately weighted to determine the water uptake. Then, it was washed several times with distilled water and placed in the oven at 37 ºC for 3 days in order to measure the dry weight and thus determine the weight loss. For each studied condition (material and solution), five samples were tested. Degradation solutions were frozen for further analysis, namely, for the quantification of the reducing sugars and calcium and silicon elements, as described below.

3.7.2. Assessment of the morphology of samples after degradation

SPCL-DLS and SPCL-DLS-Si samples after degradation under different conditions were dried at room temperatures and observed by SEM, as described previously in the section 3.5.1 of this chapter. Three samples of each material were analyzed.

3.7.3. α-Amylase activity

Degradation solutions were analyzed to determine the concentration of reducing sugars released into the solution as result of starch hydrolysis. The determination was based on the dinitrosalicyclic acid (DNS) method (46) and absorbance were read at 540 nm in a microplate reader (Synergy HT, BioTek, USA), using a standard curve of glucose.

3.7.4. Calcium and silicon concentration of the degradation solutions

In order to evaluate the effect of the enzymatic degradation on the materials, the elemental concentrations of silicon and calcium were measured in the obtained degradation solutions, after being passed through a 0.22 µm filter, using inductively coupled plasma atomic emission spectrometry (ICP; JY2000-2, Horiba Jobin Yvon, Japan). The results obtained from this assay were thought to provide additional information about the release of these elements from the materials, which have probably an important role in their *in vitro* and *in vivo* response.

3.8. Characterization of the mechanical behaviour

Mechanical tests were carried out to evaluate the tensile strength of the SPCL-DLS and SPCL-DLS-Si. Five rectangular samples with 5 x 20 mm were tested in the dry and wet state (after 24 hours of immersion in PBS). Samples were tested using a uniaxial testing system (Instron 4505 Universal Machine, USA) with a load cell of 1 kN. Tensile test was carried out at a crosshead speed of 2 mm/min. Tensile stress was taken as the maximum stress in the stress-strain curve, and the tensile modulus was estimated from the initial slope of the stress strain curve.

4. Seeding/culturing of the canine ASCs onto the materials

In Chapters V and VI of this Thesis, cASCs were seeded and cultured onto the developed scaffolds, in order to evaluate the potential of each one of the layers to accommodate the cellular adhesion and proliferation, as well to assess the potential of the wet-spun fiber meshes to induce osteogenic differentiation. For this studies, it were used cASCs from subcutaneous origin which were found, in Chapter III, to apparently have higher osteogenic potential compared to cells from omental origin regarding the expression of the studied cell markers. Furthermore, the harvesting of subcutaneous adipose tissue is associated to lower site morbidity. Additionally, envisioning an autologous or allogenic use of this source in the clinical practice, it would be the most appropriate harvesting site. As the passaging was also found to have a negative effect in the stemness, they were used in an early passage. Thus, cASCs were isolated as previously described, and expanded in basal medium until passage 2 (P2) before seeding.

Prior to cell culture experiments, all the materials were sterilized at Pronefro (Maia, Portugal) by ethylene oxide. The conditions included a temperature cycle of 37 ºC, a moisture level of 50%, a cycle time of 14 hours, and a chamber pressure of 50 kPa.

4.1. Seeding/culturing onto solvent casting membranes

In Chapters V and VI, was evaluated the potential of the membranes to sustain the adhesion and proliferation of the cASCs. The cASCs were seeded onto the patterned and non patterned membranes (SPCL-NP and SPCL-M or SPCL-P) at a concentration of 5.0×10^4 cells/sample, and then maintained in basal medium for 2h for cell attachment, and then cultured for 1, 3, 7 and 14 days in basal medium.

4.2. Seeding/culturing onto wet-spun fiber meshes

In Chapters V and VI, was evaluated the potential of the wet-spun fiber meshes to sustain the adhesion and proliferation of the cASCs, as well as to promote their osteogenic differentiation. The SPCL-WS and SPCL-WS-Si were seeded with cASCs at a concentration of 1.0×10^5 cells/sample, and then cultured for 7, 14, 21 and 28 days in either basal or osteogenic medium.

4.3. Characterization of the canine ASCs-material constructs

After each selected culturing period, the culture medium was aspirated and the cell-scaffold samples were carefully washed with sterile PBS. Then, they were prepared according to the further characterization to be performed, namely, SEM and histological analysis, MTS assay, DNA quantification, ALP activity analysis and real-time RT-PCR analysis.

4.3.1. Scanning electron microscopy

In Chapters V and VI, the cultured materials were evaluated by SEM regarding the adhesion and morphology of the cASCs. For this purpose, the samples retrieved upon the different culturing time points were fixed in 2.5% glutaraldehyde (VWR, USA) solution in PBS during 1 hour at 4 ºC and then dehydrated by in a series of ethanol-water solutions with increasing ethanol concentration (30%, 50%, 70%, 90% and 100% v/v). Afterwards, the samples were left to dry overnight before performing the SEM analysis as described previously in the section 3.5.1 of this chapter.

4.3.2. Cellular metabolic activity

In Chapters V and VI, the metabolic activity of the cells seeded/cultured onto the developed materials was assessed using the MTS assay. All the cultured materials (SPCL-NP, SPCL-P, SPCL-WS and SPCL-WS-Si), after rinsed with PBS, were immersed in a mixture consisting of serum-free cell culture medium and MTS reagent (VWR, USA) in a 5:1 ratio and incubated for 3 hours at 37 °C in a humidified atmosphere containing 5% CO_2. After this, 200 µL were transferred to 96-well plates and the optical density (O.D.) was measured on a microplate reader at an absorbance of 490 nm.

4.3.3. Cellular proliferation

In Chapters V and VI, double strain DNA (dsDNA) quantification was performed to assess the proliferation of the cASCs seeded and cultured onto all the developed materials (SPCL-NP, SPCL-P, SPCL-WS and SPCL-WS-Si). For this purposes, samples removed from culture upon the pre-setted time points, were rinsed twice in a PBS solution and transferred into 1.5 mL microtubes containing 1 mL ultra-pure water. Then, cASCs-SPCL constructs were incubated for 1 h at 37 ºC in a water-bath and stored in a -80 ºC freezer, promoting a thermal shock variation and thus inducing cell lysis. Before assessing DNA levels, constructs were thawed and sonicated for 15 min.

A fluorimetric dsDNA quantification kit (PicoGreen, Molecular Probes, USA) was used to determine the cellular content. Samples and standards (0-2 µg/mL) were prepared in triplicate. Briefly, in each well of a 96-well white plate (Costar; Becton-Dickinson, USA), were deposited 28.7 µL of sample or of each standard, 71.3 µL of PicoGreen solution and 100 µL 1X (Life Technologies, USA), then the plate was incubated for 10 min in the dark and the fluorescence was read using a microplate reader (BioTek, USA) at an excitation of 485/20 nm and an emission of 528/20 nm. A standard curve was developed in order to read DNA values of samples from the standard graph.

4.3.4. Alkaline phosphatase activity

In Chapter VI, alkaline phosphatase (ALP) activity assay was performed to assess the osteogenic differentiation of the cultured cASCs on the wet-spun fiber meshes (SPCL-WS and SPCL-WS-Si) in the same samples used for dsDNA quantification.

For this purpose, to each well of a 96-well plate (Costar; Becton-Dickinson, USA) were added 20 µL sample plus 60 µL substrate solution consisting of 0.2 wt/v% p-nytrophenyl phosphate (Sigma, Germany) in a substrate buffer with 1 M diethanolamine HCl (Merck, Germany), pH 9.8. The plate was then incubated in the dark for 45 min at 37 ºC. After the incubation period, 80 µL stop solution [2 M NaOH (Panreac, Spain) plus 0.2 mM EDTA (Sigma, Germany)] was added to each well. Standards were prepared with p-nytrophenol (10 µM/mL; Sigma, Germany) in order to achieve final concentrations in the range 0-0.3 µM/mL. Samples and standards were prepared in triplicates. Absorbance was read on a microplate reader at 405 nm and sample concentrations were read from the standard.

4.3.5. Gene expression analysis of the osteoblastic markers

In Chapters V and VI, the gene expression analysis of specific osteoblast markers were assessed on the cASCs cultured on the SPCL-WS and SPCL-WS-Si in both basal and osteogenic medium, aiming at evaluating the potential of these matrices to induce the osteogenic differentiation.

Briefly, the cell-scaffolds constructs were removed from culture, rinsed twice in a PBS solution and transferred into 1.5 mL microtubes containing in 800 µL of TRIzol Reagent and kept for further real time RT-PCR analysis as described before.

4.3.6. Histology – Donath technique

In Chapter VI, the developed fiber meshes (SPCL-WS and SPCL-WS-Si) cultured with cASCs in both basal and osteogenic conditions were evaluated by histology. In order to obtain cross sections of the cultured materials maintaining the tridimensional architecture of the matrix essential for the subsequent histological evaluation, it was decided to process the cultured scaffolds with cASCs by using the Donath technique (47). Then, the obtained slides were stained with Lévai and Laczkó staining (48). The Donath technique involved several sequential processing steps that are described below.

Dehydration

In this step, the samples were dehydrated by in a series of ethanol-water solutions with increasing ethanol concentration (70%, 80%, 96% and twice 100%).

Infiltration

Infiltration was made by emerging the samples in a solution of glycolmethacrylate plastic (Technovit 7200, Heraus Kulzer, Germany) and benzoyl peroxide (BPO; Heraus Kulzer, Germany) in 1% ethanol at different concentrations, ending with two infiltrations in pure glycolmethacrylate, with constant stirring.

Inclusion and polymerization

To carry out the inclusion, the samples were placed in polyethylene molds and subsequently filled with resin (Technovit 7200) under the effect of vacuum (Exakt 530 and 520).

The polymerization took place in two steps; first by using a low intensity light and maintaining the molds at a temperature below 40 °C for four hours to polymerize the resin, and then by using a high intensity blue light for 12 hours.

Finally, the samples remained in the oven for 24 hours to complete the polymerization process.

Preparation of the block in order to obtain a parallel surface

Once polymerized, the blocks were removed from the mold, and then cut approximately in the area of interest by using a saw (Exact 300 CP) at low speed, and irrigating to avoid sample overheating.

After cutting, in order to maintain the parallelism of the surfaces the half blocks, they were mounted in an acrylic sheet using a resin (Technovit 4000) and applying pressure. The resin is spread over the back of the block, so that the part to be examined contact becomes free for further polishing.

Preparation of the surface of interest

The following step consisted in polishing the surface of interest of the sample by using a silicon carbid sandpaper number 1200. Then, by using a press with a photopolymerization light and a specific resin (Technovit 7210), the aspect of the block aimed at be observed was sticked on the definitive slide. Then, using a saw (Exakt 400) and a vacuum sample holder was obtained a rough section of 200 µm. This section was subjected to microwear (Exakt-Griding Micro System, Exact Technologies, Germany) and polished with a sandpaper number 1200 and 4000.

At the end, there were obtained sections with thickness of approximately 30 µm.

4.3.7. Lévai Laczkó staining

The obtained slides were stained with Lévai and Laczkó staining (48) in order to identify the seeded/cultured cASCs on the surface of the fibers and identify the calcium depots existent in the functionalized fiber meshes. This procedures included the following steps: i) immersion in 30% hydrogen peroxide (Sigma, Germany) for 5 min with constant agitation, ii) rinse with tap water twice, iii) decalcification of the surface with acetic acid (VWR, USA) for 1 min, iv) rinse with tap water twice, v) immersion in a solution composed by one part of Azure II and Methylene Blue (1:1) and two parts of Na_2CO_3 for 20 min. All these reagents were ordered from Merck (Germany) and used at 1% in distilled water, vi) rinse with tap water twice, vii) submersion in 1% Pararosaniline (Sigma, Germany) in distilled water for 5 sec, and viii) rinse with tap water twice and dry.

Finally, the obtained slides were observed under a light microscope (Olympus BX51, Germany).

5. *In vivo* evaluation of the double layer scaffold in a rat mandibular defect

After accomplished the *in vitro* characterization in Chapter V and VI, the double layer scaffold was subsequently characterized *in vivo*, assessing the behaviour of the newly developed scaffold in a mandibular rodent model aiming at evaluate its potential to enhance bone formation (Chapter VII).

5.1. Study animals

Twelve, male, 10-weeks old Wistar rats (*Rattus norvegicus*) (Charles River, UK) were used in this protocol. The mean body weight was of 433.87 ± 21.69 g. The housing care and experimental protocol was performed according to national guidelines, after approval by the National Ethical Committee for Laboratory Animals and conducted in accordance with Portuguese legislation (Portaria 1005/92) and international standards on animal welfare as defined by the European Directive 2010/63/EU. The animals were fed with a maintenance diet for rats (A04/A04C/R04 diet, Safe, France) and autoclaved water, both *ad libitum*, and bedded in wood shavings (Scobis Uno, Mucedola, Italy) with suitable environment enrichment.

5.2. Experimental design

The defects were randomly assigned in the following four experimental groups (six defects per group): (i) empty defects (negative control), (ii) defects implanted with collagen membranes (positive control), (iii) defect implanted with SPCL double layer scaffolds and (iv) defect implanted with SPCL-Si double layer scaffolds. Each rat was subject of two bilateral defects which were then filled with different materials/empty defect.

5.3. Surgical procedure

The rats were premedicated with dexmedetomidine hydrochloride (Dexdomitor; Pfizer, Finland) 0.5 mg/kg intraperitoneal and anesthetized with ketamine chloride (Imalgene 1000; Merial, Portugal) 75 mg/kg intraperitoneal. The rats' head were pre-operative radiographed (Siemens, Germany) to confirm normal anatomy and to determine if the bony surface was suitable to encompass a 5 mm circular defect (Fig. 2.1).

In lateral recumbency with the neck extended, the mandibular and cervical areas were shaved and aseptically prepared with 0.1% iodopovidone (Ectodine, Portugal). Then, a mandibular skin incision was made to expose the masseter muscle and the borders pushed away rostrodorsal and ventrocaudally, taking care to prevent damage of the facial nerve and the parotid duct until access the surface of the ramus of the mandible. A bicortical 5 mm circular defect was drilled in both mandibles using a 5 mm outer diameter trephine (ACE Surgical Supply, USA) under a continuous irrigation with saline solution to reduce thermal bone damage, and then the materials were placed and fitted in the defects (Fig. 2.2).

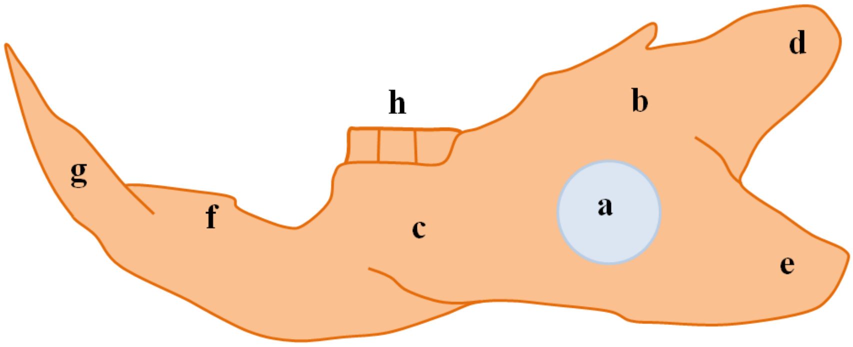

Figure 2. 1 – Schematic representation of the rat mandible (left lateral view) where is observed the induced critical size defect (a), the ramus of the mandible (b), the body of the mandible (c), the condylar process (d), the angular process (e), the diastema (f), the incisor tooth (g) and the molars teeth (h).

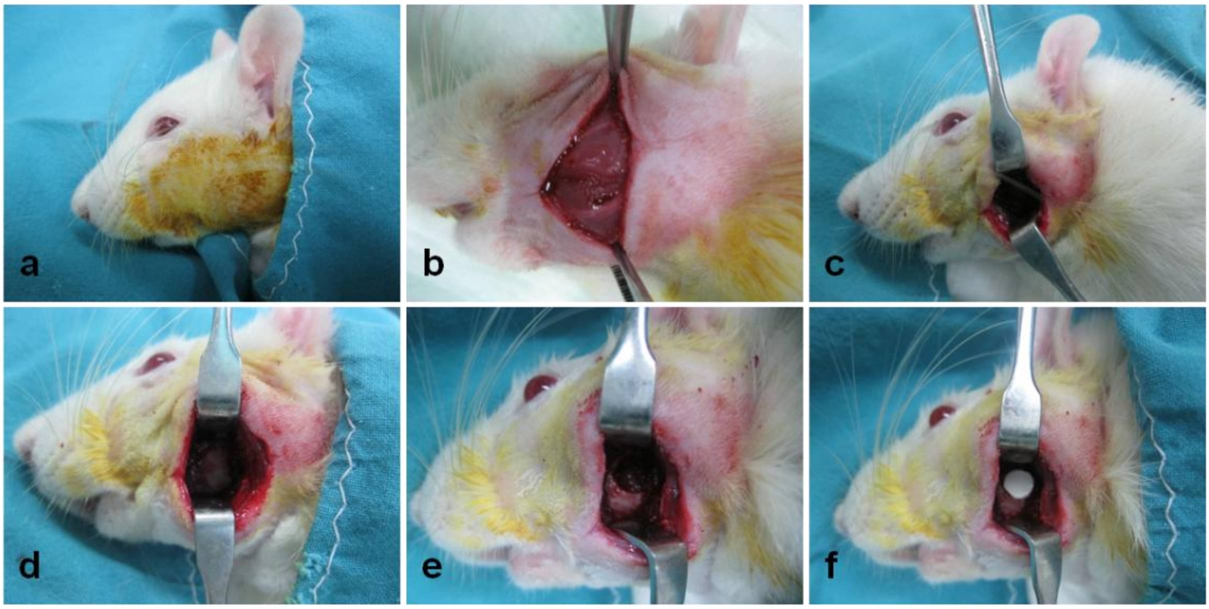

Figure 2. 2 – Surgical procedure to induce the defect and implant the material: (a) aseptic preparation of the surgical field, (b) incision of the skin to expose the masseter muscle, (c) incision and dissection of the masseter muscle, (d) exposition of the *fossa masseterica* in the lateral the ramus of the mandible, (e) induction of the circular bone defect and (f) implantation of the materials in the defect.

The surgical wound was closed in two layers using a 4-0 resorbable sutures made of glyconate (Monosyn; BBraun, Portugal) for muscle and 4-0 non-resorbable sutures made of silk (Silkan; BBraun, Portugal) for skin.

The anaesthesia was reversed using a single dose of atipamezol chlorhydrate (Antisedan; Pfizer, Germany) 1 mg/kg intraperitoneal.

5.4. Postoperative care

A single dose of butorphanol (Butador; Richterpharma, Austria) 0.4 mg/kg intraperitoneal was administrated three hours postoperatively for pain relief, and then the analgesia was maintained with meloxicam (Movalis; Boehringer Ingelheim, Germany) 1.5 mg/kg subcutaneous, once a day, during five consecutive days. For post-operative antibiotherapy, enrofloxacin (Baytril 5%; Bayer, Germany) 0.1 mg/mL of drink water was given for six consecutive days.

As the surgical procedure severely affected the mastication, the pellet food was mixed with warm water until it got soft. This mixture was given to the animals for two weeks, and then the rats were slowly introduced to the pellet food. Physiologic parameters, such as the behaviour, water and food intake, weight gain and wound healing were daily monitored.

5.5. Euthanasia and explants collection

After 8 weeks of implantation, the animals were anaesthetized as described above, and then euthanized by an intraperitoneal injection of sodium pentobarbital (Eutasil; CEVA, Portugal).The mandibles were explanted, fixed in 4% phosphate-buffered formalin (Inopat, Portugal) solution at 4 ºC for one week until further analysis.

5.6. Histology

The explanted mandibles were then analyzed using a specific technique for bone histology, the Donath technique (47), which allows to obtain histological slides without decalcifying the samples and thus obtaining an accurate image of the architecture of both the old bone in which the defect was induced and the new bone formed within the defect after eight weeks of implantation.

The explants samples were processed following the procedure already described in detailed in the section 4.3.6 of this chapter, with some minor differences that will be described herein. Regarding the explanted mandibles, the dehydratation was made by in a series of ethanol-water solutions with increasing ethanol concentration (70% for 3 days, 80% for 3 days, 96% for 3 days, and twice 100% for 3 days) under constant agitation (Exakt 510, Exakt Technologies, Germany).

Once polymerized the blocks, they were radiographed in two projections allowing to subsequently perform a cut in the exact place intended to be analyzed, namely the center of the circular mandibular bone defect. The obtained slides were then stained with Lévai and Laczkó staining which allows to distinguish the old bone and the new formed bone after induced the defect (48).

5.7. Histomorphometric analysis

The histomorphometric analysis of the explants was performed to quantify the formation of new bone. For this purpose, stained section were observed under a light microscope (Olympus BX51, Germany) and a computer-based image analysis system (Microimage 4.0, Media Cybernetics, USA) was used to assess the percentage of bone ingrowth in the defect in a defined region of interest of 5 mm of length by 1 mm of width.

6. Statistical analysis

Different statistical analyses were performed in this Thesis, according to the specific objectives of each study. All the experiments were performed with at least three replicates. Results were expressed as mean ± standard deviation.

In Chapter III, concerning the characterization of the cASCs, and in Chapter VI, regarding the seeding/culturing of cASCs on the developed materials, the results obtained were elaborated using the software JMP v9.0.1 (SAS Institute Inc., USA) and the correlation between the dataset from the same gene analyzed was investigated with the ANOVA single factor method. Data was presented as mean ± standard error of the mean (SEM) and differences between data groups were considered to be statistically significant for $p<0.05$ (Student's t-test).

In Chapter VI, about the evaluation of the physicochemical characteristics of the developed materials, the statistical analysis was performed using the GraphPad Prism v5.00 (GraphPad Software Inc., USA). The statistical significance was assessed by a two-way ANOVA followed with Bonferroni posttesting and the data was reported as mean ± standard deviation.

In Chapter VII, on the *in vivo* characterization of the double layer scaffolds, the statistical comparison of the percentage of new bone formation was performed using two-way analysis of variance (ANOVA) and Tukey post-hoc test. P-values<0.05 were considered to be statistically significant.

7. References

1. Rada T, Reis RL, Gomes ME. Adipose tissue-derived stem cells and their application in bone and cartilage tissue engineering. Tissue Engineering Part B-Reviews. 2009;15 (2):113-25.

2. Zuk PA, Zhu M, Ashjian P, De Ugarte DA, Huang JI, Mizuno H, *et al*. Human adipose tissue is a source of multipotent stem cells. Molecular Biology of the Cell. 2002;13 (12):4279-95.

3. Albuquerque C, Morinha F, Requicha J, Martins T, Dias I, Guedes-Pinto H, *et al*. Canine periodontitis the dog as an important model for periodontal studies. Vet J. 2012;191 (3):299-305.

4. Struillou X, Boutigny H, Soueidan A, Layrolle P. Experimental animal models in periodontology: a review. Open Dent J. 2010;4:37-47.

5. Dumitrescu A. Animal Models in Periodontal Research. Understanding Periodontal Research: Springer Berlin Heidelberg; 2012. p. 655-763.

6. Plumb DC. Plumb's Veterinary Drug Handbook: Desk. 7th ed: Wiley-Blackwell; 2011.

7. Fossum TW. Small Animal Surgery. 4th ed. St. Louis, Missouri: Elsevier Mosby; 2013.

8. Carvalho PP, Wu X, Yu G, Dias IR, Gomes ME, Reis RL, *et al*. The Effect of Storage Time on Adipose-Derived Stem Cell Recovery from Human Lipoaspirates. Cells Tissues Organs. 2011.

9. Gimble JM, Guilak F. Adipose-derived adult stem cells: isolation, characterization, and differentiation potential. Cytotherapy. 2003;5 (5):362-9.

10. Dominici M, Le Blanc K, Mueller I, Slaper-Cortenbach I, Marini FC, Krause DS, *et al*. Minimal criteria for defining multipotent mesenchymal stromal cells. The International Society for Cellular Therapy position statement. Cytotherapy. 2006;8 (4):315-7.

11. Spitz SN, Requicha AAG. Accessibility analysis using computer graphics hardware. Ieee T Vis Comput Gr. 2000;6 (3):208-19.

12. Vassena R, Montserrat N, Carrasco Canal B, Aran B, de Onate L, Veiga A, *et al*. Accumulation of instability in serial differentiation and reprogramming of parthenogenetic human cells. Hum Mol Genet. 2012;21 (15):3366-73.

13. Arutyunyan IV, Rzhaninova AA, Volkov AV, Goldstein DV. Effect of Dexamethasone on Differentiation of Multipotent Stromal Cells from Human Adipose Tissue. Bulletin of Experimental Biology and Medicine. 2009;147 (4):503-8.

14. de Girolamo L, Sartori MF, Albisetti W, Brini AT. Osteogenic differentiation of human adipose-derived stem cells: comparison of two different inductive media. Journal of Tissue Engineering and Regenerative Medicine. 2007;1 (2):154-7.

15. Tuli R, Tuli S, Nandi S, Huang X, Manner PA, Hozack WJ, *et al*. Transforming Growth Factor-β-mediated Chondrogenesis of Human Mesenchymal Progenitor Cells Involves N-cadherin and Mitogen-activated Protein Kinase and Wnt Signaling Cross-talk. Journal of Biological Chemistry. 2003;278 (42):41227-36.

16. Shoulders MD, Raines RT. Collagen structure and stability. Annu Rev Biochem. 2009;78:929-58.

17. Jensen EC. Real-Time Reverse Transcription Polymerase Chain Reaction to Measure mRNA: Use, Limitations, and Presentation of Results. Anatomical Record-Advances in Integrative Anatomy and Evolutionary Biology. 2012;295 (1):1-3.

18. Misumi Y, Ogata S, Ohkubo K, Hirose S, Ikehara Y. Primary structure of human placental 5'-nucleotidase and identification of the glycolipid anchor in the mature form. Eur J Biochem. 1990;191 (3):563-9.

19. Kisselbach L, Merges M, Bossie A, Boyd A. CD90 Expression on human primary cells and elimination of contaminating fibroblasts from cell cultures. Cytotechnology. 2009;59 (1):31-44.

20. Pierelli L, Bonanno G, Rutella S, Marone M, Scambia G, Leone G. CD105 (endoglin) expression on hematopoietic stem/progenitor cells. Leukemia & Lymphoma. 2001;42 (6):1195-206.

21. Chu ML, de Wet W, Bernard M, Ramirez F. Fine structural analysis of the human pro-alpha 1 (I) collagen gene. Promoter structure, AluI repeats, and polymorphic transcripts. Journal of Biological Chemistry. 1985;260 (4):2315-20.

22. Liu TM, Lee EH. Transcriptional Regulatory Cascades in Runx2-Dependent Bone Development. Tissue Eng Part B Rev. 2012.

23. Long F. Building strong bones: molecular regulation of the osteoblast lineage. Nat Rev Mol Cell Biol. 2012;13 (1):27-38.

24. Miron RJ, Zhang YF. Osteoinduction: a review of old concepts with new standards. J Dent Res. 2012;91 (8):736-44.

25. Livak KJ, Schmittgen TD. Analysis of relative gene expression data using real-time quantitative PCR and the 2 (T) (-Delta Delta C) method. Methods. 2001;25 (4):402-8.

26. Gregory CA, Gunn WG, Peister A, Prockop DJ. An Alizarin red-based assay of mineralization by adherent cells in culture: comparison with cetylpyridinium chloride extraction. Analytical Biochemistry. 2004;329 (1):77-84.

27. Zeeman SC, Delatte T, Messerli G, Umhang M, Stettler M, Mettler T, *et al*. Starch breakdown: recent discoveries suggest distinct pathways and novel mechanisms. Funct Plant Biol. 2007;34 (6):465-73.

28. Puppi D, Chiellini F, Piras AM, Chiellini E. Polymeric materials for bone and cartilage repair. Progress in Polymer Science. 2010;35 (4):403-40.

29. Salgado AJ, Coutinho OP, Reis RL. Bone tissue engineering: State of the art and future trends. Macromolecular Bioscience. 2004;4 (8):743-65.

30. Woodruff MA, Hutmacher DW. The return of a forgotten polymer-Polycaprolactone in the 21st century. Progress in Polymer Science. 2010;35 (10):1217-56.

31. Puppi D, Piras AM, Chiellini F, Chiellini E, Martins A, Leonor IB, *et al*. Optimized electro- and wet-spinning techniques for the production of polymeric fibrous scaffolds loaded with bisphosphonate and hydroxyapatite. Journal of Tissue Engineering and Regenerative Medicine. 2011;5 (4):253-63.

32. Martins A, Chung S, Pedro AJ, Sousa RA, Marques AP, Reis RL, *et al*. Hierarchical starch-based fibrous scaffold for bone tissue engineering applications. Journal of Tissue Engineering and Regenerative Medicine. 2009;3 (1):37-42.

33. Rodrigues MT, Gomes ME, Viegas CA, Azevedo JT, Dias IR, Guzon FM, *et al*. Tissue-engineered constructs based on SPCL scaffolds cultured with goat marrow cells:

functionality in femoral defects. Journal of Tissue Engineering and Regenerative Medicine. 2011;5 (1):41-9.

34. Leonor IB, Rodrigues MT, Gomes ME, Reis RL. In situ functionalization of wet-spun fibre meshes for bone tissue engineering. J Tissue Eng Regen Med. 2011;5 (2):104-11.

35. Oliveira AL, Pedro AJ, Arroyo CS, Mano JF, Rodriguez G, San Roman J, *et al*. Biomimetic Ca-P coatings incorporating bisphosphonates produced on starch-based degradable biomaterials. Journal of Biomedical Materials Research Part B-Applied Biomaterials. 2010;92B (1):55-67.

36. Duarte ARC, Mano JF, Reis RL. Supercritical phase inversion of starch-poly (epsilon-caprolactone) for tissue engineering applications. Journal of Materials Science-Materials in Medicine. 2010;21 (2):533-40.

37. Tuzlakoglu K, Pashkuleva I, Rodrigues MT, Gomes ME, van Lenthe GH, Muller R, *et al*. A new route to produce starch-based fiber mesh scaffolds by wet spinning and subsequent surface modification as a way to improve cell attachment and proliferation. Journal of Biomedical Materials Research Part A. 2010;92A (1):369-77.

38. da Silva MA, Crawford A, Mundy J, Martins A, Araujo JV, Hatton PV, *et al*. Evaluation of Extracellular Matrix Formation in Polycaprolactone and Starch-Compounded Polycaprolactone Nanofiber Meshes When Seeded with Bovine Articular Chondrocytes. Tissue Engineering Part A. 2009;15 (2):377-85.

39. Gomes ME, Sikavitsas VI, Behravesh E, Reis RL, Mikos AG. Effect of flow perfusion on the osteogenic differentiation of bone marrow stromal cells cultured on starch-based three-dimensional scaffolds. Journal of Biomedical Materials Research Part A. 2003;67A (1):87-95.

40. Rodrigues AI, Gomes ME, Leonor IB, Reis RL. Bioactive starch based scaffolds and human adipose stem cells are a good combination for bone tissue engineering. Acta Biomaterialia. 2012;8:3765–76.

41. Gomes ME, Azevedo HS, Moreira AR, Ella V, Kellomaki M, Reis RL. Starch-poly (epsilon-caprolactone) and starch-poly (lactic acid) fibre-mesh scaffolds for bone tissue engineering applications: structure, mechanical properties and degradation behaviour. Journal of Tissue Engineering and Regenerative Medicine. 2008;2 (5):243-52.

42. Azevedo HS, Gama FM, Reis RL. In vitro assessment of the enzymatic degradation of several starch based biomaterials. Biomacromolecules. 2003;4 (6):1703-12.

43. Santos TC, Marques AP, Horing B, Martins AR, Tuzlakoglu K, Castro AG, *et al*. In vivo short-term and long-term host reaction to starch-based scaffolds. Acta Biomater. 2010;6 (11):4314-26.

44. Oyane A, Kawashita M, Nakanishi K, Kokubo T, Minoda M, Miyamoto T, *et al*. Bonelike apatite formation on ethylene-vinyl alcohol copolymer modified with silane coupling agent and calcium silicate solutions. Biomaterials. 2003;24 (10):1729-35.

45. Tvedten H. Listing of selected reference values. In: Willard M, Tvedten H, editors. Small Animal Clinical Diagnosis by Laboratory Methods. 5th ed. St. Louis: Elsevier Saunders; 2012. p. 399-402.

46. Ghose T. Measurement of cellulase activities. Pure and Applied Chemistry 1987 (59):257-68.

47. Donath K, Breuner G. A method for the study of undecalcified bones and teeth with attached soft tissues. J Oral Pathol. 1982;11:318–26.

48. Laczkó J, Lévai G. A simple differential staining method for semi-thin sectionsof ossifying cartilage and bone tissues emhedded in epoxy resin. Mikroskopie 1975;31:1-4.

Section III

New tissue-engineered matrix for periodontal regeneration based on a biodegradable material combined with canine adipose-derived stem cells

Chapter III

Effect of anatomical origin and cell passage number on the stemness and osteogenic differentiation potential of canine adipose-derived stem cells

Abstract

Mesenchymal stem cells have a great potential for application in cell based therapies, such as Tissue Engineering. Adipose derived stem cells have shown the capacity to differentiate into several lineages, and have been isolated in many animal species. Dog is a very relevant animal model to study several human diseases and simultaneously an important subject in veterinary medicine. Thus, in this study we assessed the potential of canine adipose tissue derived stem cells (cASCs) to differentiate into the osteogenic and chondrogenic lineages by performing specific histological stainings, and studied the cell passaging effect on the cASCs stemness and osteogenic potential. We also evaluated the effect of the anatomical origin of the adipose tissue, namely from abdominal subcutaneous layer and from greater omentum. The stemness and osteogenic differentiation was followed by real time RT-PCR analysis of typical markers of mesenchymal stem cells (MSCs) and osteoblasts.

The results obtained revealed that cASCs exhibit a progressively decreased expression of the MSCs markers along passages and also a decreased osteogenic differentiation potential. In the author's knowledge, this work presents the first data about the MSCs markers profile and osteogenic potential of cASCs along cellular expansion. Moreover, the obtained data showed that the anatomical origin of the adipose tissue has an evident effect in the differentiation potential of the ASCs. Due to the observed resemblances with the human ASCs, we conclude that canine ASCs can be used as a model cells in Tissue Engineering research envisioning human applications.

---

*This Chapter is based on the following publication:

Requicha JF, Viegas CA, Albuquerque CM, Azevedo JM, Reis RL, Gomes ME. 2012. Effect of anatomical origin and cell passage number on the stemness and osteogenic differentiation potential of canine adipose-derived stem cells. Stem Cell Reviews and Reports, 8 (4):1211-22

1. Introduction

Stem cells play a vital role in regenerative medicine approaches due to their self-renew capacity and differentiation potential when cultured under specific biochemical and/or mechanical stimulus (1-3). Several adult tissues derived from mesodermal layer of the embryo are known sources of mesenchymal stem cells (MSCs), such as, the bone marrow (3), adipose tissue (1, 2, 4), umbilical cord blood (5), muscle tissue (6), neuronal tissue (7), bone (8), periosteum (9), periodontal ligament (10), dental pulp (11), exfoliated deciduous teeth (12), dental follicle (13) and pancreatic or hepatic tissues (14).

Human adipose-derived stem cells (hASCs) were firstly isolated by Zuk and colleagues, in 2001 (4) and have gained importance in the last years, mainly due to the wide availability of the adipose tissue (15, 16), enabling to collect larger quantities and due to the easiness of its harvesting procedures, minimizing site morbidity. ASCs can be isolated by enzymatic digestion (16) and, in culture, they are characterized by their adherence to the plastic substrate of culture plates, in opposition to hematopoietic stem cells (2, 17). Furthermore, ASCs are able to differentiate in different lineages (1, 15, 18), such as, osteoblasts (4, 15, 19, 20), chondroblasts (1, 4, 15, 20), adipocytes (4, 15, 20, 21), skeletal, smooth and cardiac myocytes (4, 20, 22), neuronal cells (20, 23-26), tendon cells (27) and intervertebral disc cells (28).

This source of multipotent cells has been mostly studied in humans, but also in other species, such as mice (29), rat (30), rabbit (31), sheep (32), horse (27, 33), non-human primate (25, 34) and dogs (24, 35-37).

Canine ASCs have been isolated from visceral (24, 35, 38) and subcutaneous (35, 36, 38-40) adipose tissue and it has been proved their potential to differentiated, *in vitro*, into the osteogenic (35), chondrogenic (35), adipocytic (35, 38), neuronal (24) and myogenic (37) lineages. Canine animal models are very important to study a variety of human diseases; simultaneously, dog is a very important subject in veterinary medicine, therefore it is essential to know more about canine ASCs. These cells can also be used in autologous Tissue Engineering approaches, as it has already been reported in previous works related to the regeneration of periodontal defects (36), cranial defects (41) and in osteoarthritis clinical trials (39), in all cases demonstrating promising results. In fact, stem cells based therapies have gained increasing importance in veterinary medicine and have already went into the clinical routine in some countries.

The aim of this study was to compare canine adipose-derived stem cells derived from different anatomical sites, namely, subcutaneous and omental fat depots, and to characterize their stemness along its proliferative process by analyzing the expression of typical MSC genes at different passages. The multipotency of these cells was assessed by inducing their differentiation into different cellular lineages, including osteogenic and chondrogenic and analysing the production of specific extra cellular matrix, as well as the expression of specific osteoblastic genes.

The results obtained provide essential information for the future application of canine ASCs in new stem cells based therapies in veterinary medicine, as well as for the use of the dog as a model (42) for developing new human regenerative medicine approaches.

2. Materials and Methods

2.1. Harvesting of canine adipose tissue

Adipose tissue was collected from 6 adult dogs (3 males and 3 females), between 1 and 5 years of age, subject of convenience surgery in the Veterinary Hospital of University of Trás-os-Montes e Alto Douro in accordance with Portuguese legislation (Portaria no1005/92) and international standards on animal welfare as defined by the European Communities Council Directive (86/609/EEC), and with previous informed consent of the owners.

The dogs were sedated by an intramuscular administration of 0.2 mg/kg IM butorphanol (Torbugesic 1%; Fort Dodge, the Netherlands) and 30 µg/kg IM acepromazine (Vetranquil; CEVA Sante Animal, France). Anaesthesia was achieved by an intravenous administration of 0.25 mg/kg IV diazepam (Diazepam MG; Labesfal, Portugal), 4 mg/kg IV ketamine (Imalgene 1000; Merial, France) and 4 mg/kg IV propofol (Lipuro 2%; Braun, Germany) and was maintained using 1% isoflurane (IsoFlo; Abbott Animal Health, USA), administered in oxygen through an endotracheal tube.

After anesthetized, the animals were placed in dorsal recumbence and it was made a careful tricothomy and asepsis of the abdominal region. A small surgical incision was made through the skin, subcutaneous tissue and muscular wall of the abdominal region.

In all the animals of the study, a small amount of abdominal subcutaneous and omental adipose tissue was resected using scalpel and surgical scissors and placed into labeled sterile containers with PBS (Phosphate Buffer Solution; Sigma Aldrich, Germany) with 10%

antibiotic/antimycotic (100 IU/ml penicillin and 100 IU streptomycin; Fluka, UK). Samples were refrigerated at 4 ºC and transported to the laboratory for further processing.

2.2. Isolation and expansion of canine ASCs

All the samples were processed within 12 hours upon harvesting. Adipose tissue samples were washed with PBS containing 10% antibiotics/antimycotic and minced into small fragments using a scissor. The fragments were digested with a solution of 0.1% collagenase type IA (Sigma Aldrich, Germany) in PBS at 37 ºC under shacking at 200 rpm for 40 min (10 ml/10 cc Tissue). Collagenase was inactivated with an equal volume of culture medium containing 10% FBS (Foetal Bovine Serum; Invitrogen, USA).

The digested tissue was filtered with a 100 µm nylon mesh and centrifuged at 1250 rpm for 5 min at 20 °C and the supernatant removed. The obtained cells were resuspended in culture medium (basal medium, BM) composed of DMEM (Dulbecco's Minimum Essential Medium Eagle; Sigma Aldrich, Germany), 10% FBS, sodium bicarbonate (Sigma Aldrich, Germany) and 1% antibiotic/antimycotic and then seeded in 25 cm^2 culture flasks. After 48 hours, the cells were rinsed with PBS and the medium was changed to remove non-adherent cells, such as hematopoietic cells or dead cells, as performed in other studies (32).

2.3. Canine ASCs expansion and differentiation

The cells were cultured in plastic adherent culture flasks, using basal medium, which was changed three times a week until reaching a confluence of around 80%, along four passages (P1, P2, P3 and P4).

2.3.1. Osteogenic differentiation

Canine ASCs, at P1, P2, P3 and P4, were seeded at a density of 5×10^4 cells per culture flask (75 cm^2 T-flask), and further cultured for 14, 21, 28 and 35 days in osteogenic medium (OM) composed of αMEM (Alpha Minimum Essential Medium Eagle; Sigma Aldrich, Germany) supplemented with 10% FBS, sodium bicarbonate, 1% antibiotic/antimycotic, ascorbic acid (Sigma, USA), 10^{-8} M dexamethasone (Sigma, USA) and 10 mM β-glycerophosphate (Sigma, USA); culture medium was changed twice a week.

2.3.2. Chondrogenic differentiation

Canine ASCs (about 5×10^5 cells), at P1, P2, P3 and P4, were resuspended in chondrogenic medium and centrifuged at 800 G for 5 min, in order to obtain cell pellets. Pellets were cultured in the same medium for up to 21 days at 37 ºC and 5% CO_2, in 15 ml falcon tubes. Chondrogenic medium was composed of DMEM supplemented with 5% FBS, sodium bicarbonate, 1% antibiotic/antimycotic, 1 mM dexamethasone, 17 mM ascorbic acid, 10 ng/ml TGF-β1 (Human Transforming Growth Factor Beta 1; eBioscience, USA), 10% Insulin-Transferrin-Selenium (ITS) (Sigma, USA), 35 mM L-proline (Sigma, USA) and 0.1 M sodium pyruvate (Sigma, USA) and was changed twice a week.

2.4. Canine ASCs characterization

2.4.1. Gene expression analysis of MSCs markers

Real time RT-PCR analysis was used to characterize the phenotype of cASCs, obtained from tissue collected from different anatomical sites (subcutaneous and omental) at different passages, namely, through the relative expression of *CD73*, *CD90* and *CD105* genes (17), which are the widely accepted markers of the mesenchymal stem cells. The fact that is difficult to find in the market specific antibodies for cells of canine origin, was the main reason to select real time RT-PCR analysis and not flow cytometry or other immune-based assays, for the assessment of the MSCs and osteoblasts markers

For this purpose, cASCs were detached using trypsin, and samples consisting of $1×10^6$ cells at P0, P1, P2, P3 and P4 cultured in basal media, were retrieved and kept in 800 µL of TRIzol Reagent (Invitrogen, USA). The mRNA was extracted with TRIzol following the procedure provide by the supplier. Briefly, after an incubation of 5 min, additional 160 µL of chloroform (Sigma Aldrich, Germany) were added; the samples were then incubated for 15 min at 4 °C and centrifuged at the same temperature and 13000 rpm for 15 min. After the centrifugation, the aqueous part was collected and an equal part of isopropanol (VWR, USA) was added. After an incubation of 2 hours at -20 °C, the samples were washed in ethanol, centrifuged at 4 °C and 9000 rpm for 5 min and resuspended in 12 µL of RNase/DNase free water (Gibco, UK). The samples were quantified using a NanoDrop ND1000 Spectrophotometer (NanoDrop Technologies, USA). For the cDNA synthesis, it were used the samples with a 260/280 ratio between 1.7 and 2.0. The cDNA synthesis was performed in the Mastercycler real time PCR equipment (Eppendorf, USA) using the iScript cDNA Synthesis Kit (Quanta Biosciences, USA) and an initial amount of mRNA of 2 µg and a total volume of 20 µL RNAse free water (Gibco, UK) was used as a negative control.

After the synthesis of the cDNA, real time PCR analysis was carried in the Mastercycler real time PCR equipment (Eppendorf, USA) using the PerfeCta Sybr-Green FastMix (Quanta Biosciences, USA) to analyze the relative expression of the genes *CD73*, *CD90* and *CD105* in each sample, using *GAPDH* as housekeeping gene. The primers were previously designed using the Primer 3 Plus v0.4.0 (MWG Biotech, Germany) (Table 3.1).

Delta Delta Ct method, according to Livak and Schmittgen (2011) (43), was performed, using the results corresponding to cells at P0 as calibrator of data obtained from cell at P1, P2, P3 and P4.

2.4.2. Canine ASCs osteogenic potential assessment

Alizarin red staining

Cells cultured in osteogenic medium for 14, 21, 28 and 35 days, were fixed with 4% formalin (Sigma Aldrich, Germany) and washed with PBS and then with distilled water. Afterwards, the cells were stained with a 2% Alizarin Red solution (Merk, Germany) in distilled water with a pH of 4.1-4.3, for 10 min, and finally washed with distilled water. Stained cells were observed under an optical microscope (Axivert 40 CFL; Zeiss; Germany) and photographed using an Axio Cam MRm (Zeiss, Germany) camera.

Gene expression analysis of specific osteoblasts markers

Cells at different passages (P1-4) and further cultured for up 14, 21, 28 and 35 days in osteogenic medium were trypsinized and samples (of 1×10^6 cells) were kept in 800 µL of TRIzol. After extraction of the mRNA, the samples were quantified using the NanoDrop ND1000 Spectrophotometer. The cDNA synthesis was performed in the Mastercycler real time PCR equipment using the iScript cDNA Synthesis Kit. Real time PCR analysis was carried in the Mastercycler real time PCR equipment using the PerfeCta Sybr-Green FastMix to assess the relative expression of *collagen I alpha 1* (*COLIA1*), *runt-related transcription factor 2* (*RUNX2*) and *Osteocalcin* genes, using *GAPDH* as housekeeping gene (Table 3.1).

Delta Delta Ct method was performed, using the data corresponding to undifferentiated cells (cultured in basal medium) at the respective passage (P1-4) as calibrator of the results obtained for cells after 14, 21, 28 and 35 days in osteogenic medium (44).

Table 3. 1 – Primer sequences for targeted cDNAs.

Primer	**RefSeqID**	**Product length** (**bp**)	**5′-3′ sequence** (**F, forward; R, reverse**)
CD73	ENSCAFT00000004810	191	F: ATCCTGCCGCTTTAAGGAAT R: GTACAGCAGCCAGGTTCTCC
CD90	ENSCAFT00000019082	214	F: CGTGATCTATGGCACTGTGG R: GCCCTCACACTTGACCAGTT
CD105	ENSCAFT00000032002	161	F: AGGAGTCAACACCACGGAAC R: GATTGCAGAAGGACGGTGAT
COL1A1	ENSCAFT00000026953	170	F: ATGCCATCAAGGTTTTCTGC R: CTGGCCACCATACTCGAACT
Osteocalcin	ENSCAFT00000026668	166	F: GATCGTGGAAGAAGGCAAAG R: AGCCTCTGCCAGTTGTCTGT
RUNX2	ENSCAFT00000020482	148	F: CAGACCAGCAGCACTCCATA R: CAGCGTCAACACCATCATTC
GAPDH	NM_001003142.1	238	F: CCAGAACATCATCCCTGCTT R: GACCACCTGGTCCTCAGTGT

2.4.3. Canine ASCs chondrogenic potential assessment

After 21 days of culture in chondrogenic medium, cASCs pellets were fixed with 4% formalin, washed with PBS, embedded in paraffin and cut into sections of 3 μm; finally section were fixed on a slide and deparaffinised.

In order to observe cells and matrix formed, sections were stained with hematoxylin & eosin (H&E; Sigma, USA). Cartilage-like matrix deposition (mucopolysaccharides and glycosaminoglycans) was assessed by staining the samples sections with 1% Toluidine Blue (Sigma, USA), 0.1% Safranin O (Sigma, USA) and 1% Alcian Blue (Sigma, USA).

In all cases, the stained sections were subsequently rinsed with distilled water and dehydrated using 100% ethylene alcohol and allowed to dry overnight. Afterwards, the slides were observed under an optical microscope (Axivert 40 CFL; Zeiss; Germany), and photographed using an Axio Cam MRm (Zeiss, Germany) camera.

2.5. Statistical analysis

The results obtained from the real time RT PCR analysis were elaborated using the software JMP® v9.0.1 (SAS Institute Inc., USA) and the correlation between the dataset from the same gene analyzed was investigated with the ANOVA single factor method. Data was presented as mean ± standard error of the mean (SEM) and differences between data groups were considered to be statistically significant for $p<0.05$ (Student's t-test).

3. Results

Canine adipose tissue derived stem cells were successfully isolated from adipose tissue harvested from subcutaneous abdominal region, as well as from the omental fat depots. After isolation through enzymatic digestion, the obtained stromal vascular fraction adhered to the plastic culture flaks, and revealed a fibroblastic morphology in a monolayer growth (Fig. 3.1).

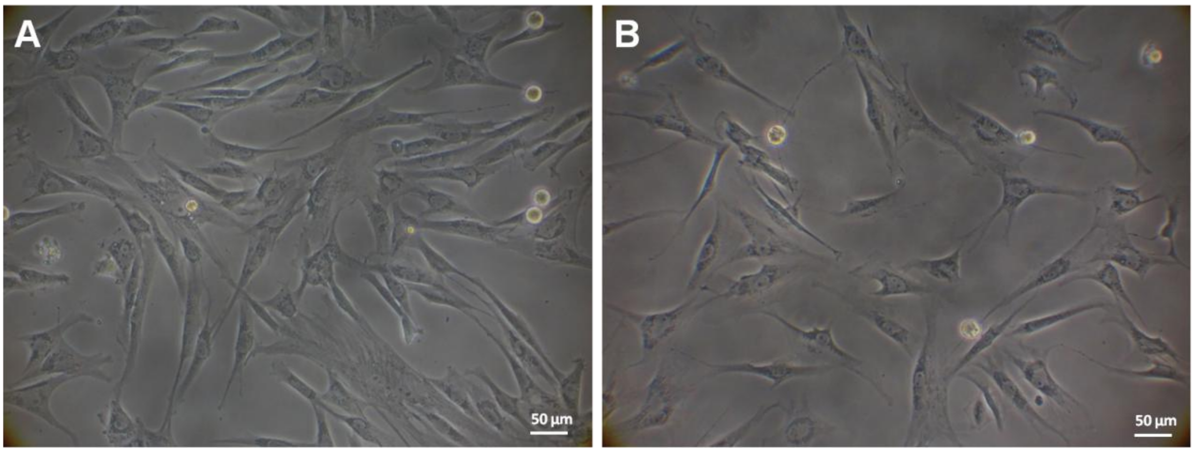

Figure 3. 1 – Representative light microscopy images of cASCs obtained by enzymatic digestion from different anatomical sites, namely subcutaneous (A) and omental (B), after 48h of culturing in basal medium.

The morphology of these cells does not seem to be affected by the number of passages, maintaining their characteristic spindle like shape and showing signals of cell viability and integrity along all studied passages.

3.1. Effect of the passage number in the undifferentiated canine ASCs

The isolated cells were subsequently cultured along four passages in basal medium without differentiation factors, and characterized through the expression of typical MSCs markers, namely CD73 (NT5E), CD90 (Thy1) and CD105 (Endoglin) (17), assessed by real time RT-PCR analysis. In general, the results revealed a decrease in the expression levels of these markers in the canine ASCs cultured in basal medium along passages, from P1 until P4 (Fig. 3.2).

The registered down-regulation of the above mentioned MSCs markers was found always statistically significant from P1 to P2 and from P2 to P3, being more evident in the *CD90* and *CD105* genes, independently of the anatomical origin. Changes on the expression fold were not observed between P3 and P4.

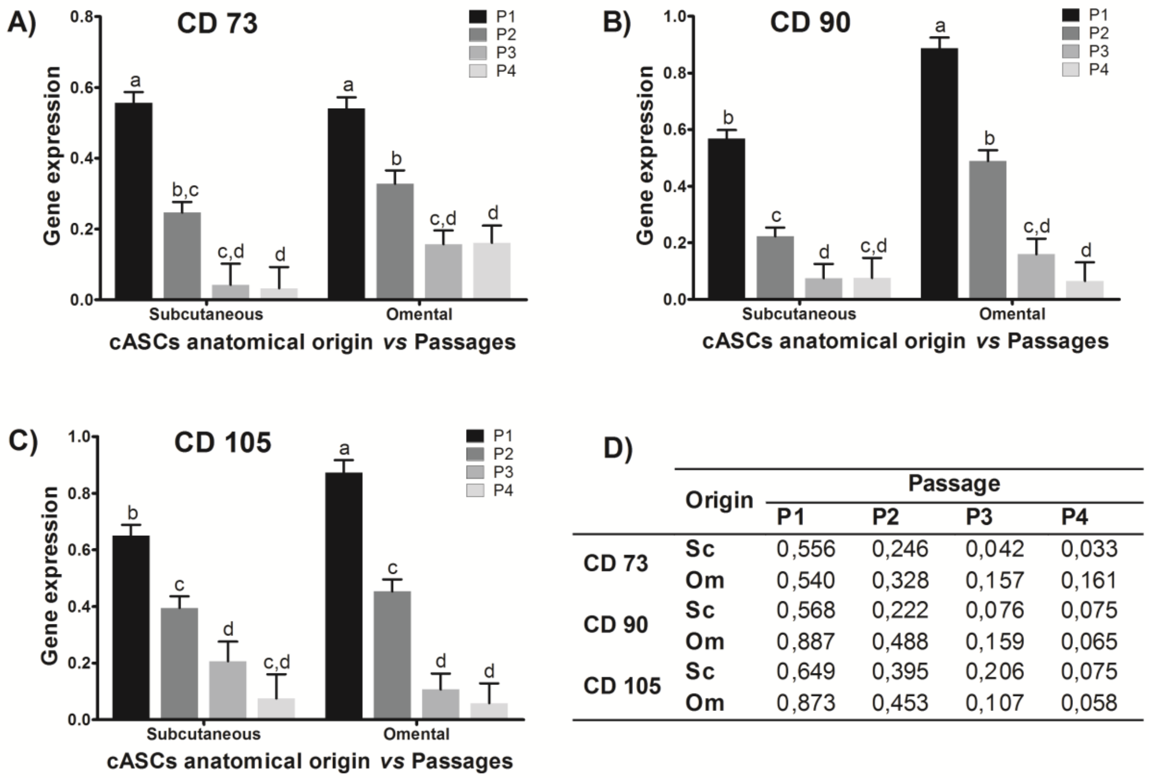

	Origin	Passage			
		P1	P2	P3	P4
CD 73	Sc	0,556	0,246	0,042	0,033
	Om	0,540	0,328	0,157	0,161
CD 90	Sc	0,568	0,222	0,076	0,075
	Om	0,887	0,488	0,159	0,065
CD 105	Sc	0,649	0,395	0,206	0,075
	Om	0,873	0,453	0,107	0,058

Figure 3. 2 – Real time RT-PCR analysis results of the various genes, namely A) CD73, B) CD90 and C) CD105 in canine ASCs isolated by enzymatic digestion and cultured in basal medium along four passages (mean ± SEM). Considering each marker independently, levels not connected by the same letter are significantly different ($p<0.05$, Student's t-test). Table shown in D) refers to the means. Abbreviations: P - passage; Sc - subcutaneous; Om - omental.

3.2. Effect of the anatomical site in the undifferentiated canine ASCs

Regarding the influence of the anatomical site of origin on the cASCs stemness, in general, it was found a higher expression of the three markers analyzed in the cASCs obtained from omental fat depots. No differences were observed in the *CD73* expression on cASCs from both anatomical origins. Significant differences were registered in the *CD90* and *CD105* expression at P1. As this work did not concern the evaluation of the proliferative capacity of the cASCs, no data regarding cell or colonies count were obtained; Nevertheless, no evident microscopic differences in terms of cellular proliferation were observed between subcutaneous and omental cASCs during expansion, and they usually reached the confluence at the same time, after seeding with the same cell density.

3.3. Osteogenic differentiation assessment

The osteogenic differentiation was induced by supplementing culture medium with well known osteogenic factors, such as ascorbic acid, β-glycerophosphate and dexamethasone (45). The osteogenic differentiation was firstly demonstrated as observed by Alizarin Red staining (Fig. 3.3) of the cells after 21 days of culture, which showed an increase of matrix mineralization along culturing time. Analysis of cells stained with H&E revealed no evident differences in terms of cellular morphology and matrix mineralization between cASCs obtained from subcutaneous or from omental adipose tissue.

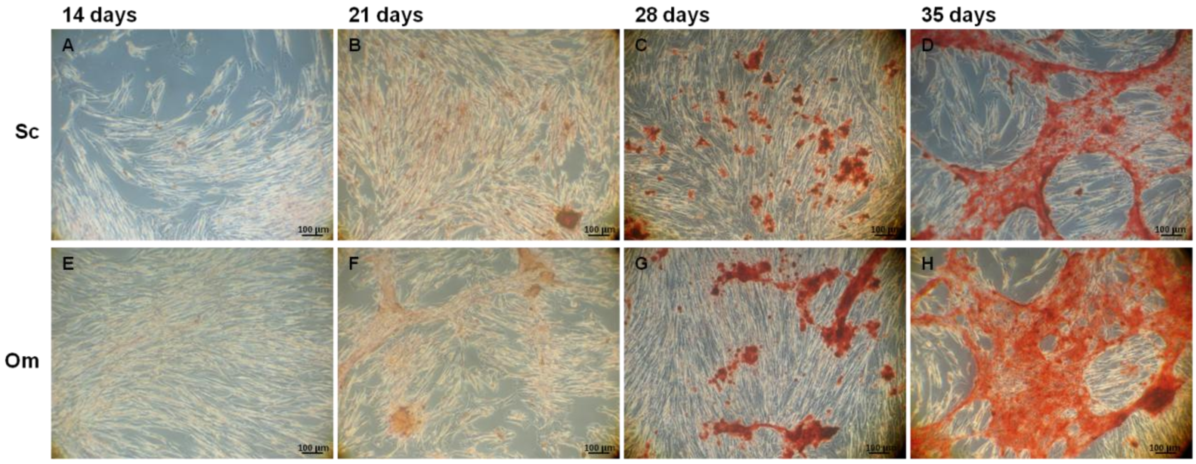

Figure 3. 3 – Light microscopy images of cASCs from subcutaneous (Sc, A-D) and omental (Om, E-H) origins and expanded up to passage 2, cultured for 14 (A, E), 21 (B, F), 28 (C, G) and 35 (D, H) days in osteogenic conditions, stained with Alizarin Red.

The osteogenic differentiation was further evaluated by real time RT-PCR analysis of the expression profile of three different osteogenic markers, namely *COLIA1*, *RUNX2* and *Osteocalcin* along culturing. In the Fig. 3.4, it is possible to observe the different expression profiles of the genes analyzed at different culturing time points. A down-regulation of *COLIA1* is evident along time and is significantly different between the first three culturing times in all conditions. Regarding the *RUNX2* gene, an early marker for osteoblastic differentiation, it was found a significant up-regulation from day 14 to 21 followed by a decrease in all conditions. *Osteocalcin*, a late marker, increased its expression along culturing time, but more evidently between day 21 and 28.

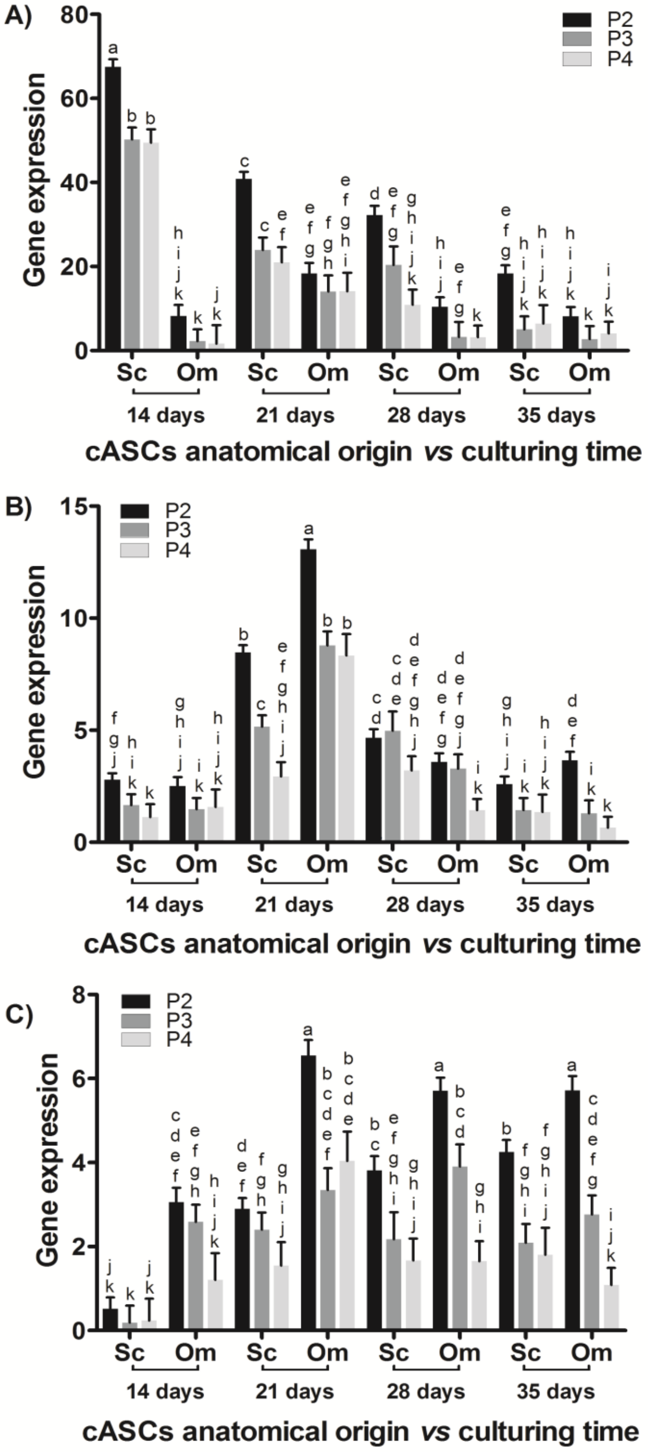

COL1A1

D)

Days	Origin	Passage P2	 P3	 P4
14	Sc	67,48	50,27	49,43
	Om	8,22	2,24	1,64
21	Sc	40,82	23,92	20,98
	Om	18,34	14,06	14,11
28	Sc	32,26	20,40	10,93
	Om	10,43	3,22	3,18
35	Sc	18,30	5,06	6,42
	Om	8,13	2,75	4,03

RUNX2

E)

Days	Origin	Passage P2	 P3	 P4
14	Sc	2,79	1,66	1,12
	Om	2,51	1,47	1,58
21	Sc	8,47	5,17	2,94
	Om	13,07	8,78	8,33
28	Sc	4,66	4,98	3,20
	Om	3,59	3,29	1,44
35	Sc	2,59	1,43	1,35
	Om	3,65	1,29	0,65

OSTEOCALCIN

F)

Days	Origin	Passage P2	 P3	 P4
14	Sc	0,52	0,19	0,24
	Om	3,06	2,59	1,20
21	Sc	2,90	2,41	1,55
	Om	6,55	3,35	4,04
28	Sc	3,81	2,18	1,67
	Om	5,71	3,91	1,65
35	Sc	4,25	2,09	1,81
	Om	5,72	2,77	1,09

Figure 3. 4 – Real time RT-PCR analysis results of the various osteoblastic genes: A) COLIA1, B) RUNX2 and C) Osteocalcin analyzed in canine ASCs, obtained from subcutaneous and omental origin and expanded up to four passages, cultured in osteogenic conditions during 14, 21, 28 and 35 days (mean ± SEM). Considering each marker independently, levels not connected by same letter are significantly different ($p<0.05$, Student's t-test). Tables shown in D), E) and F) mention the means. Abbreviations: P, passage; Sc, subcutaneous; Om, omental.

The number of passages has also shown to have a strong influence in the osteogenic differentiation potential of cASCs, since it was observed a higher expression of the studied markers in the cells from lower passages. Concerning *COLIA1*, the differences were significant in the cells from subcutaneous origin. In the case of the *RUNX2*, significant differences were identified in the cells from subcutaneous origin at day 14 and 21 and in cells from omental origin at the 21th day. Moreover, the passaging effect was observed in almost all conditions when evaluated the *Osteocalcin* gene, particularly, when comparing the P2 and P4.

Taking in account the anatomical origin of the cells, it was observed a higher expression of *COLIA1* in those from subcutaneous depots, drastically different in the first culturing time, and also in other some punctual conditions. In the *RUNX2* profile, it was not observed significant differences, except in the 21th day of culture. *Osteocalcin* gene was up-regulated in the omental cASCs, mostly in the 14th and 21th culturing times.

Comparing the effect of anatomical origin of cASCs in the osteogenic potential, it was observed a different expression profile of the osteogenic markers analyzed for ASCs of omental and subcutaneous origin. Specifically, early markers (*COLIA1* and *RUNX2*) expression was higher in subcutaneous ASCs, except at 21 days of culture, while the late marker analyzed (*Osteocalcin*) exhibit a higher expression level in omental ASCs, but this result was only statistically significant for the cells in passage 2.

3.4. Chondrogenic differentiation assessment

The chondrogenic differentiation of cASCs was induced by culturing cell pellets with medium supplemented with well established chondrogenic factors, namely, TGF-β1, insulin-transferrin-selenium, ascorbic acid, dexamethasone, L-proline and sodium pyruvate (46). The Fig. 3.5 shows the positive staining of cartilage matrix components, demonstrating the ability of cASCs to differentiate into the chondrogenic lineage. No visible differences were observed comparing samples from the various passages and from different anatomical origins, all of them revealing round cell morphology, low cell density and extensive cartilaginous matrix deposition.

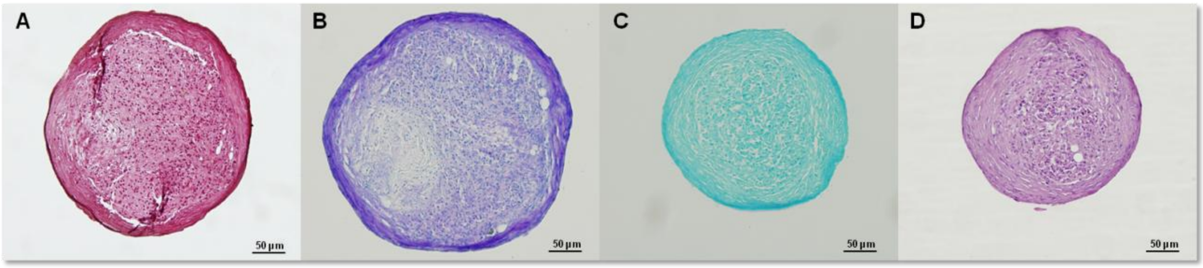

Figure 3. 5 – Representative light microscopy images of subcutaneous cASCs cultured for 21 days in chondrogenic conditions stained with Toluidine Blue (A), Safranin O (B), Alcian Blue (C) and H&E (D).

4. Discussion

Adipose tissue is a promising source for adult mesenchymal stem cells due to its abundance and easiness of harvesting. Adipose-derived stem cells from canine origin (cASCs) have been poorly studied as patented in the relatively low number of scientific publications (24, 35, 37, 40, 47). In this work, we characterized the stemness of these cells obtained from different anatomical sites, assessing the expression of three typical markers of MSCs (17) along successive passages, from passage 0 (P0) to passage 4 (P4). Additionally, we evaluated the cASCs potential to differentiate into two distinct cellular lineages, namely the osteogenic and chondrogenic. The osteogenic potential was further analysed, considering the influence of passaging, assessing mineralization by alizarin red staining and also by real time RT-PCR analysis of typical osteogenic markers expression.

While in humans it was found a significant variability on the ASCs behaviour when obtained from donors of different ages (48), there is no such data on canine ASCs. In this study, we have obtained cASCs from donors of different ages, but as we had only one donor of each age, it was not possible to obtain conclusive data on this issue.

The cASCs obtained by enzymatic digestion of both omental and subcutaneous tissue revealed the fibroblast-like shape typical of MSCs (17). This morphology is characteristic of the ASCs obtained from human, rodents, rabbit, sheep, horse and dogs (20, 30, 32, 33, 35, 49) from distinct anatomical origins, as subcutaneous abdominal and inguinal regions, omentum, arms and legs, breast, buttocks and footpad (35, 48, 50, 51).

Cell-based therapies often require *in vitro* expansion of cells collected from small tissues samples, in order to obtain clinically relevant cell numbers, i.e, to enable a specific therapeutic effect in a given application. The obtained results regarding the cASCs stemness, a parameter directly related to the cellular proliferative potential, have shown us that along passages there is a decrease of MSCs markers expression, particularly evident in the cells from subcutaneous origin. The decreasing expression of one or several MSCs markers along passages herein assessed for ASCs, and previously reported for human (34), equines (subcutaneous tissue from tail's region) (33), rabbit and sheep (32), may compromise their proliferation and/or differentiation potential and thus limit their *in vitro* expansion. However, this potential limitation can probably be overcome by the large amount of adipose tissue samples and high cell yields which can be safely harvested and isolated, as compared to other stem cell sources.

Previous studies on cASCs, reported the positive expression of CD90 and negative expression of CD73 and CD105 (37), assessed by flow cytometry (FC), which are in disagreement with our data. These differences might be due to the method of collection, (liposuction instead of surgical collection) or due to the use of unspecific antibodies for flow cytometry. Oh *et al*. (2011) reported a positive expression (determined by FC) only of CD90 (40) for cASCs, however, this data is difficult to compare because in the referred studies, human-specific antibodies, and not dog-specific antibodies, were used to assess CD73 and CD105 expression.

Apart from the MSCs markers, it is has been demonstrated that cASCs express pluritotency genes, such as *OCT4*, *NANOG* and *SOX2*, typical of the embryonic stem cells (26, 35), as it has been also reported for rhesus monkey and human ASCs (34). Lim *et al*. (2010) added that *CD90* is expressed until the 7th passage of cASCs and that at the same moment, the embryonic markers found previously, are not present anymore (26).

Additionally to the markers above mentioned, many others were identified in ASCs of other species. In human ASCs, was already observed the positive expression of HLA-ABC, CD9, CD10, CD13, CD29, CD34, CD44, CD49d, CD49e, CD54, CD51, CD55, CD71, CD166, SH3, STRO1, OCT4, UTF1 and Snail2, and the negative expression of HLA-DR (1, 20). The decrease of MSCs and embryonic markers expression, like *OCT4* and *SOX9*, along passaging has also been reported for human ASCs (34). Baglioni *et al*. (2009) concluded that, as observed in this work for cASCs, in the early passages of hASCs the expression levels of MSCs markers are higher, adding that there was no evident difference between the visceral and subcutaneous ASCs due to the heterogeneity of the cellular populations (52). In human and monkey, a strong positive expression of CD90 and a positive expression of CD105, among other markers, was identified by FC remaining stable trough passage 20-30 (34). In equines, it was proved, by flow cytometry, the negative expression of CD13 and the positive expression of CD44 and CD90 with variations along the first three passages (33). Also in horses, was referred the expression of the same MSCs markers that we have studied, but variations in the proliferative pattern were observed until P4, being the propagation cessed after P8 (53). Rabbit and sheep ASCs have been reported to have higher proliferative capacity as compared to humans (32), however, these studies did not address the gene expression of the MSCs markers.

In this study it was shown that the cASCs from both anatomical sites analysed, subcutaneous and omental, expressed the typical MSCs markers. The adipose tissue can be collected from subcutaneous (superficial and deep) and visceral depots and from many internal organs (44). Other authors have already evaluated the proliferative potential of cASCs obtained from different anatomical sites (35, 38, 54, 55) in dogs. Neupane *et al*. (2008) observed that subcutaneous cASCs reveal higher proliferation capacity comparing to omental (35). Wu and colleagues (2000) have registered differences in the adipogenic potential, which was found lower in the cells from omental and perineum as compared to the cells from inguinal origin (38). In humans it has been also reported that subcutaneous adipose tissue has a higher proliferation rate (1, 31). Furthermore, Dragoo *et al*. (2003) stated the number of cells harvested from human patellar adipose tissue was higher comparing to fat pad (55). Oedayrajsingh-Varma *et al*. (2006) concluded that human subcutaneous adipose tissue from the abdomen had a higher yield of stromal vascular cells in comparison to mammary fat, but all type of cells demonstrated similar viability. In the same study, was observed that three different collection techniques (surgical resection, tumescent and ultrasound-assisted liposuction) did not affect the number and viability of the hASCs, however, when used the ultrasounds the proliferation was negatively affected (54).

In the present work, all the samples were collected by surgical resection, avoiding contaminating the tissue with blood and vessels, where also exist cells which express MSCs markers. The higher *CD105* (endoglin) expression in the omental tissue, where more vessels were observed during the surgeries, can be due to the fact that endoglin has an important role in the vascular remodelling (56).

Recently, a work on ASCs from canine, equine as porcine origin proved that, apart from the passaging and anatomical site effect, the cellular kinetics can be influenced by the way the cells are cultured. They demonstrated that the cASCs, when cultured with 10% FBS supplementation start to proliferate more quickly in comparison to those cultured with serum free medium supplemented with 2% UltroserG; however in both cultures the same number of cells was obtained at the end of the 14th culturing day (57). These findings evidence that the culturing protocols should be taken into account when we compare data between different studies, even when referring to the same cells source.

As mentioned before, canine adipose-derived stem cells have demonstrated ability to differentiate into many lineages, namely osteogenic, chondrogenic, adipogenic (35, 37, 40, 47), myogenic (37, 40) and neurogenic (24, 40). In the present work, we evaluated the osteogenic potential of these cells, isolated from fat tissue harvested from distinct anatomical sites, and observed that cASCs cultured under osteogenic stimuli, expressed the three osteoblastic markers analysed, namely *COLIA1*, *RUNX2* and *Osteocalcin*. The later one, which is a late marker of osteogenesis, increased its expression along culturing time, but more evidently between day 21 and 28, as observed in human ASCs by PCR analysis, that showed a higher expression at the 28th day (23), and similarly to a report in mice where the *Osteocalcin* expression was higher at the 25th day, and earlier (15th day) on the cells cultured with retinoic acid supplementation (29). In another study on human ASCs, the secretion of *Osteocalcin* were registered by ELISA at the 18th culturing day (58). Thus, in terms of their osteogenic differentiation potential, canine, rodent and human ASCs can be considered similar.

Canine ASCs from both anatomical origins expressed the three studied osteogenic markers as previously reported by Neupane *et al*. (2009) and by Vieira *et al*. (2010), and exhibit the typical expression profile along the osteogenic process described in the literature. Alonso *et al*. (2008) observed that *Osteocalcin* started to be expressed after 2nd week of osteogenic induction as found in the present study (59).

The passaging effect, herein demonstrated by the decrease of expression levels of the typical MSCs markers, was also evident on the osteogenic differentiation; however, cells from later passages maintain the expression of the osteoblastic markers, leading us to conclude that the negative effect on the stemness is not directly followed by a negative effect on the osteogenic potential, and thus it does not seem to compromise the use of canine subcutaneous or omental adipose tissue in potential applications envisioning bone regeneration, as observed in previous studies in humans or in mice (23, 29, 58).

Izadpanah and colleagues (2006) observed that in primates, including humans, the percentage of colonies that underwent osteogenic differentiation, decrease along time, comparing the lower passages (50-65%) and the higher passages (20-25% at P20) (34), contrary to the findings reported by Alonso and colleagues (2008), who conclude that human ASCs reveal similar osteoblastic potential between P1 and P4 (59).

Human ASC have already been isolated from different fat depots, being reported that subcutaneous adipose tissue has a higher proliferation rate while visceral fat has a higher osteogenic differentiation capacity (1, 31). Aksu and colleagues (2008) revealed that the

ASCs from superficial subcutaneous layers had higher osteogenic potential, namely in males, comparing to deeper subcutaneous depots, adding that the ASCs from male donors had better proliferative behaviour (48). In addition, Marcassus *et al*. (2006) observed that the density of osteogenic clusters was significantly lower in cultures from epidydimal fat pads as compared to inguinal depot (60).

Other osteoblastic genes, such as *Bone sialoprotein* (*BSP*) (35, 37), *Osterix* (37) and *Osteoprogesterin* (47), were previously assessed in canine ASCs cultured in osteogenic medium. In humans, the *Collagen type II*, *Osteopontin*, *Osteonectin* (61), *Parathyroid hormone receptor*, *Bone morphogenic proteins* (*BMP*) *2* and *4* and *BMP receptors types IA, IB and II* have been reported as markers of ASCs previously exposed to culture medium supplemented with ascorbic acid, β-glycerophosphate and dexamethasone (58). In murine ASCs, cultured both in 2D and 3D conditions, *Osteopontin*, *RUNX2*, and *Osteocalcin* were also expressed (29). As observed in studies on ASCs from other animal species, including dog, these cells have the capacity to maintain the chondrogenic potential along passages, even until P10 (32). Recently, a study on cASC registered the positive expression of *SOX9* and *collagen type II*, after culturing with chondrogenic media. Nevertheless, the expression levels were lower comparing to those registered for MSCs from canine bone marrow (62). In humans, the *collagen type II* expression was also found higher in BMSCs than in ASCs, when cultured with chondrogenic medium supplemented with TGF-β3 up to 21 days (50).

In summary, these results obtained in the present work clearly demonstrate the capacity of the canine adipose-derived stem cells to differentiate into the osteogenic and chondrogenic lineage, making them promising candidates for bone and cartilage regeneration approaches and disease management based on veterinary regenerative medicine approaches.

In the authors' knowledge, this study brought about the first data on the stemness and osteogenic potential of cASCs upon subsequent culturing periods. The results obtained revealed that cASCs exhibit a progressively decreased expression of the typical stem cells markers along passages and also a decreased osteogenic differentiation potential. Moreover, the anatomical origin of the adipose tissue has an evident effect in the differentiation potential of the ASCs. In the literature, many other factors, such as, age, sex, isolation and conservation methods are proved to have effect in the biologic behaviour these cells in humans (21, 48) but the effect of such factors in canine ASCs behaviour remains unclear.

As observed in other animal species, the cASCs show resemblances to human ASCs profile, regarding stemness and osteogenic potential along culturing time and passages, which allow us to conclude that canine adipose tissue is a source of cells which could be used in Tissue Engineering research envisioning human application.

5. Acknowledgments

Authors acknowledge the support from the Portuguese Foundation for Science and Technology (FCT) project (ref. MIT/ECE/0047/2009) and for João Filipe Requicha PhD scholarship (SFRH/BD/44143/2008).

6. References

1. Rada T, Reis RL, Gomes ME. Adipose tissue-derived stem cells and their application in bone and cartilage tissue engineering. Tissue Engineering Part B-Reviews. 2009;15 (2):113-25.

2. Horwitz EM, Le Blanc K, Dominici M, Mueller I, Slaper-Cortenbach I, Marini FC, *et al*. Clarification of the nomenclature for MSC: The international society for cellular therapy position statement. Cytotherapy. 2005;7 (5):393-5.

3. Friedens AJ, Petrakov KV, Kuroleso AI, Frolova GP. Heterotopic Transplants of Bone Marrow - Analysis of Precursor Cells for Osteogenic and Hematopoietic Tissues. Transplantation. 1968;6 (2):230-&.

4. Zuk PA, Zhu M, Mizuno H, Huang J, Futrell JW, Katz AJ, *et al*. Multilineage cells from human adipose tissue: Implications for cell-based therapies. Tissue Engineering. 2001;7 (2):211-28.

5. Kern S, Eichler H, Stoeve J, Kluter H, Bieback K. Comparative analysis of mesenchymal stem cells from bone marrow, umbilical cord blood, or adipose tissue. Stem Cells. 2006;24 (5):1294-301.

6. Jankowski RJ, Deasy BM, Huard J. Muscle-derived stem cells. Gene Therapy. 2002;9 (10):642-7.

7. Gage FH, Ray J, Fisher LJ. Isolation, Characterization, and Use of Stem-Cells from the Cns. Annual Review of Neuroscience. 1995;18:159-92.

8. Noth U, Osyczka AM, Tuli R, Hickok NJ, Danielson KG, Tuan RS. Multilineage mesenchymal differentiation potential of human trabecular bone-derived cells. Journal of Orthopaedic Research. 2002;20 (5):1060-9.

9. Nakahara H, Goldberg VM, Caplan AI. Culture-Expanded Human Periosteal-Derived Cells Exhibit Osteochondral Potential Invivo. Journal of Orthopaedic Research. 1991;9 (4):465-76.

10. Seo BM, Miura M, Gronthos S, Bartold PM, Batouli S, Brahim J, *et al*. Investigation of multipotent postnatal stem cells from human periodontal ligament. Lancet. 2004;364 (9429):149-55.

11. Gronthos S, Mankani M, Brahim J, Robey PG, Shi S. Postnatal human dental pulp stem cells (DPSCs) in vitro and in vivo. Proceedings of the National Academy of Sciences of the United States of America. 2000;97 (25):13625-30.

12. Miura M, Gronthos S, Zhao M, Lu B, Fisher LW, Robey PG, *et al*. SHED - Stem cells from human exfoliated deciduous teeth. Journal of Dental Research. 2003;82:B305-B.

13. Morsczeck C, Gotz W, Schierholz J, Zellhofer F, Kuhn U, Mohl C, *et al*. Isolation of precursor cells (PCs) from human dental follicle of wisdom teeth. Matrix Biology. 2005;24 (2):155-65.

14. Lechner A, Habener JF. Stem/progenitor cells derived from adult tissues: potential for the treatment of diabetes mellitus. American Journal of Physiology-Endocrinology and Metabolism. 2003;284 (2):E259-E66.

15. Mitchell JB, McIntosh K, Zvonic S, Garretta S, Floyd ZE, Kloster A, *et al*. Immunophenotype of human adipose-derived cells: Temporal changes in stromal-associated and stem cell-associated markers. Stem Cells. 2006;24 (2):376-85.

16. Tapp H, Hanley EN, Patt JC, Gruber HE. Adipose-Derived Stem Cells: Characterization and Current Application in Orthopaedic Tissue Repair. Experimental Biology and Medicine. 2009;234 (1):1-9.

17. Dominici M, Le Blanc K, Mueller I, Slaper-Cortenbach I, Marini FC, Krause DS, *et al*. Minimal criteria for defining multipotent mesenchymal stromal cells. The International Society for Cellular Therapy position statement. Cytotherapy. 2006;8 (4):315-7.

18. Fraser JA, Huang CL. Quantitative techniques for steady-state calculation and dynamic integrated modelling of membrane potential and intracellular ion concentrations. Prog Biophys Mol Biol. 2007;94 (3):336-72.

19. Gabbay JS, Heller JB, Mitchell SA, Zuk PA, Spoon DB, Wasson KL, *et al*. Osteogenic potentiation of human adipose-derived stem cells in a 3-dimensional matrix. Annals of Plastic Surgery. 2006;57 (1):89-93.

20. Gimble JM, Guilak F. Adipose-derived adult stem cells: isolation, characterization, and differentiation potential. Cytotherapy. 2003;5 (5):362-9.

21. Aust L, Devlin B, Foster SJ, Halvorsen YDC, Hicok K, du Laney T, *et al*. Yield of human adipose-derived adult stem cells from liposuction aspirates. Cytotherapy. 2004;6 (1):7-14.

22. Mizuno H, Zuk PA, Zhu M, Lorenz HP, Benhaim P, Hedrick MH. Myogenic differentiation by human processed lipoaspirate cells. Plastic and Reconstructive Surgery. 2002;109 (1):199-209.

23. Zuk PA, Zhu M, Ashjian P, De Ugarte DA, Huang JI, Mizuno H, *et al*. Human adipose tissue is a source of multipotent stem cells. Molecular Biology of the Cell. 2002;13 (12):4279-95.

24. Sago K, Tamahara S, Tomihari M, Matsuki N, Asahara Y, Takei A, *et al*. In vitro differentiation of canine celiac adipose tissue-derived stromal cells into neuronal cells. Journal of Veterinary Medical Science. 2008;70 (4):353-7.

25. Kang SK, Putnam LA, Ylostalo J, Popescu IR, Dufour J, Belousov A, *et al*. Neurogenesis of Rhesus adipose stromal cells. Journal of Cell Science. 2004;117 (18):4289-99.

26. Lim JH, Boozer L, Mariani CL, Piedrahita JA, Olby NJ. Generation and characterization of neurospheres from canine adipose tissue-derived stromal cells. Cell Reprogram. 2010;12 (4):417-25.

27. Richardson LE, Dudhia J, Clegg PD, Smith R. Stem cells in veterinary medicine - attempts at regenerating equine tendon after injury. Trends in Biotechnology. 2007;25 (9):409-16.

28. Lu ZF, Doulabi BZ, Wuisman PI, Bank RA, Helder MN. Differentiation of adipose stem cells by nucleus pulposus cells: Configuration effect. Biochemical and Biophysical Research Communications. 2007;359 (4):991-6.

29. Wan DC, Siedhoff MT, Kwan MD, Nacamuli RP, Wu BM, Longaker MT. Refining retinoic acid stimulation for osteogenic differentiation of murine adipose-derived adult stromal cells. Tissue Eng. 2007;13 (7):1623-31.

30. Tobita M, Uysal AC, Ogawa R, Hyakusoku H, Mizuno H. Periodontal tissue regeneration with adipose-derived stem cells. Tissue Engineering Part A. 2008;14 (6):945-53.

31. Peptan IA, Hong L, Mao JJ. Comparison of osteogenic potentials of visceral and subcutaneous adipose-derived cells of rabbits. Plastic and Reconstructive Surgery. 2006;117 (5):1462-70.

32. Martinez-Lorenzo MJ, Royo-Canas M, Alegre-Aguaron E, Desportes P, Castiella T, Garcia-Alvarez F, *et al*. Phenotype and chondrogenic differentiation of mesenchymal cells from adipose tissue of different species. J Orthop Res. 2009;27 (11):1499-507.

33. Carvalho AD, Alves ALG, Golim MA, Moroz A, Hussni CA, de Oliveira PGG, *et al*. Isolation and immunophenotypic characterization of mesenchymal stem cells derived from equine species adipose tissue. Veterinary Immunology and Immunopathology. 2009;132 (2-4):303-6.

34. Izadpanah R, Trygg C, Patel B, Kriedt C, Dufour J, Gimble JM, *et al*. Biologic properties of mesenchymal stem cells derived from bone marrow and adipose tissue. Journal of Cellular Biochemistry. 2006;99 (5):1285-97.

35. Neupane M, Chang C-C, Kiupel M, Yuzbasiyan-Gurkan V. Isolation and characterization of canine adipose-derived mesenchymal stem cells. Tissue Engineering Part A. 2008;14 (6):1007-15.

36. Tobita M, Mizuno H, Uysal CA, Xin G, Hyakusoku H. Behavior of adipose-derived stem cells in canine periodontal tissue regeneration. Stem Cells. 2007;25 (12):3288-.

37. Vieira N, Brandalise V, Zucconi E, Secco M, Strauss B, Zatz M. Isolation, characterization and differentiation potential of canine adipose-derived stem cells. Cell Transplant. 2010;19 (3):279-89.

38. Wu PX, Sato K, Yukawa S, Hikasa Y, Kagota K. Differentiation of stromal-vascular cells isolated from canine adipose tissues in primary culture. Journal of Veterinary Medical Science. 2001;63 (1):17-23.

39. Black LL, Gaynor J, Gahring D, Adams C, Aron D, Harman S, *et al*. Effect of adipose-derived mesenchymal stem and regenerative cells on lameness in dogs with chronic osteoarthritis of the coxofemoral joints: A randomized, double-blinded, multicenter, controlled trial. Veterinary Therapeutics. 2007;8 (4):272-84.

40. Oh HJ, Park JE, Kim MJ, Hong SG, Ra JC, Jo JY, *et al*. Recloned dogs derived from adipose stem cells of a transgenic cloned beagle. Theriogenology. 2011;75 (7):1221-31.

41. Cui L, Liu B, Liu G, Zhang W, Cen L, Sun J, *et al*. Repair of cranial bone defects with adipose derived stem cells and coral scaffold in a canine model. Biomaterials. 2007;28 (36):5477-86.

42. Albuquerque C, Morinha F, Requicha J, Martins T, Dias I, Guedes-Pinto H, *et al*. Canine periodontitis the dog as an important model for periodontal studies. Vet J. 2012;191 (3):299-305.

43. Livak KJ, Schmittgen TD. Analysis of relative gene expression data using real-time quantitative PCR and the 2 (T) (-Delta Delta C) method. Methods. 2001;25 (4):402-8.

44. Avram AS, Avram MM, James WD. Subcutaneous fat in normal and diseased states: 2. Anatomy and physiology of white and brown adipose tissue. J Am Acad Dermatol. 2005;53 (4):671-83.

45. Jaiswal N, Haynesworth SE, Caplan AI, Bruder SP. Osteogenic differentiation of purified, culture-expanded human mesenchymal stem cells in vitro. J Cell Biochem. 1997;64 (2):295-312.

46. Goncalves A, Costa P, Rodrigues MT, Dias IR, Reis RL, Gomes ME. Effect of flow perfusion conditions in the chondrogenic differentiation of bone marrow stromal cells cultured onto starch based biodegradable scaffolds. Acta Biomaterialia. 2011;7 (4):1644-52.

47. Spencer ND, Chun R, Vidal MA, Gimble JM, Lopez MJ. In vitro expansion and differentiation of fresh and revitalized adult canine bone marrow-derived and adipose tissue-derived stromal cells. Vet J. 2011.

48. Aksu AE, Rubin JP, Dudas JR, Marra KG. Role of gender and anatomical region on induction of osteogenic differentiation of human adipose-derived stem cells. Ann Plast Surg. 2008;60 (3):306-22.

49. Vidal MA, Kilroy GE, Lopez MJ, Johnson JR, Moore RM, Gimble JM. Characterization of equine adipose tissue-derived stromal cells: adipogenic and osteogenic capacity and comparison with bone marrow-derived mesenchymal stromal cells. Vet Surg. 2007;36 (7):613-22.

50. Afizah H, Yang Z, Hui JHP, Ouyang HW, Lee EH. A comparison between the chondrogenic potential of human bone marrow stem cells (BMSCs) and adipose-derived stem cells (ADSCs) taken from the same donors. Tissue Engineering. 2007;13 (4):659-66.

51. Sachs PC, Francis MP, Zhao M, Brumelle J, Rao RR, Elmore LW, *et al*. Defining essential stem cell characteristics in adipose-derived stromal cells extracted from distinct anatomical sites. Cell Tissue Res. 2012.

52. Baglioni S, Francalanci M, Squecco R, Lombardi A, Cantini G, Angeli R, *et al*. Characterization of human adult stem-cell populations isolated from visceral and subcutaneous adipose tissue. Faseb Journal. 2009;23 (10):3494-505.

53. Braun J, Hack A, Weis-Klemm M, Conrad S, Treml S, Kohler K, *et al*. Evaluation of the osteogenic and chondrogenic differentiation capacities of equine adipose tissue-derived mesenchymal stem cells. Am J Vet Res. 2010;71 (10):1228-36.

54. Oedayrajsingh-Varma MJ, van Ham SM, Knippenberg M, Helder MN, Klein-Nulend J, Schouten TE, *et al*. Adipose tissue-derived mesenchymal stem cell yield and growth characteristics are affected by the tissue-harvesting procedure. Cytotherapy. 2006;8 (2):166-77.

55. Dragoo JL, Samimi B, Zhu M, Hame SL, Thomas BJ, Lieberman JR, *et al*. Tissue-engineered cartilage and bone using stem cells from human infrapatellar fat pads. Journal of Bone and Joint Surgery-British Volume. 2003;85B (5):740-7.

56. Sanz-Rodriguez F, Guerrero-Esteo M, Botella LM, Banville D, Vary CP, Bernabeu C. Endoglin regulates cytoskeletal organization through binding to ZRP-1, a member of the Lim family of proteins. J Biol Chem. 2004;279 (31):32858-68.

57. Schwarz C, Leicht U, Rothe C, Drosse I, Luibl V, Rocken M, *et al*. Effects of different media on proliferation and differentiation capacity of canine, equine and porcine adipose derived stem cells. Res Vet Sci. 2012;93 (1):457-62.

58. Halvorsen YD, Franklin D, Bond AL, Hitt DC, Auchter C, Boskey AL, *et al*. Extracellular matrix mineralization and osteoblast gene expression by human adipose tissue-derived stromal cells. Tissue Eng. 2001;7 (6):729-41.

59. Alonso M, Claros S, Becerra J, Andrades JA. The effect of type I collagen on osteochondrogenic differentiation in adipose-derived stromal cells in vivo. Cytotherapy. 2008;10 (6):597-610.

60. Prunet-Marcassus B, Cousin B, Caton D, Andre M, Penicaud L, Casteilla L. From heterogeneity to plasticity in adipose tissues: site-specific differences. Exp Cell Res. 2006;312 (6):727-36.

61. Gimble JM, Katz AJ, Bunnell BA. Adipose-derived stem cells for regenerative medicine. Circulation Research. 2007;100 (9):1249-60.

62. Reich CM, Raabe O, Wenisch S, Bridger PS, Kramer M, Arnhold S. Isolation, culture and chondrogenic differentiation of canine adipose tissue- and bone marrow-derived mesenchymal stem cells-a comparative study. Vet Res Commun. 2012.

Chapter IV

Evaluation of the response to the implantation of canine adipose-derived stem cells in a healthy mice subcutaneous model

Abstract

Canine adipose-derived stem cells (cASCs) have great interest for applications in Tissue Engineering and other cell-based therapies to be used in Veterinary Medicine or as a model for translation to human clinical therapies. As the behaviour of these cells when implanted in non-autologous recipients is not deeply characterized, the research in this field is mandatory in order to develop new animal models to assess therapies based on cASCs.

In this work, cASCs were injected subcutaneously in mice and these cells were detected in the xenogenic tissue by immunohistochemistry using vimentin, CD44 and keratin. The local response evaluated by routine histology did not reveal signals of significant inflammatory reaction around the local were cASCs were injected neither in the lymph nodes or other organs, namely lungs, liver, kidney, intestine, spleen, hearth and brain. Detection of cASCs was confirmed by histology and immunohistochemistry, through the positivity to vimentin and CD44 and a negative expression of keratin, demonstrating the presence of cASCs in mice tissue after transplantation.

This study showed that the implantation of cASCs in mice induced a scarce inflammatory response. This finding contributed to propose the mouse as an animal model to study the *in vivo* behaviour of the cASCs and to validate new tissue engineered approaches based on cASCs avoiding or reducing the use of dogs in research.

---

*This Chapter is based on the following publication:

Requicha JF, Carvalho PP, Pires MA, Dias I, Gomes ME, Reis RL, Viegas CA. Evaluation of the response to the implantation of canine adipose-derived stem cells in a healthy mice subcutaneous model. Submitted

1. Introduction

The use of mesenchymal stem cells (MSCs) has been proposed for a wide number of Regenerative Medicine strategies, mainly due to their ability to self-renew and potential to differentiate towards different cell lineages. These cells have been initially isolated from the bone marrow (1) but, since then, it has been reported its existence in many other adult tissues, including the adipose tissue (2, 3), placenta, amniotic fluid (4), umbilical cord blood (5) and periodontal ligament or other dental tissues (6, 7).

Adipose-derived stem cells (ASCs) have shown remarkable properties with great potential to be used in Tissue Engineering and other cell-based therapies (8, 9), regarding their ability to differentiate into several cellular lineages, easiness of harvesting with low morbidity and discomfort to the patient (8).

The canine adipose-derived stem cells (cASCs) have recently been reported in several studies in Regenerative Medicine with promising results. Concerning clinical studies, cASCs have been used in combination with scaffolds based on hydroxyapatite and chitosan (30:70 wt%) for the treatment of radius and ulna non-union fracture in dog (10), or in the treatment of dogs with lameness associated with osteoarthritis of the coxofemoral (11) and humeroradial (12, 13) joints. Although without effective clinical improvement, cASCs have also been tested in the treatment of canine atopic dermatitis (14).

At a preclinical stage, cASCs have been studied in canine models for the regeneration of intervertebral disc (15) or the inhibition of its degeneration (16), and for the regeneration of cranial bone defects by autologous (17) or allogenic (18) cASCs combined with coral scaffolds. Additionally, cASCs have also been assessed as cellular delivery system of interferon-β gene for cancer therapy using a mouse melanoma model (19).

Despite the increasing interest in this cell source, there is not enough information to enables to assess cASCs in smaller animal models. In order to reduce or avoid the use of the dog as an animal model to study new therapeutic approaches based on cASCs, it is mandatory to develop alternative animal models to gather information on the *in vivo* behaviour of the cASCs upon implantation and on the host response against the cASCs both when transplanted alone or as part of tissue-engineered constructs.

In this work, the cASCs were xenotransplanted in a mouse subcutaneous model without any specific induced disease. The implanted cells were immunodetected throughout the timeline of the experiment and the host response was evaluated. The obtained data contributed to the characterization of the mouse as model to assess cASCs before their study in canine preclinical models and their further translation to the veterinary clinical practice.

2. Materials and Methods

2.1. Surgical harvesting of the canine adipose tissue

Subcutaneous abdominal adipose tissue was harvested from three adult healthy dogs subjected to convenience surgery at the Veterinary Hospital of University of Trás-os-Montes e Alto Douro with previous informed consent of the owners.

2.2. Isolation and expansion of the canine ASCs

The adipose tissue samples were processed within 12 hours upon harvesting, and the canine adipose-derived stem cells (cASCs) were isolated by an enzymatic digestion method, as described previously (2).

The cASCs were expanded in basal medium composed of Dulbecco Modified Eagle Medium (DMEM) (Sigma Aldrich, Germany) supplemented with 10% fetal bovine serum (FBS; Invitrogen, USA) and 1% antibiotic/antimicotic (amphotericin B/streptomycin sulfate; Sigma, USA) up to passage 2 as reported before (2) in order to obtain the necessary number of cells to use in this study.

2.3. Preparation of the canine ASCs suspension

The cASCs were resuspended in phosphate buffer solution (PBS; Sigma Aldrich, Germany), obtaining a cellular suspension of 1×10^7 cells ml^{-1} to be subsequently injected in the mice.

From the same culture, a cellular suspension of 2×10^6 cASCs per ml was also obtained, washed with PBS and fixed in 4% phosphate-buffered formalin for further cytology and immunostaining assays.

2.4. Study animals

Thirty five immunocompetent 10 weeks old Hsd:CD1 (ICR), outbred and SPF male mice (Harlan Laboratories, Spain) were used in this protocol. The housing care and experimental protocol was performed according to the national guidelines, after approval by the National Ethical Committee for Laboratory Animals and conducted in accordance with Portuguese legislation (Portaria 1005/92) and international standards on animal welfare as defined by the European Directive 2010/63/EU.

The animals were housed in groups of five individuals, fed *ad libitum* with maintenance diet for mice (4RF21/C diet, Mucedola, Italy) and autoclaved water, and bedded in corn cob (Scobis Due, Mucedola, Italy) with suitable environment enrichment and with a day/night cycle of 14/10 hrs.

2.5. Subcutaneous injection of the canine ASCs

The animals were placed in dorsal recumbence for subcutaneous injection in the abdominal right flank with 100 µL of suspension containing 1 × 10^7 cells ml^{-1} by using a 1 mL syringe with a 26 G needle.

2.6. Euthanasia and explants collection

All animals were euthanized by an intravenous injection of sodium pentobarbital (Eutasil, CEVA, France). A group of five animals injected with PBS with no cells (time 0) were considered the negative control. Throughout the following 28 days, the remaining six experimental groups (n=5) were sacrificed at 12 hours, and 1, 3, 7, 21 and 28 days after injection.

The abdominal skin and adjacent muscle, around the site of injection, were collected with a safety margin of 1 cm, in order to assess the local response against the xenotransplanted cASCs.

The organs, namely, mesenteric and inguinal lymph nodes, liver, kidney, lung, heart, spleen, brain, and intestine were also collected, in order to evaluate the presence of cASCs at distance and also the host response against these cells. All samples were fixed in 4% phosphate-buffered formalin (Inopat, Portugal) during 24 hours.

2.7. Preparation of the canine ASCs’ cytoblocks

A cellular culture suspension of 2 × 10^6 cASCs ml^{-1} was fixed in 4% phosphate-buffered formalin and centrifuged in the Shandon CytoSpin 3 centrifuge (Thermo Scientific, USA) to a proper cassette.

2.8. Hematoxylin and eosin

Explants retrieved from mice and the cASCs' cytoblock were processed in an automatic tissue processor Shandon Hypercenter XP (ThermoFisher Scientific, USA) and embedded in paraffin. Paraffin blocks were cut at 3 µm to silane-coated slides and stained by routine with hematoxylin and eosin (H&E) and mounting with Entelan (Merck, Germany).

2.9. Immunohistochemistry

Mouse monoclonal anti-human antibodies to Vimentin, (clone V9, Leica Biosystems, UK) and to Keratin (clone AE1/AE3, Dako, USA), and rat monoclonal anti-human CD44 (clone 8E2F3, Santa Cruz Biotechnology, Germany) (Table 4.1) were used to perform indirect avidin-biotin immunohistochemistry (IHC) technique in order to characterize the injected cASCs in the host tissue.

Table 4. 1 – Characteristics of the antibodies used in this study.

	Vimentin	Keratin	CD44
Type	Monoclonal	Monoclonal	Monoclonal
Clone	V9	AE1/AE3	IM7
Dilution	1:100	1:400	1:100
Antigen recovery	Sodium citrate, 90 ºC, 20 min		
Incubation	Room temperature, 4 hours	Room temperature, 4 hours	4 ºC, overnight

Antigen retrieval was performed in a water bath at 96 ºC for 20 min, in citrate buffer (pH=6). The slides were washed with PBS and endogenous peroxidase was blocked with 3% hydrogen peroxide (Sigma, Germany) at room temperature for 30 min.

RTU Vectastain Universal Elite ABC Kit (Vector PK-7200, UK) in combination with the Mouse-on-Mouse (MOM) Basic Kit (Vector BMK-2202, UK) was used for antibody incubation, according to the instructions of the manufacturers, in order to reduce the background and cross reactivity.

The mouse-on-mouse kit aimed to block the endogenous mouse's immunoglobulins was essential to avoid the detection of the studied antibodies in the host tissue, ensuring that only the canine xenotransplanted cells were identified through histological stainings of the explants. Briefly, non-specific binding of primary antibodies was blocked using a horse serum for 5 min, and the mice's immunoglobulins blocked for 1 hour. Then, after an overnight incubation with the primary antibody, at 4 ºC in a humidified atmosphere, tissue sections were incubated with biotinylated antibody, followed by incubation with streptavidin-peroxidase.

After washing with PBS, antibody detection was revealed using the peroxidase substrate kit DAB (Vector SK-4100, UK). Slides were washed in water for 5 min and then counterstained with Gill’s hematoxylin (Sigma, Germany) for nuclear contrast.

The sections of the cASCs’ cytoblock were submitted to the same procedure and used as positive control of the immunohistochemistry analysis. Finally, the sections were observed under a light microscope (E600 Nikon Instruments, UK) and the images were obtained using the digital camera Nikon DXM200.

3. Results

The subcutaneous injections of cells promoted the formation of small papules immediately after the injection of the cellular suspension. A few minutes upon implantation, it was observed the regularization of the skin and no local signs of inflammation were detected after that. In each timepoint, all the animals revealed good body condition and also no clinical signs of inflammation were detected.

During the samples collection for histological processing, it was observed a certain degree of local skin swelling in first experimental group corresponding to 12 hours post-transplantation.

3.1. Histology of the explants

Histological analysis of the local of injection in the abdominal skin (Fig. 4.1A) revealed normal skin architecture in the negative control group, comprising the animals where no cells were transplanted. On other groups, at 12 hours, one and seven days after cells injection, cellular agglomerates on the dermis morphologically compatible with the injected cells were observed in 60%, 20% and 20% of the animals, respectively. In the later timepoints, these cells were no longer observed.

Around the clusters it was observed a mild inflammatory infiltrate, mainly at 12 hours, comprising mostly lymphocytes and macrophages that decreased along the experiment. At the 7th day of injection, a central necrosis with macrophages was observed inside the clusters.

Moreover, the histological observation of the organs did not reveal any inflammatory, degenerative or necrotic reaction which could be associated to the xenotransplanted cells. Local and regional lymph nodes presented normal morphology with brown pigment in some cases.

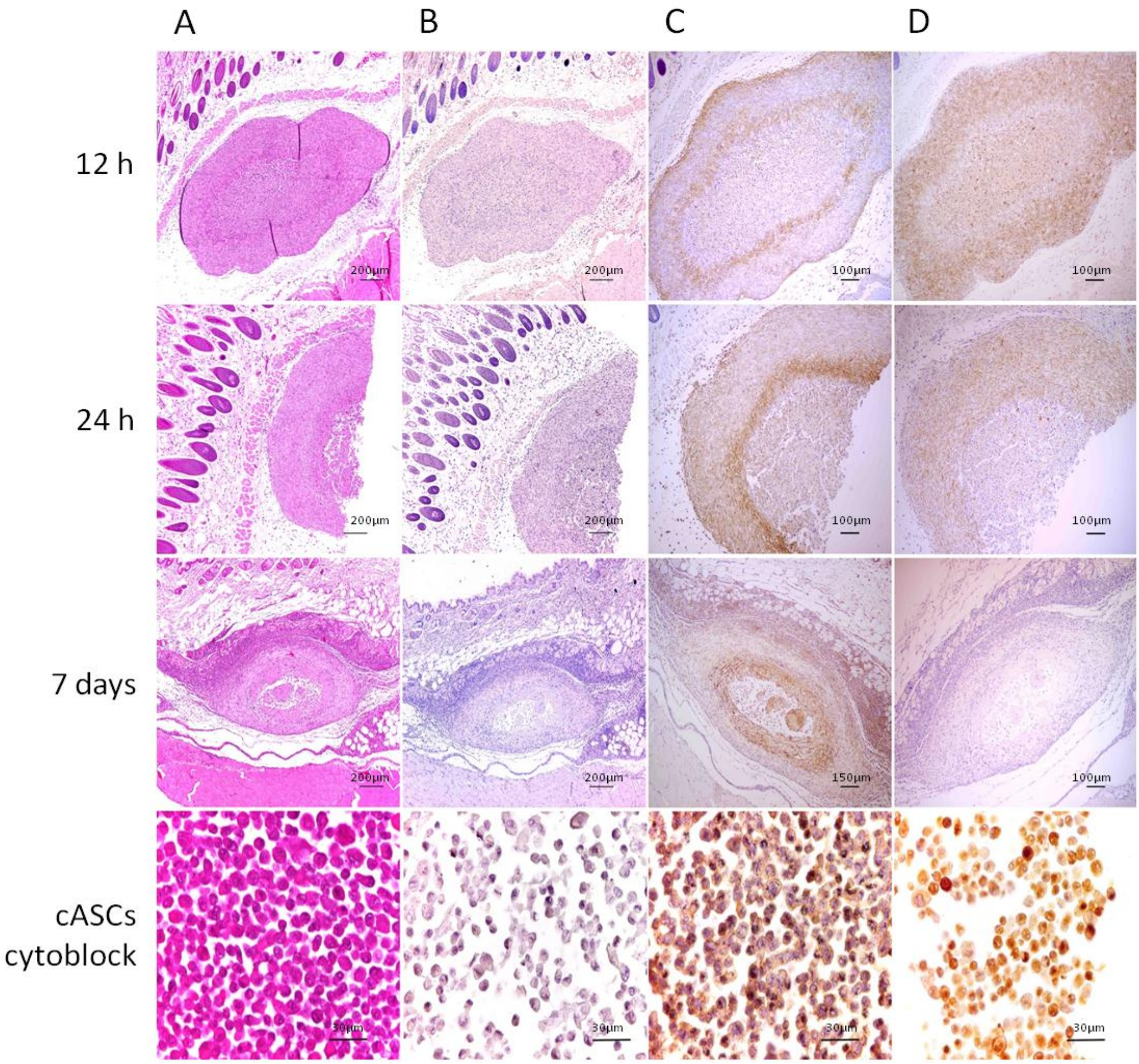

Figure 4. 1 – Histological images of the observed clusters on the dermis and the cASCs' cytoblock stained with H&E (A) and immunostained against keratin (B), vimentin (C) and CD44 (D) counterstained with Gill's hematoxilin.

3.2. Immunohistochemistry of the explants

The skin samples with the cellular agglomerates were submitted to IHC in order to identify the cASCs according to their phenotype. As shown in Fig. 4.1B-D, those cells were also positive to vimentin and CD44 and negative to keratins as in the cASCs' cytoblock used as control. The intensity of expression of the different markers used varied along the experimental period.

4. Discussion

The cASCs used in this study were isolated from subcutaneous tissue by a previously optimized methodology (2). These cells display properties of MSCs namely adherence to culture flasks, positivity to the three main characteristic MSCs markers, namely, CD105, CD73 and CD90, as well as the potential to differentiate into osteogenic and chondrogenic lineages (2), fulfilling the minimal criteria for been considered MSCs (20).

Although different cell tracking methodologies could have been implemented in this study, we were interested in assessing the implanted cells in its pure form, as they are envisioned to be used in future clinical applications and, therefore without any permeabilization steps or using any type of cell surface modification such as fluorochromes, or genetic modifications such as transfection. Taking this into consideration we decided to detect cASCs according to their phenotype, through the positive expression of vimentin and CD44, and the negative expression of keratins.

Vimentin and keratin, among others, are cytoskeleton intermediate filaments. For instance, MSCs are known to contain vimentin (21). Vimentin is involved in modulating cell-matrix interactions (22) and this filament it has already been detected in cASCs after inducing differentiation into the neuronal lineage (23), and in MSCs isolated from rodent skin was highly expressed (24).

The large spectrum keratin used in the present work is a combination of acidic and neutral-basic keratins, thus covering broad spectra of this protein and, in that sense, minimizing the probability of false negatives for keratins' expression on the injected cells. In human ASCs committed to the epithelial lineage, cytokeratin-18 has been detected, while vimentin reduced its positive expression (25).

The CD44 is a membrane glycoprotein and functions as the major hyaluronan receptor on most cell types (26), and is one of primary stable positive ASCs’ markers (27). The expression of this marker on cASCs has already been shown by Kang *et al*. (2008) who found immunomodulatory behaviour on co-cultured with allogenic leukocyte (28). Others studies on cASCs revealed the positive expression of CD44 by flow citometry and immunocytochemistry (23, 29, 30), however, in our knowledge, the detection of this marker in cASCs after transplantation in an *in vivo* model was not yet been reported.

Several mouse models of disease, such as muscular dystrophy (31), colitis (32), rheumatoid arthritis (33), acute kidney injury (34), autoimmune hearing loss (35) and systemic lupus erythematosus (36) have already been used in the study of the human ASCs behaviour and therapeutic application. In this work, the study animals were immunocompetent and healthy prior to the cells implantation and thus without any chemotactic stimulus which could attract the cells into a specific body location. The presence of the cASCs in the subcutaneous tissue could be related to the physical trauma induced during by the inoculation. The observed mild post-trauma inflammatory reaction could have mimetized a disease and, thus, promote the inflammatory response and the cluster formation of the implanted cells, similar to what happens in the disease models (37).

Apart from the subcutaneous injection, other ways of injection have been reported in different disease models or clinical studies, namely, the intraarticular injection (11, 12), the intravenous injection (14) or the direct injection into a spinal cord injury (29). Transplantation of cASCs have been described to be carried out by combining them with platelet rich plasma (13), hyaluronic acid (13) or PBS (11, 12) as performed in this study.

The immunomodulation of the ASCs has been examined in a variety of animal models (37). One of the first *in vivo* studies on systemic infusion of ex-vivo expanded allogenic ASCs dates of 2006, when Yanez and colleagues reported that these cells were able to control an induced graft-versus-host disease in mice (38). Human ASCs have been shown not to express the MHC-II and did not stimulate allogenic peripheral blood mononuclear cells when in co-culture (39). The immunomodulatory potential of the studied cASCs needs to be deeply assessed, paving the way for the application of cASCs in medicine regenerative approaches not only in the donor patient but also in allogenic patients.

The present work also gave a contribution to the study of cASCs behaviour in a non-autologous host. Envisioning the use of cASCs in allogenic therapies, it is important to assess their behaviour also in canine recipients in the future. Taking into consideration that long-term cryopreservation of cASCs did not affect their stem-like features (40), it is feasible to create a cell bank of cASCs ready to use in autologous or allogenic approaches.

The present study demonstrated for the first time, in our knowledge, the presence of cASCs in healthy mice tissue after transplantation. Moreover, the obtained data showed that only a mild inflammatory local reaction was observed contributing to the characterization of the cASCs when implanted in a xenogenic host. The scarce inflammatory response against the cASCs could also be useful to propose the mouse as animal model to study the *in vivo* behaviour of the cASCs and to validate new tissue engineered matrices combining cASCs avoiding or reducing the use of dogs in research.

5. Conclusion

In the present study, canine adipose-derived stem cells injected subcutaneously in healthy mouse model were detected in the host tissue through the positive expression of vimentin and CD44 markers and the negative expression of keratin along the experiment by immunochemistry.

In summary, the histological analysis of the host tissue revealed a mild inflammatory response, mainly comprising macrophages and lymphocytes, against the cASCs. Therefore, the outcomes of this study provided new insights on the characterization of the subcutaneous mouse model as an alternative model for the study of regenerative medicine strategies based on canine ASCs.

6. Acknowledgments

The research leading to these results has received funding from the European Union's Seventh Framework Programme (FP7/2007-2013) under grant agreement n° REGPOT-CT2012-316331-POLARIS and from the Portuguese Foundation for Science and Technology (FCT) under the projects MIT/ECE/0047/2009 and PEst-OE/AGR/UI0772/2011). J.F. Requicha and P.P. Carvalho acknowledge the FCT for their PhD scholarship (SFRH/BD/44143/2008) and Post-Doc scholarship (SFRH/BPD/89454/2012), respectively. The authors thank Lígia Lourenço (UTAD) for her technical expertise in the histology.

7. References

1. Friedens AJ, Petrakov KV, Kuroleso AI, Frolova GP. Heterotopic Transplants of Bone Marrow - Analysis of Precursor Cells for Osteogenic and Hematopoietic Tissues. Transplantation. 1968;6 (2):230-&.

2. Requicha J, Viegas C, Albuquerque C, Azevedo J, Reis R, Gomes M. Effect of anatomical origin and cell passage number on the stemness and osteogenic differentiation potential of canine adipose-derived stem cells. Stem Cell Reviews and Reports. 2012;8 (4):1211-22.

3. Zuk PA, Zhu M, Ashjian P, De Ugarte DA, Huang JI, Mizuno H, *et al*. Human adipose tissue is a source of multipotent stem cells. Molecular Biology of the Cell. 2002;13 (12):4279-95.

4. in 'tAnker PS, Scherjon SA, Kleijburg-van der Keur C, Noort WA, Claas FHJ, Willemze R, *et al*. Amniotic fluid as a novel source of mesenchymal stem cells for therapeutic transplantation. Blood. 2003;102 (4):1548-9.

5. Bieback K, Kern S, Kluter H, Eichler H. Critical parameters for the isolation of mesenchymal stem cells from umbilical cord blood. Stem Cells. 2004;22 (4):625-34.

6. Seo BM, Miura M, Gronthos S, Bartold PM, Batouli S, Brahim J, *et al*. Investigation of multipotent postnatal stem cells from human periodontal ligament. Lancet. 2004;364 (9429):149-55.

7. Requicha JR, Viegas CA, Muñoz F, Reis RL, Gomes ME. Periodontal tissue engineering strategies based on non-oral stem cells. The Anatomical Record. 2013;invited review:accepted for publication.

8. Rada T, Reis RL, Gomes ME. Adipose tissue-derived stem cells and their application in bone and cartilage tissue engineering. Tissue Engineering Part B-Reviews. 2009;15 (2):113-25.

9. Carvalho PP, Gomes ME, Reis RL, Gimble JM. Adipose Tissue-Derived MSCs: Moving to the Clinic. In: Hematti P, Keating A, editors. esenchymal Stromal Cells: Biology and Clinical Applications, Stem Cell Biology and Regenerative Medicine. New York: Springer; 2013.

10. Lee HB, Chung YS, Heo SY, Kim NS. Augmentation of bone healing of nonunion fracture using stem cell based tissue engineering in a dog: a case report. Veterinarni Medicina. 2009;54 (4):198-203.

11. Black LL, Gaynor J, Gahring D, Adams C, Aron D, Harman S, *et al*. Effect of adipose-derived mesenchymal stem and regenerative cells on lameness in dogs with chronic osteoarthritis of the coxofemoral joints: A randomized, double-blinded, multicenter, controlled trial. Veterinary Therapeutics. 2007;8 (4):272-84.

12. Black L, Gaynor J, Adams C, Dhupa S, Sams A, Taylor R, *et al*. Effect of Intraarticular Injection of Autologous Adipose-Derived Mesenchymal Stem and Regenerative Cells on Clinical Signs of Chronic Osteoarthritis of the Elbow Joint in Dogs. Veterinary Therapeutics. 2008;9 (3).

13. Guercio A, Di Marco P, Casella S, Cannella V, Russotto L, Purpari G, *et al*. Production of canine mesenchymal stem cells from adipose tissue and their application in dogs with chronic osteoarthritis of the humeroradial joints. Cell Biology International. 2012;36 (2):189-94.

14. Hall MN, Rosenkrantz WS, Hong JH, Griffin CE, Mendelsohn CM. Evaluation of the Potential Use of Adipose-Derived Mesenchymal Stromal Cells in the Treatment of Canine Atopic Dermatitis: A Pilot Study. Veterinary Therapeutics. 2010;11 (2).

15. Ganey T, Hutton WC, Moseley T, Hedrick M, Meisel HJ. Intervertebral disc repair using adipose tissue-derived stem and regenerative cells: experiments in a canine model. Spine (Phila Pa 1976). 2009;34 (21):2297-304.

16. Hiyama A, Mochida J, Iwashina T, Omi H, Watanabe T, Serigano K, *et al*. Transplantation of mesenchymal stem cells in a canine disc degeneration model. Journal of Orthopaedic Research. 2008;26 (5):589-600.

17. Cui L, Liu B, Liu G, Zhang W, Cen L, Sun J, *et al*. Repair of cranial bone defects with adipose derived stem cells and coral scaffold in a canine model. Biomaterials. 2007;28 (36):5477-86.

18. Liu G, Zhang Y, Liu B, Sun J, Li W, Cui L. Bone regeneration in a canine cranial model using allogeneic adipose derived stem cells and coral scaffold. Biomaterials. 2013;34 (11):2655-64.

19. Seo KW, Lee HW, Oh YI, Ahn JO, Koh YR, Oh SH, *et al*. Anti-tumor effects of canine adipose tissue-derived mesenchymal stromal cell-based interferon-beta gene therapy and cisplatin in a mouse melanoma model. Cytotherapy. 2011;13 (8):944-55.

20. Dominici M, Le Blanc K, Mueller I, Slaper-Cortenbach I, Marini FC, Krause DS, *et al*. Minimal criteria for defining multipotent mesenchymal stromal cells. The International Society for Cellular Therapy position statement. Cytotherapy. 2006;8 (4):315-7.

21. Eriksson JE, Dechat T, Grin B, Helfand B, Mendez M, Pallari HM, *et al*. Introducing intermediate filaments: from discovery to disease. Journal of Clinical Investigation. 2009;119 (7):1763-71.

22. Eckes B, Dogic D, Colucci-Guyon E, Wang N, Maniotis A, Ingber D, *et al*. Impaired mechanical stability, migration and contractile capacity in vimentin-deficient fibroblasts. Journal of Cell Science. 1998;111:1897-907.

23. Lim JH, Boozer L, Mariani CL, Piedrahita JA, Olby NJ. Generation and characterization of neurospheres from canine adipose tissue-derived stromal cells. Cell Reprogram. 2010;12 (4):417-25.

24. Toma JG, Akhavan M, Fernandes KJ, Barnabe-Heider F, Sadikot A, Kaplan DR, *et al*. Isolation of multipotent adult stem cells from the dermis of mammalian skin. Nat Cell Biol. 2001;3 (9):778-84.

25. Brzoska M, Geiger H, Gauer S, Baer P. Epithelial differentiation of human adipose tissue-derived adult stem cells. Biochemical and Biophysical Research Communications. 2005;330 (1):142-50.

26. Thorne RF, Legg JW, Isacke CM. The role of the CD44 transmembrane and cytoplasmic domains in co-ordinating adhesive and signalling events. J Cell Sci. 2004;117 (Pt 3):373-80.

27. Bourin P, Bunnell BA, Casteilla L, Dominici M, Katz AJ, March KL, *et al*. Stromal cells from the adipose tissue-derived stromal vascular fraction and culture expanded adipose tissue-derived stromal/stem cells: a joint statement of the International Federation for Adipose Therapeutics and Science (IFATS) and the International Society for Cellular Therapy (ISCT). Cytotherapy. 2013;15 (6):641-8.

28. Kang JW, Kang KS, Koo HC, Park JR, Choi EW, Park YH. Soluble factors-mediated immunomodulatory effects of canine adipose tissue-derived mesenchymal stem cells. Stem Cells Dev. 2008;17 (4):681-93.

29. Ryu HH, Lim JH, Byeon YE, Park JR, Seo MS, Lee YW, *et al*. Functional recovery and neural differentiation after transplantation of allogenic adipose-derived stem cells in a canine model of acute spinal cord injury. J Vet Sci. 2009;10 (4):273-84.

30. Vieira N, Brandalise V, Zucconi E, Secco M, Strauss B, Zatz M. Isolation, characterization and differentiation potential of canine adipose-derived stem cells. Cell Transplant. 2010;19 (3):279-89.

31. Rodriguez AM, Pisani D, Dechesne CA, Turc-Carel C, Kurzenne JY, Wdziekonski B, *et al*. Transplantation of a multipotent cell population from human adipose tissue induces dystrophin expression in the immunocompetent mdx mouse. J Exp Med. 2005;201 (9):1397-405.

32. Gonzalez MA, Gonzalez-Rey E, Rico L, Buscher D, Delgado M. Adipose-derived mesenchymal stem cells alleviate experimental colitis by inhibiting inflammatory and autoimmune responses. Gastroenterology. 2009;136 (3):978-89.

33. Gonzalez MA, Gonzalez-Rey E, Rico L, Buscher D, Delgado M. Treatment of experimental arthritis by inducing immune tolerance with human adipose-derived mesenchymal stem cells. Arthritis Rheum. 2009;60 (4):1006-19.

34. Li K, Han Q, Yan X, Liao L, Zhao RC. Not a process of simple vicariousness, the differentiation of human adipose-derived mesenchymal stem cells to renal tubular epithelial cells plays an important role in acute kidney injury repairing. Stem Cells Dev. 2010;19 (8):1267-75.

35. Zhou Y, Yuan J, Zhou B, Lee AJ, Lee AJ, Ghawji Jr M, *et al*. The therapeutic efficacy of human adipose tissue-derived mesenchymal stem cells on experimental autoimmune hearing loss in mice. Immunology. 2011;133 (1):133-40.

36. Choi EW, Shin IS, Park SY, Park JH, Kim JS, Yoon EJ, *et al*. Reversal of serologic, immunologic, and histologic dysfunction in mice with systemic lupus erythematosus by long-term serial adipose tissue-derived mesenchymal stem cell transplantation. Arthritis Rheum. 2012;64 (1):243-53.

37. Lin CS, Lin GT, Lue TF. Allogeneic and Xenogeneic Transplantation of Adipose-Derived Stem Cells in Immunocompetent Recipients Without Immunosuppressants. Stem Cells and Development. 2012;21 (15):2770-8.

38. Yanez R, Lamana ML, Garcia-Castro J, Colmenero I, Ramirez M, Bueren JA. Adipose tissue-derived mesenchymal stem cells have in vivo immunosuppressive properties applicable for the control of the graft-versus-host disease. Stem Cells. 2006;24 (11):2582-91.

39. Niemeyer P, Kornacker M, Mehlhorn A, Seckinger A, Vohrer J, Schmal H, *et al*. Comparison of immunological properties of bone marrow stromal cells and adipose tissue-derived stem cells before and after osteogenic differentiation in vitro. Tissue Engineering. 2007;13 (1):111-21.

40. Martinello T, Bronzini I, Maccatrozzo L, Mollo A, Sampaolesi M, Mascarello F, *et al*. Canine adipose-derived-mesenchymal stem cells do not lose stem features after a long-term cryopreservation. Research in Veterinary Science. 2011;91 (1):18-24.

Chapter V

Design and characterization of a biodegradable double layer scaffold aimed at periodontal tissue engineering applications

Abstract

The inefficacy of the currently used therapies in achieving the regeneration *ad integrum* of the periodontium stimulates the search for alternative approaches, such as Tissue Engineering strategies. Therefore, the core objective of this study was to develop a biodegradable double layer scaffold for periodontal Tissue Engineering.

The design philosophy was based on a double layered construct obtained from a blend of starch and poly (ε-caprolactone) (30:70 wt%) (SPCL). A SPCL fiber mesh functionalized with silanol groups to promote osteogenesis was combined with a SPCL solvent casting membrane aiming at acting as a barrier against the migration of gingival epithelium into the periodontal defect. Each layer of the double layer scaffolds was characterized in terms of morphology, surface chemical composition, degradation behaviour and mechanical properties. Moreover, it was assessed the behaviour of seeded/cultured canine adipose-derived stem cells (cASCs).

In general, the developed double layered scaffolds demonstrated adequate degradation and mechanical behaviour for the target application. Furthermore, the biological assays revealed that both layers of the scaffold allow adhesion and proliferation of the seeded undifferentiated cASCs, and the incorporation of silanol groups into the fiber mesh layer enhance the expression of a typical osteogenic marker.

This work allowed to develop an innovative construct combining a tridimensional scaffold with osteoconductive properties and with potential to assist periodontal regeneration, carrying new possible solutions to current clinical needs.

---

*This Chapter is based on the following publication:

Requicha JF, Viegas CA, Hede S, Leonor IB, Reis RL, Gomes ME. Design and characterization of a biodegradable double layer scaffold aimed at periodontal tissue engineering applications. Journal of Tissue Engineering and Regenerative Medicine. doi: 10.1002/term.1816

1. Introduction

Periodontium, the organ which surrounds and sustains the tooth, is constituted by the alveolar bone, the cementum, the periodontal ligament (PDL) and the gingiva (1). The periodontium is often affected by periodontitis, an inflammatory disease highly prevalent both in humans and dogs, which can progresses with bone resorption, cementum necrosis and gingival recession or hyperplasia and ultimately, when untreated, leads to tooth exfoliation (2). Periodontitis has been identified as an important health problem owing to its enormous prevalence and life threatening implications on humans and animals systemic health (3).

Currently, there are several therapies used in the clinical practice, namely the gingival flap techniques (2, 4), scaling and root planning (2), root conditioning with demineralizing agents (2, 4, 5), direct injection of growth or differentiation factors into the root surface [e.g. platelet derived growth factor (PDGF), insulin growth factor-1 (IGF-1), bone morphogenetic proteins-2 and -7 (BMPs)] (2) or concentrate of factors [platelet rich plasma (PRP), enamel matrix derivatives (EMD)] (1, 6), *in situ* application of filler materials, such as autografts, allografts and alloplastic materials, namely hydroxyapatite (HA) and tricalcium phosphate (TCP) (5), and application of guided tissue regeneration (GTR) membranes.

GTR was proposed (5, 7) to selectively guide cells to proliferate in different compartments of the alveolar bone and PDL. This technique allows preventing the gingival epithelium and connective tissue expansion, ankylosis and radicular resorption phenomenon and at same time avoiding the collapse of the periodontal defect (2, 8).

The materials that have been used to produce GTR membranes are several, namely, non-absorbable polymers, as for example ePTFE (8); absorbable polymers of synthetic origin, such as polylactic acid (PLA) (9), poly (lactic-co-glycolic acid (PGLA) (10), polyglactin (11) and biosynthetic cellulose (12) or absorbable polymers of natural origin, such as collagen (13, 14), cargile (15) and chitosan (16, 17). Besides those materials, composite membranes composed of PGLA with HA (13) or nano-apatite with poly (ε-caprolactone) (PCL) (18) has also been tested for this application. Other membranes have also been developed to work as vehicles for delivering biological molecules, namely growth factors (PDGF, BMPs, PRP) or antibiotics, as metronidazole (10), doxycycline (19) or tetracycline (9), in order to promote an effective and aseptic cellular proliferation and differentiation in the desire tissue. In spite of all therapeutic strategies developed until today for periodontal regeneration, there is still no treatment that could restore the functionality of all the damaged periodontal tissues. For this reason, clinicians tend to combine several of techniques mentioned above in attempts to reach the desired effect, resulting in complex treatments with unpredictable outcomes (20, 21).

Recently, Tissue Engineering has paved the way for the development of new therapeutic strategies, trying to understand and mimic the role of the cellular and matrix components of the tissues along the regenerative process. The regeneration of the mesoderm-origin tissues, including the periodontal tissues, rely on the use of adult mesenchymal stem cells (MSCs) (22) which are proved to have the capacity to differentiate into various cellular lineages (1, 6, 23, 24). A prime consideration in periodontal Tissue Engineering should be the design of tridimensional supportive matrix/scaffolds, which will support the periodontal tissues.

Therefore, the purpose of the present study was to develop an innovative scaffold with potential to regenerate periodontal defects. Thus, a scaffold was designed into a construct composed of two different layers: a membrane and a 3D fiber mesh, both made of a blend of starch and poly (ε-caprolactone) (SPCL). The membrane is expected to act as GTR barrier, avoiding the gingival epithelium growth into the periodontal defect when placed between the gingiva and the defect and also to promote the adhesion and recruitment of the native undifferentiated cells responsible for new ligament tissue formation. The SPCL 3D fiber mesh layer is aimed to provide a support matrix for the ingrowth of alveolar bone that comprises the osseous compartment of the periodontium. This fiber mesh was further functionalized with silanol groups that are known to activate bone-related genes expression and stimulate osteoblast proliferation and differentiation (25-27). This aforementioned double layer scaffold was characterized in terms of morphology and surface chemical composition, mechanical properties and degradability. Furthermore, we have studied the behaviour of canine adipose-derived stem cells (cASCs) on both layers to assess their *in vitro* functionality.

2. Materials and methods

2.1. Production of the materials

A double layer scaffold based on SPCL, a biodegradable and thermoplastic blend of starch and poly (ε-caprolactone) (30:70 wt%) (Novamont, Italy), was produced by combining two layers. These layers were obtained using two different processing techniques, solvent casting and wet-spinning, as shown in Fig. 5.1a.

To obtain the solvent casting membrane (SPCL-M), the SPCL were dissolved in chloroform (Sigma-Aldrich, Germany) at a concentration of 20 wt%. At room temperature, 3 mL of the polymeric solution was casted onto a 5 cm diameter patterned Teflon mold to obtain the SPCL-M, which was then dried in a hood and cut into discs samples of 6 mm of diameter.

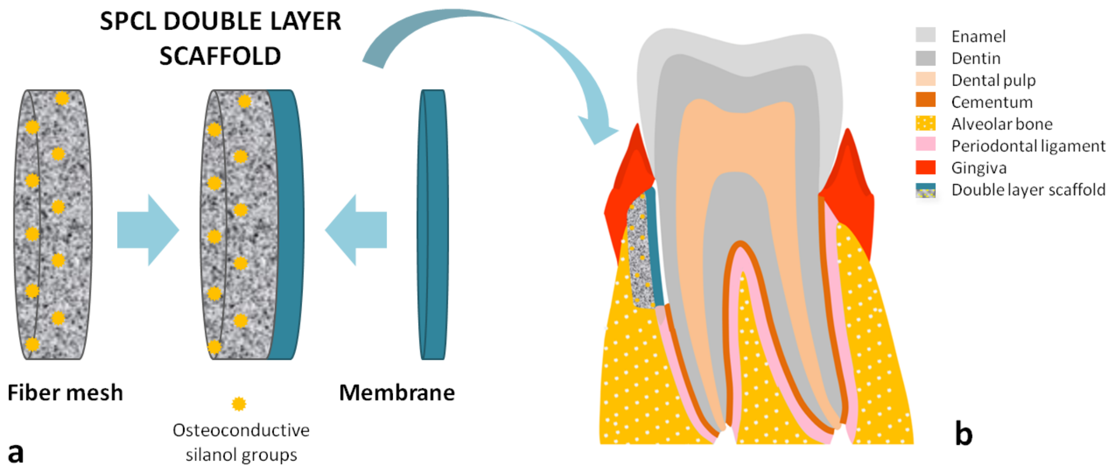

c

Layers	Description	Abbreviation	Characterization
SPCL membrane		SPCL-M	SEM, biological studies
SPCL wet-spun fiber mesh	Non-functionalized with silanol groups	SPCL-WS	SEM, FTIR, biological studies
	Functionalized with silanol groups	SPCL-WS-Si	
SPCL double layer scaffold	Patterned membrane plus wet-spun fiber mesh non-functionalized with silanol groups	SPCL-DLS	SEM, micro-CT, degradability, mechanical properties
	Patterned membrane plus wet-spun fiber mesh functionalized with silanol groups	SPCL-DLS-Si	

Figure 5. 1 – Schematic representation of the developed double layer scaffold comprising the membrane and the fiber mesh. The yellow spots represent the osteoconductive silanol groups incorporated into the material (a). Schematic picture of the implantation of the double layer scaffold in a periodontal defect (b). Table summarizing the components of the double layer scaffold that were developed and characterized (c).

In order to prepare the wet-spun fiber meshes, the same SPCL solution was loaded into a 5 mL plastic syringe with a metallic needle (21 G×1.5”). The syringe was connected to a programmable syringe pump (KD Scientific, World Precision Instruments, UK) to inject the polymer solution at a controlled pumping rate of 5 mL per hour to allow the formation of the fiber mesh directly into the coagulation bath. The wet-spun fiber mesh structure was formed during the process by the random movement of the coagulation bath. Two different coagulation baths were used: methanol (Vaz Pereira, Portugal) as control (SPCL-WS) and calcium silicate solution previously studied and described in previous works (SPCL-WS-Si) (25, 26, 28). Using methanol, the formed fiber meshes were dried at room temperature overnight in order to remove any remaining solvent and designated as SPCL-WS. In the case of using calcium silicate solution, the fiber meshes were dried in an oven at 60 °C for 24 hours, and designated as SPCL-WS-Si.

After the preparation of each layer as described above, the two layers were combined together by dropping chloroform onto the top side of the SPCL-M, allowing it to become slightly soften, and then, by applying an certain pressure the fiber mesh was attached. The combined layers were dried in a hood and cut into discs with 6 mm of diameter. All samples were disinfected by ethylene oxide before cell culture studies.

In Fig. 5.1c it is described the composition and the characterization of the two developed layers. The double layer scaffolds, comprising the SPCL-M/SPCL-WS or SPCL-M/SPCL-WS-Si, were also characterized in terms of morphology, degradability and mechanical behaviour.

2.2. Morphology characterization

2.2.1. Scanning electron microscopy

Scanning electron microscopy (SEM) was performed using a Leica Cambridge S-360 model (Cambridge, UK). Prior to any SEM observations, all the scaffolds were sputter-coated with gold by ion sputtering (Polaron SC502, Fisons Instruments, UK). Three samples of each material were used, and the micrographs analyzed by using the software ImageJ (NIH, USA).

2.2.2. Micro-computed tomography

Micro-computed tomography was carried out using a high-resolution micro-CT Skyscan 1072 scanner (Skyscan, Kontich, Belgium). X-ray scans of SPCL-DLS and SPCL-DLS-Si were performed in triplicate using a resolution of pixel size of 8.7 µm and integration time of 1.9 sec. The X-ray source was set at 49 keV of energy and 122 µA of current. Approximately 400 projections were acquired over a rotation range of 180º with a rotation step of 0.45º. Data sets were reconstructed using standardized cone-beam reconstruction software (NRecon v1.4.3, SkyScan). Representative data sets of 200 slices were segmented into binary images with a dynamic threshold of 37 to 120 to identify the organic and inorganic phases. This data were used to build 3D models (CTAnalyser, v 1.5.1.5, SkyScan).

2.3. Fourier transform attenuated total reflectance infrared spectroscopy

The surface of the SPCL-WS and SPCL-WS-Si was analyzed by Fourier-transformed IR spectroscopy with attenuated total reflectance (FTIR-ATR) in an IRPrestige 21 (Shimadzu, Japan). Spectra were collected at 4 cm^{-1} resolution using 60 scans in the spectral range 4400-800 cm^{-1}. For each sample, three individual measurements were performed.

2.4. Degradation behaviour

2.4.1. Water uptake and weight loss

In order to simulate *in vivo* conditions, SPCL-DLS and SPCL-DLS-Si were incubated in different enzymatic solutions at physiological conditions (pH 7.4, 37ºC). Pre-weighed materials were individually immersed in 2.5 mL of four different solutions: (i) phosphate-buffered saline (PBS, 0.01 M, pH 7.4; Sigma-Aldrich, Germany), (ii) PBS solution containing 400 U/L α-amylase from *Bacillus* sp. (Sigma-Aldrich, Germany), (iii) PBS solution containing 500 U/L lipase from *Pseudomonas* sp. (Sigma-Aldrich, Germany) and (iv) PBS containing lipase and amylase at the same concentrations (50:50 vol%). The samples were incubated at 37 ºC for 1, 3, 7, 14, 21 and 28 days, and the solutions were changed weekly. All the prepared solutions were sterilized using a 0.2 µm syringe filter and kept at 4 ºC until further usage.

The enzymatic degradation of polymeric scaffolds was carried out using amylase and lipase, enzymes to study their effect on starch and PCL hydrolysis. Additionally, these two enzymes are found in healthy dogs' serum at concentration in the range of 373-1503 U/L and 90-527 U/L, respectively (29). The reason of using dog reference values is based on the fact that dog is an animal with natural occurrence of the periodontal disease and is considered the best model in Periodontology pre-clinical research.

At the end of each degradation period, the samples were removed from the solution and placed between two filter papers, to remove excess of liquid, and immediately weighted to determine the water uptake. Then, it was washed several times with distilled water and placed in the oven at 37 ºC for 3 days in order to measure the dry weight and thus determine the weight loss. For each study condition (material and solution), five samples were tested. Degradation solutions were frozen for further analysis, namely, for the quantification of the reducing sugars and calcium and silicon elements, as described below.

2.4.2. Morphology after degradation

SPCL-DLS and SPCL-DLS-Si samples after degradation under different conditions were dried at room temperatures and observed by SEM, as described previously. Three samples of each material were analyzed.

2.4.3. α-Amylase activity

Degradation solutions were analyzed to determine the concentration of reducing sugars released into the solution as result of starch hydrolysis. The determination was based on the dinitrosalicyclic acid (DNS) method and absorbance were red at 540 nm in a microplate reader (Synergy HT, BioTek Instruments, USA), using a standard curve of glucose.

2.4.4. Calcium and silicon concentration of the degradation solutions

Elemental concentrations of silicon (Si) and calcium (Ca) were measured in the degradation solutions, after passed through a 0.22 µm filter, using inductively coupled plasma atomic emission spectrometry (ICP: JY2000-2, Jobin Yvon, Horiba, Japan).

2.5. Mechanical behaviour

Mechanical tests were carried out to evaluate the tensile strength of the SPCL-DLS and SPCL-DLS-Si. Five rectangular samples with 5 x 20 mm were tested in the dry and wet state (after 24 hours of immersion in PBS). Samples were tested using a uniaxial testing system (Instron 4505 Universal Machine, USA) with a load cell of 1 kN. Tensile test was carried out at a crosshead speed of 2 mm/min. Tensile stress was taken as the maximum stress in the stress-strain curve, and the elastic modulus was estimated from the initial slope of the stress strain curve.

2.6. Culturing of canine adipose-derived stem cells

Canine adipose-derived stem cells (cASCs) were isolated from subcutaneous abdominal tissue collected from adult healthy dogs in the Veterinary Hospital of University of Trás-os-Montes e Alto Douro in accordance with Portuguese legislation (Portaria no 1005/92) and international standards on animal welfare as defined by the European Directive 2010/63/EU, and with previous informed consent of the owners. cASCs were expanded in basal medium composed of Dulbecco Modified Eagle Medium (DMEM) (Sigma Aldrich, Germany) supplemented with 10% fetal bovine serum (FBS; Invitrogen, USA) and 1% antibiotic/antimicotic (Sigma, USA) as previously reported (24), until passage 2 before seeding. As previously referred, dog is an important animal model in periodontal regeneration research. For that reason, we envision, ultimately, the autologous assessment of this tissue engineered construct with canine cells in the Wikësjo model, which is considered the most adequate animal model aimed at extrapolate results for future applications in veterinary and human dentistry (5, 20). The harvesting, isolation and characterization of the canine adipose derived stem cells has been addressed in a previous study (24).

The cASCs were seeded onto the SPCL-M a concentration of 5.0×10^4 cells/sample and then cultured for 1 and 14 days in basal medium. The cells morphology and proliferation were characterized by scanning electron microscopy (SEM) and DNA quantification, respectively, as it is described below.

The SPCL-WS and SPCL-WS-Si were seeded with cASCs at a concentration of 1.0×10^5 cells/sample and then cultured in either basal or osteogenic medium for 7 and 28 days. Osteogenic medium was composed of alpha Modification Eagle Medium (α-MEM) (Sigma Aldrich, Germany), 10% FBS, 1% antibiotic/antimicotic and osteogenic supplements, ascorbic acid (50 µg/mL) (Sigma, USA), dexamethasone (10^{-8} M) (Sigma, USA) and β-glycerophosphate (10 mM) (Sigma, USA). Cell-scaffolds constructs were evaluated in terms of the cellular morphology and proliferation, as described below. The relative gene expression of a specific osteoblast marker, Osteocalcin, was also assessed by real time RT-PCR analysis to evaluate the effect of the functionalization of the polymer fibers with silanol groups in the osteogenic differentiation of cASCs.

2.6.1. Scanning electron microscopy

To observe the morphology of cASCs cultured onto the membrane and fiber meshes, the samples were fixed in 2.5% glutaraldehyde solution in PBS during 1 hour at the 4 ºC and then dehydrated in a series of ethanol solutions with increasing concentration (30%, 50%, 70%, 90% and 100%, v/v). Afterwards, the samples were left to dry overnight.

2.6.2. dsDNA quantification

A fluorimetric dsDNA quantification kit (PicoGreen, Molecular Probes, USA) was used and the fluorescence was read using a microplate ELISA reader (BioTek, USA) at an excitation of 485/20 nm and an emission of 528/20 nm. The number of cells in each timepoint was obtained by using previously created standard curve dsDNA content versus cASCs number.

2.6.3. Real time RT-PCR analysis

For the Osteocalcin gene expression analysis, the cultured materials were retrieved and kept in 800 µL of TRIzol Reagent (Invitrogen, USA). The mRNA was extracted with TRIzol following the procedure provide by the supplier. Briefly, after an incubation of 5 min, additional 160 µL of chloroform (Sigma Aldrich, Germany) were added; the samples were then incubated for 15 min at 4 °C and centrifuged at the same temperature and 13 000 rpm for 15 min. After the centrifugation, the aqueous part was collected and an equal part of isopropanol (VWR, USA) was added. After an incubation of 2 hours at -20 °C the samples were washed in ethanol, centrifuged at 4 °C and 9 000 rpm for 5 min and resuspended in 12 µL of RNase/DNase free water (Gibco, UK). The samples were quantified using the NanoDrop ND1000 Spectrophotometer (NanoDrop Technologies, USA). For the cDNA synthesis were used the samples with a 260/280 ratio between 1.7 and 2.0. The cDNA synthesis was performed in the Mastercycler real time PCR equipment (Eppendorf, USA) using the iScript cDNA Synthesis Kit (Quanta Biosciences, USA) with an initial amount of mRNA of 2 µg in a total reaction volume of 20 µL. RNAse free water (Gibco, UK) was used as a negative control. After the synthesis of the cDNA, real time PCR analysis was carried in the Mastercycler real time PCR equipment (Eppendorf, USA) using the PerfeCta Sybr-Green FastMix (Quanta Biosciences, USA) to analyze the relative expression of Osteocalcin gene (ENSCAFT00000026668, F: GATCGTGGAAGAAGGCAAAG, R: AGCCTCTGCCAGTTGTC TGT) in each sample, using GAPDH as housekeeping gene (NM_001003142.1, F: CCAGAACATCATCCCTGCTT, R: GACCACCTGGTCCTCAGTGT). The primers have been designed using the Primer 3 Plus v0.4.0 (MWG Biotech, Germany). Delta-delta Ct method according to Livak and Schmittgen (2011) (30) was performed using the materials after seeding as calibrator.

2.7. Statistical analysis

Statistical analysis was performed using the GraphPad Prism v5.00 (GraphPad Software Inc., USA). The statistical significance was assessed by a two-way ANOVA followed with Bonferroni posttesting. Data are reported as mean ± standard deviation.

3. Results

3.1. Morphology characterization

The micro-computed tomography images showed that the combination of the two different layers was effectively achieved, allowing to obtain a single asymmetric scaffold, comprising two distinct parts (Fig. 5.2). SEM showed that the SPCL-M presents an irregular and rough surface, which can be due to the textures of the mould used and the stretching of the SPCL during mechanical detachment from the mould (Fig. 5.2). The SPCL-WS and SPCL-WS-Si were mainly composed by a random arrangement of interconnected fibers. The diameter of the SPCL-WS fibers was about 192 ± 23.5 µm and SPCL-WS-Si fibers were around 195 ± 24.6 µm. At higher magnifications, it was possible to observe the rough surface of SPCL fibers, which could be due to the evaporation of chloroform. In SPCL-WS-Si, the surface of the fibers was much smoother and presents some cracks which probably resulted from the drying process typical of the materials prepared by the sol-gel process.

3.2. Fourier transform attenuated total reflectance infrared spectroscopy

The effectiveness of the functionalization of the fiber mesh layer with Si-OH groups was investigated by FTIR-ATR (Fig. 5.2). Regarding the SPCL-WS, it was observed a high intensity band at 1700-1750 cm^{-1} for C=O, corresponding to the characteristic band of poly (ε-caprolactone) (31, 32). In the SPCL-WS-Si, obtained using a calcium silicate solution as a coagulation bath, the C=O band was also detected. In addition, siloxane (Si-O-Si) reflection peaks were observed at 1020 cm^{-1}, 1080 cm^{-1} and1180 cm^{-1} and a shoulder at 1110 cm^{-1}.

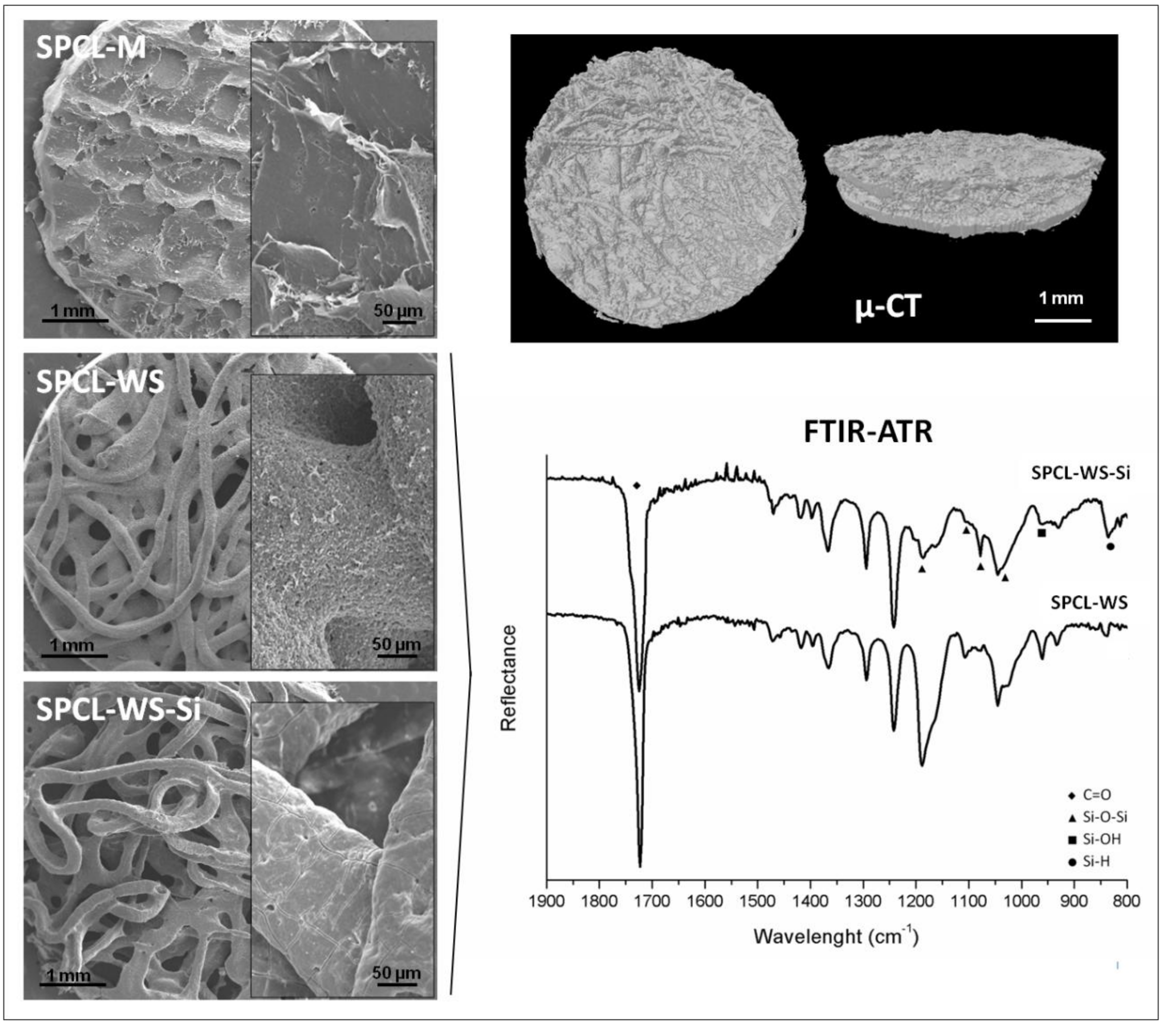

Figure 5. 2 – SEM micrographs of the SPCL-M, SPCL-WS and SPCL-WS-Si. The images embedded in the right corner of each SEM micrographs correspond to higher magnifications. At the right, the micro-CT image of the double layer scaffold and the FTIR-ATR spectrum of the SPCL-WS and SPCL-WS-Si.

A shoulder of Si-OH was observed at 960 cm^{-1} and a peak at 840 cm^{-1} for Si-OH typically observed in silica gel (33, 34) proving the functionalization of the SPCL with silanol groups.

3.3. Degradation behaviour

3.3.1. Water uptake and weight loss

The SPCL-DLS and SPCL-DLS-Si showed different water uptake ability along the immersion time in the different degradation media used, as it can be observed in the Fig. 5.3a. When immersed in PBS buffer, both scaffolds did not change their water uptake along the immersion period, maintaining a stable value bellow 60%.

In contrast, scaffolds immersed in the enzymatic solutions showed a water uptake of around 50 to 60%, after only one day of immersion. In the case of SPCL-DLS, it was observed a gradually increase of the water uptake in PBS + lipase and PBS + amylase + lipase, although it was more significant for PBS + lipase, reaching values of 96.5% comparing to the 82.7% in PBS + amylase + lipase. Samples immersed in PBS + amylase solution remains constant with time. The SPCL-DLS-Si exhibits a lower water uptake comparing to non-functionalized scaffolds. In general, the water uptake in degradation solutions increases by the following order: PBS, PBS + amylase, PBS + amylase plus lipase and PBS + lipase.

In terms of weight loss (Fig. 5.3b), it was observed a faster degradation of the SPCL-DLS-Si, comparing to the SPCL-DLS after 1 day of immersion under all conditions. However, as the degradation time increases, it is observed a higher weight loss for the SPCL-DLS, especially at day 7 (56.9% weight loss) in PBS + lipase. The SPCL-DLS-Si, exhibited a similar degradation profile, but showed lower degradation rate in PBS + lipase (41.1% weight loss) comparing with SPCL-DLS. In PBS solution, devoid of enzymes, both materials showed lower degradation rate.

3.3.2. Morphology after degradation

SEM images of the double layer scaffolds under the different enzymatic conditions as function of degradation time are presented in Fig. 5.3c. In general, along the degradation time, the structure of both scaffolds (with or without silanol groups) at the surface level showed profound morphological changes with the formation of pores and increase of roughness, being more visible in the SPCL-DLS. After 14th day of degradation in PBS + lipase and PBS + amylase + lipase, gradual increasing on the number of pores on the surface of SPCL-DLS was observed.

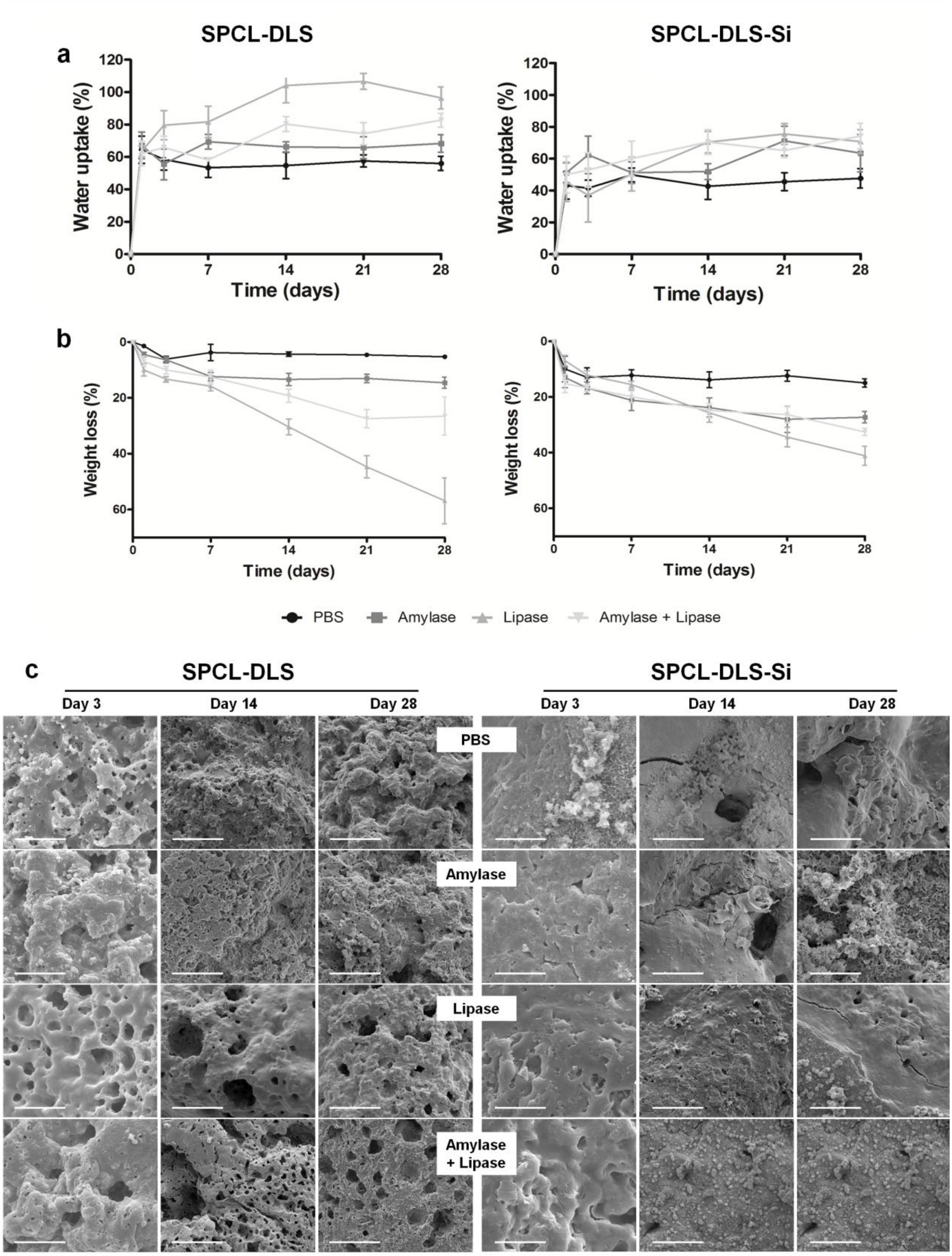

Figure 5. 3 – SEM micrographs (c) and degradation profile in terms of water uptake (a) and weight loss (b) of the SPCL-DLS and SPCL-DLS-Si in PBS solution and in presence of enzymes at physiological conditions (pH 7.4, 37 ºC).

When both scaffolds were immersed in PBS buffer, no evident changes in their morphology were possible to observe. Respecting SPCL-DLS-Si samples, it was also observed a more evident action on the polymer structure after the 14th day of degradation time. The formation of calcium phosphate crystals onto the surface was evident for all conditions, particularly, in PBS + lipase and PBS + amylase + lipase solutions.

3.3.3. α-Amylase activity

Along the degradation time, it was observed a gradual increasing in the concentration of sugars in the solutions for all conditions (Fig. 5.4).

For the SPCL-DLS, the amount of reducing sugars released was higher in PBS + amylase solution, particularly at day 14, indicating a high activity of this enzyme in this substrate. In the presence of the lipase, although it is known this enzyme degrades PCL based materials, some sugars were also detected. Regarding the SPCL-DLS-Si, it was also observed the presence of higher amounts of reducing sugars in PBS + amylase solution. Reducing sugars were also detected after immersion of the scaffolds in PBS, although in lower quantities. In PBS + amylase + lipase solution it was observed lower amounts of reducing sugars for both materials comparing with PBS + amylase solution.

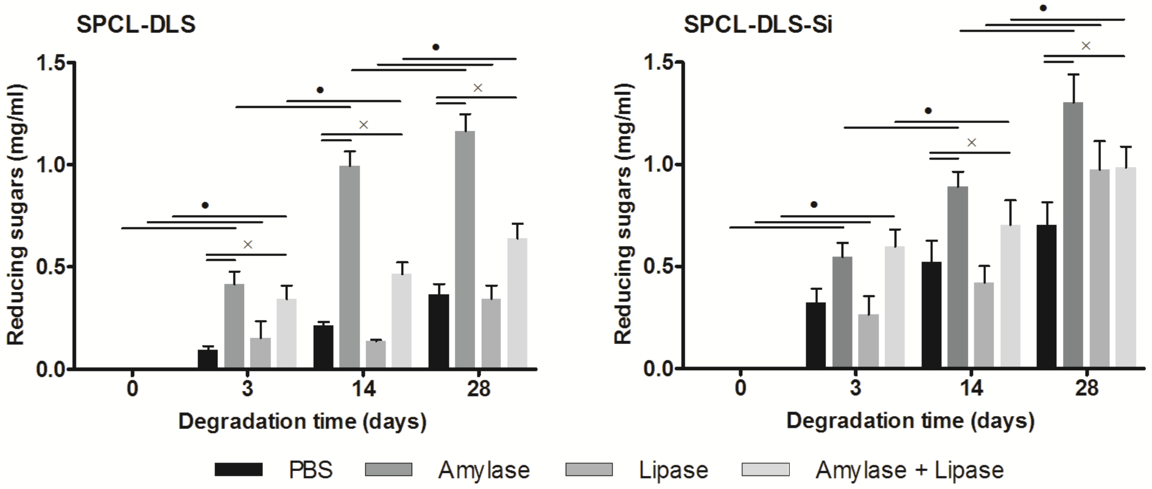

Figure 5. 4 – Cumulative release of reducing sugars as function of degradation time in PBS solution and in presence of enzymes at physiological conditions (pH 7.4, 37 ºC) of SPCL-DLS and SPCL-DLS-Si. The symbol (×) compares the enzyme effect within the same degradation time. The symbol (•) compares the effect of the degradation time within the same enzymatic condition. ($p<0.001$, n=9).

3.3.4. Calcium and silicon concentration of the degradation solutions

In general, it was observed an increasing release of calcium and silicon ions from the SPCL-DLS-Si along the degradation time (Fig. 5.5). Between 3rd and 14th days of immersion, there was increase in calcium and silicon concentration in all solution, although the silicon concentration increase was higher. At day 14, an accentuate increase in calcium concentration was observed. The release of calcium was higher for the samples immersed in PBS + lipase and PBS + amylase + lipase solutions than in PBS + amylase, while the release of silicon was much higher in samples immersed in PBS + amylase and PBS + amylase + lipase solutions.

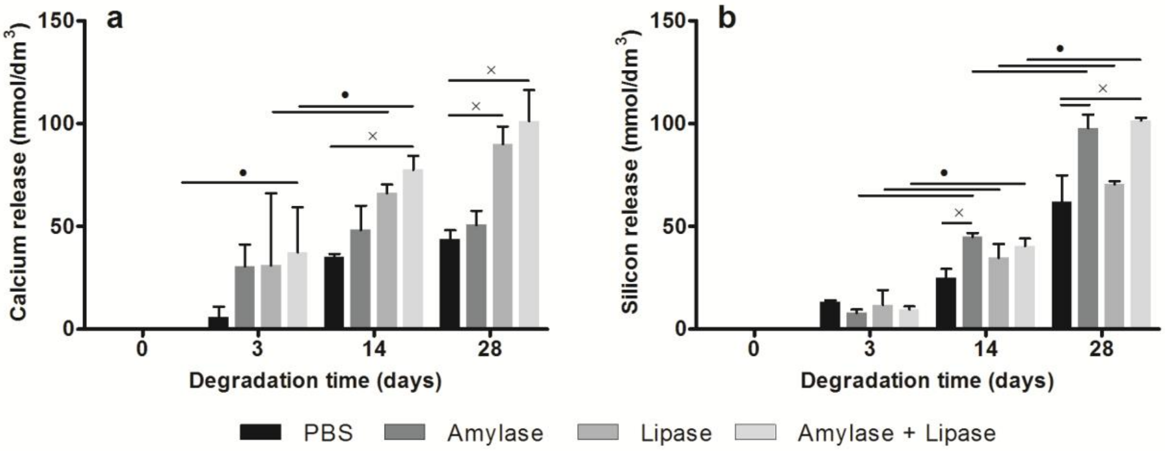

Figure 5. 5 – Cumulative release of calcium (a) and silicon (b) as function of degradation time in PBS solution and in presence of enzymes at physiological conditions (pH 7.4, 37 ºC) of SPCL-DLS-Si. The symbol (×) compares the enzyme effect within the same degradation time. The symbol (•) compares the effect of the degradation time within the same enzymatic condition. ($p<0.001$, n=5).

3.4. Mechanical behaviour

The tensile properties of SPCL-DLS and SPCL-DLS-Si, in wet and dry state, are reported in Table 5.1. In general, the mechanical properties were better for SCPL-DLS than for SPCL-DLS-Si in dry state. In the wet state, both scaffolds present a lower Modulus that is statistically different ($p<0.001$) from the samples in dry state. In terms of elasticity, it was observed a significant increase for both materials ($p<0.001$) under wet state.

Table 5. 1 – Mechanical properties of the SPCL-DLS and SPCL-DLS-Si, before and after soaked in PBS for 24 hours.

Material	SPCL-DLS dry	SPCL-DLS wet	SPCL-DLS-Si dry	SPCL-DLS-Si wet
Tensile Stress (MPa)	4,08 ± 0,877	2,873 ± 0,453	3,211 ± 1,096	2,441 ± 0,295
Modulus (MPa)	167,73 ± 33,52	45,839 ± 5,38	142,46 ± 38,477	34,153 ± 5,772
Elongation (%)	8,646 ± 6,502	35,854 ± 2,925	0,878 ± 0,175	29,209 ± 1,675

3.5. Culturing of canine ASCs

SEM micrographs revealed a good adhesion of cASCs to the SPCL-M exhibiting a flat and elongated shape and the cell number increase was highly significant between the first and the final culturing day (Fig. 5.6a). SEM analysis of the SPCL-WS and SPCL-WS-Si revealed that, in basal medium, both materials have the ability to support and sustain cell proliferation (Fig. 5.6b). The observation of the respective graphic shows the functionalization of the polymer with silanol groups has a positive effect in cellular proliferation, evident at the 28th day of culture.

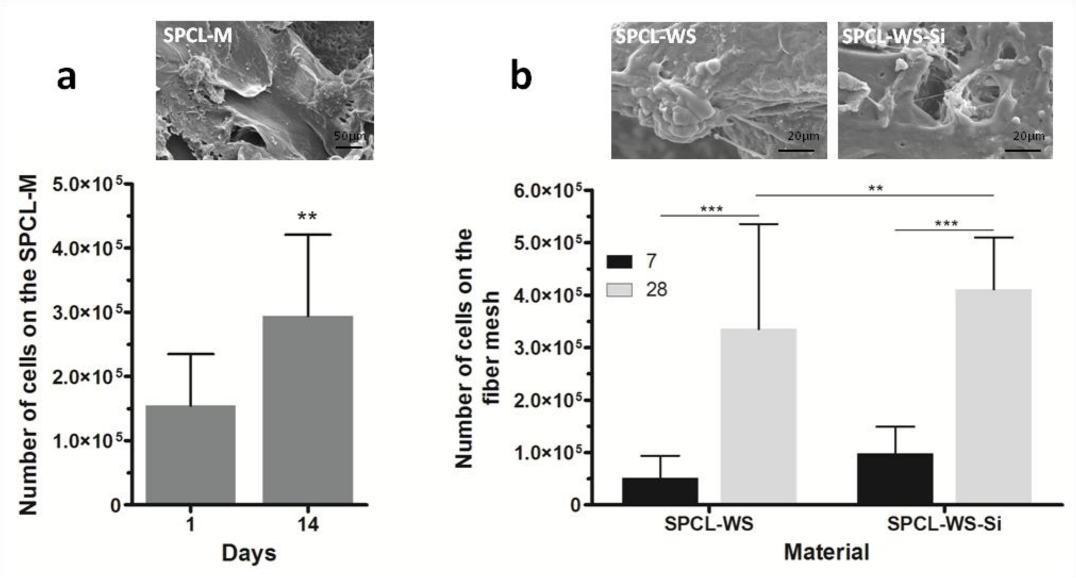

Figure 5. 6 – Canine ASCs proliferation in the (a) SPCL-M cultured for 1 and 14 days and in the (b) SPCL-WS and SPCL-WS-Si cultured for 7 and 28 days in basal medium. (**p<0.01, ***p<0.001, n=9). SEM micrographs represent the latter time point of each type of material.

The analysis of the Osteocalcin expression by real time PCR (Fig. 5.7) shown an increase of expression along the culturing, higher in the samples cultured in osteogenic medium. In the 28th day of culture, there was a significant expression of this marker in the SPCL-WS-Si comparing to SPCL-WS.

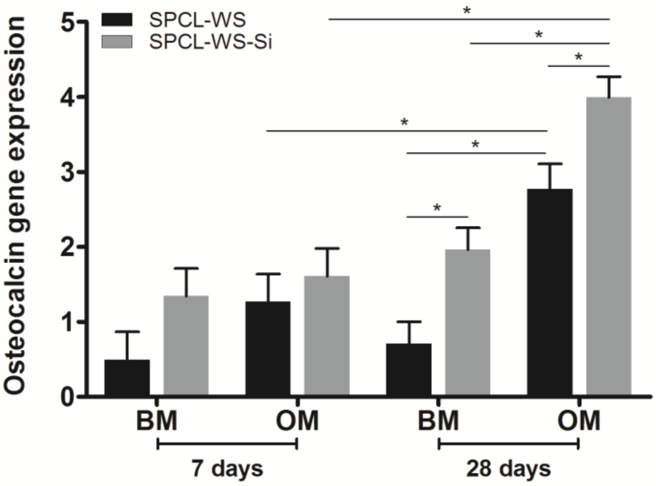

Figure 5. 7 – Osteocalcin gene expression in cASCs cultured onto SPCL-WS and SPCL-WS-Si for 7 and 28 days in basal (BM) and osteogenic (OM) medium. (*p<0.05, n=9).

4. Discussion

This work proposed the development of an innovative double layer scaffold that could support the regeneration of the different tissues that compose the periodontium. The developed scaffold results from the assembling of two distinct layers, a membrane obtained by solvent casting and a fiber mesh obtained by wet-spinning (35), with different functions aiming the regeneration of various tissue components of a periodontal defect. This scaffold design is expected to fulfil two main goals: (a) to provide a matrix with an osteoconductive potential in one side (layer) for the formation of new alveolar bone and (b) to simultaneously act as a barrier against the migration of gingival epithelium into the bone compartment and at same time, promoting the formation of the PDL between bone and the tooth surface on the opposite side (layer) of the construct.

The biocompatibility and versatility of SPCL polymeric blend was the main criteria for the selection of this material since it has already been used to produce 3D structures and microparticles with different physicochemical characteristics using various technologies, namely electrospinning (35, 36), fiber bonding (37), wet-spinning (25), rapid prototyping (36), injection molding (38) or supercritical phase inversion (39) for applications in Tissue

Engineering and regenerative medicine. Furthermore, the SPCL based scaffolds have been extensively assessed both *in vitro* (26, 35, 40) and *in vivo* (37, 41).

SEM and micro-CT imaging showed that the methodology used to combine both layers did not affect the surface morphology of each layer and, at the same time, enabled to obtain a solid integration of the membrane layer with the fiber mesh layer.

The functionalization of the wet-spun fiber meshes with silanol groups, by using the calcium silicate bath, was comproved by the FTIR results. The presence of Si–OH groups came from the hydrolyzed and incomplete polycondensation reaction of TEOS, which can lead to the formation of hydrogen-bonding interactions with carbonyls of PCL, as reported in previous works (25, 33, 34, 37). In these works, the inorganic–organic hybrids are prepared via an *in situ* sol–gel process of TEOS in the presence of PCL.

The functionalized fiber mesh layer of the construct was obtained in a single step by combining wet-spinning technology and a calcium silicate solution, which allows a bioactive structure with Si–OH functional groups to be developed. Thus, this methodology offers clear advantages in scaling up technologies, in terms of reduction of time and costs of production.

Regarding the degradability of the double layer scaffold in terms of morphology and weight loss, instead of be higher in the SPCL-DLS, it was not observed a complete degradation of the studied materials, leading us to conclude that a period of 28 days of digestion by the serum enzymes is not enough to degrade completely the newly developed scaffolds.

The developed double layer scaffold was found to be degraded by two enzymes found in dog serum (α-amylase and lipase) at physiological concentrations, as reported in previous studies using human-like enzymatic solutions to study their effect on the degradation of SPCL-DLS (42, 43). Lipase is one of the most effective enzymes on this process, because it is able to catalyze the hydrolysis of ester bonds in PCL, which in our blend, 70% in weigh is from PCL (42, 43). In PBS + amylase + lipase solution it was observed lower amounts of reducing sugars for both materials comparing with PBS + amylase solution, maybe because, in the first solution there is a competition effect between the two enzymes.

Although, the degradation rate of the SPCL-DLS was higher in terms of weight loss comparing with the SPCL-DLS-Si, the production of sugars was observed higher in SPCL-DLS-Si maybe influenced by the presence of silicon and calcium elements which means that the amylase has more important role in degrade this material than in the SPCL-DLS-Si.

Gradual degradation observed for the material is essential for maintaining its integrity during the regeneration period. Along with the degradation of the material, it is expected that the pool of periodontal undifferentiated cells could be recruited, proliferate and differentiated in the desired phenotypes, both ligament and bone, at the same time that the epithelial cells of the gingiva are selectively blocked out of the defect. If the material degrades quickly, the GTR barrier function of the membrane would disappear and the previously existent cells would not colonize the defect.

Concerning the mechanical properties of the SPCL-DLS and SPCL-DLS-Si, it was observed that, in general, they exhibit similar properties to the ones obtained in previous works (44) or also, to the commercially available membranes (45) for periodontal regeneration. In terms of elastic modulus, the study materials in wet state present higher values comparing to electro-spun nano-apatite/PCL membrane, which can be due to the incorporation of the bioceramic particles into the polymeric structure (18). It was demonstrated that a hybrid PCL membrane containing 40% silica xerogel exhibited five and eight times higher strength and elastic modulus comparing with pure PCL membrane (46).

The SPCL-DLS-Si modulus is lower than SPCL in bond states, which might be due to the bond between the carbonyl groups of PCL with the silanol groups as demonstrated in the FTIR-ATR spectrum. These bonds can cause some constraints on the mobility of the PCL chains (33, 47). The mechanical properties of a scaffold for this target application should enable to maintain the space and the stability of the defect during the periodontal regeneration, mainly, during the early phase of wound healing (1). As the *in vivo* environment is wet, good elasticity could be advantageous for an easier suiting of the scaffold in irregular defects. Moreover, the fact that SPCL-DLS-Si scaffold was not completely degraded after 28 days of immersion can be advantageous. In fact, this finding is desired because in periodontal defects the stability provided by the structure of the construct is very important to enable the mechanical stability and prevent the epithelial invasion while retaining space for regeneration.

The biological behaviour of the developed scaffold was assessed using adipose derived stem cells, envisioning the future application of the constructs in Tissue Engineering approaches. ASCs have revealed potential for use in Tissue Engineering and other cell-based therapies, similarly with bone marrow mesenchymal stem cells (BMSCs). Moreover, the adipose tissue is ubiquitous and easily obtainable in large quantities with little patient discomfort (48, 49). Canine ASCs were used to assess the studied material in terms of cellular adhesion, proliferation and osteogenic differentiation, because ultimately, the obtained tissue engineered scaffold will be assessed in a preclinical dog model, following an autologous approach. Given the fact the ASCs are similar to periodontal ligament stem cells in terms of phenotype and differentiation potential (50), they could be a suitable alternative for cell-based therapies of periodontal damages (22).

Both layers of the double layer scaffold revealed potential to allow cellular adhesion and proliferation. The cultured cells exhibited a flat and elongated shape typical of the mesenchymal stem cells (23, 24, 49). In SPCL-WS and SPCL-WS-Si, the effect of the functionalization with osteoconductive silanol groups in the cell proliferation and osteogenic differentiation was assessed because the main aim of this layer is to enable cell attachment and promote the formation of new alveolar bone inside the periodontal defect. Although the membrane should have a barrier function, it should allow the adhesion of cells, namely the epithelial cells when placed in contact with the gingiva, or the ligament cells when fitted to the tooth root surface.

The reported release of silicon in the SPCL-WS-Si, as shown in previous studies (25, 26, 51, 52), induced the osteogenesis, as patent by the overexpression of Osteocalcin at the 28th culturing day. In fact, previous works shown that silicon enhances osteoblasts proliferation, differentiation and collagen production, and also have effects on the osteoclasts (52-54). The increased release of calcium and silicon to the solution may favor some degree of reprecipitation which in combination with other important ions like phosphate, existent in stimulated buffer solution (55), in the cell culture medium (54), or in the tissues, can contribute to the formation of the hydroxyapatite on the material and further induce the undifferentiated cells to the osteogenic lineage (25, 26), a key factor for the regeneration of the osseous compartment of the periodontium.

Considering that the scaffold is composed by the two distinct layers, it was possible to obtain an asymmetric material with osteoconductive potential in only one side. This bioactive aspect was developed aiming at be fitted on the alveolar bone defect in order to promote selectively the regeneration of this compartment of the periodontium. The porous structure of the 3D fiber mesh structure is expected to induce the proliferation of the bone cells and the integration of the scaffold in the adjacent bone tissue and ingrowth of new bone.

Depending on the type of defect, which can vary in terms of size, shape and type of damaged tissue, the scaffold might be implanted differently in order to fit adequately in the defect. The membrane layer is important to be placed adjacently to the gingiva in order to avoid the migration of epithelial cells into the periodontal defect through the root surface. Moreover, when the lesion affects the radicular periodontal ligament and cementum, it is important to mold the scaffold in order to make sure that the membrane layer is adjusted to the tooth root creating an occlusive space for regeneration of periodontal ligament avoiding the influence of the gingival epithelium migration and avoiding the risk of ankylosis with the adjacent bone.

5. Conclusion

This work proposed an innovative approach for designing a double layer scaffold to address the structural and biological requirements for the regeneration of periodontal defects.

The obtained data allowed to demonstrate that this scaffold, combining the advantageous features of the two different layers in a single construct, exhibits adequate physicochemical and biological characteristics to be used in therapeutic approaches leading to the regeneration of periodontal tissues.

Therefore, this construct may provide a new solution to the current clinical needs, being an alternative to the mixed techniques using allograft and autografts bone combined with guided tissue regeneration membranes in the dentistry and orthopaedic medical field, both in human and in veterinary medicine. Nevertheless, further studies, particularly using animal models, are required to demonstrate the full potential of the proposed construct in the regeneration of periodontal defects.

6. Acknowledgements

The research leading to these results has received funding from the European Union's Seventh Framework Programme (FP7/2007-2013) under grant agreement n° REGPOT-CT2012-316331-POLARIS and from the Portuguese Foundation for Science and Technology (FCT) under the project (ref. MIT/ECE/0047/2009). João Requicha acknowledges the FCT for his PhD scholarship (SFRH/BD/44143/2008).

7. References

1. Chen FM, Jin Y. Periodontal tissue engineering and regeneration: current approaches and expanding opportunities. Tissue Engineering Part B-Reviews. 2010;16 (2):219-55.

2. Bosshardt DD, Sculean A. Does periodontal tissue regeneration really work? Periodontology 2000. 2009;51:208-19.

3. Kuo L-C, Polson AM, Kang T. Associations between periodontal diseases and systemic diseases: A review of the inter-relationships and interactions with diabetes, respiratory diseases, cardiovascular diseases and osteoporosis. Public Health. 2008;122 (4):417-33.

4. Lin NH, Gronthos S, Bartold PM. Stem cells and periodontal regeneration. Australian Dental Journal. 2008;53 (2):108-21.

5. Wikesjo UME, Nilveus R. Periodontal repair in dogs: Healing patterns in large circumferential periodontal defects. Journal of Clinical Periodontology. 1991;18 (1):49-59.

6. Tobita M, Uysal AC, Ogawa R, Hyakusoku H, Mizuno H. Periodontal tissue regeneration with adipose-derived stem cells. Tissue Engineering Part A. 2008;14 (6):945-53.

7. Karring T, Nyman S, Gottlow JAN, Laurell L. Development of the biological concept of guided tissue regeneration - animal and human studies. Periodontology 2000. 1993;1 (1):26-35.

8. Wikesjo UME, Lim WH, Thomson RC, Hardwick WR. Periodontal repair in dogs: gingival tissue occlusion, a critical requirement for GTR? Journal of Clinical Periodontology. 2003;30 (7):655-64.

9. Park YJ, Lee YM, Park SN, Lee JY, Ku Y, Chung CP, *et al*. Enhanced guided bone regeneration by controlled tetracycline release from poly (L-lactide) barrier membranes. Journal of Biomedical Materials Research. 2000;51 (3):391-7.

10. Kurtis B, Unsal B, Cetiner D, Gultekin E, Ozcan G, Celebi N, *et al*. Effect of polylactide/glycolide (PLGA) membranes loaded with metronidazole on periodontal regeneration following guided tissue regeneration on dogs. Journal of Periodontology. 2002;73 (7):694-700.

11. Quinones CR, Caton JG, Polson AM, Wagener CJ, Mota LF. Evaluation of a synthetic biodegradable barrier to facilitate guided tissue regeneration. . Advances in Dental Research. 1991;5 (1):85.

12. Galgut PN. Oxidized cellulose mesh used as a biodegradable barrier membrane in the technique of guided tissue regeneration. A case report. J Periodontol. 1990;61 (12):766-8.

13. Liao S, Wang W, Uo M, Ohkawa S, Akasaka T, Tamura K, *et al*. A three-layered nano-carbonated hydroxyapatite/collagen/PLGA composite membrane for guided tissue regeneration. Biomaterials. 2005;26 (36):7564-71.

14. Pitaru S, Tal H, Soldinger M, Noff M. Collagen membranes prevent apical migration of epithelium and support new connective-tissue attachment during periodontal wound-healing in dogs. Journal of Periodontal Research. 1989;24 (4):247-53.

15. Card SJ, Caffesse RG, Smith BA, Nasjleti CE. New attachment following the use of a resorbable membrane in the treatment of periodontitis in dogs. Int J Periodontics Restorative Dent. 1989;9 (1):58-69.

16. Ho MH, Hsieh CC, Hsiao SW, Thien DVH. Fabrication of asymmetric chitosan GTR membranes for the treatment of periodontal disease. Carbohydrate Polymers. 2010;79 (4):955-63.

17. Mota J, Yu N, Caridade SG, Luz G, Gomes ME, Reis RL, *et al*. Chitosan/bioactive glass nanoparticle composite membranes for periodontal regeneration. Acta Biomaterialia. 2012;8 (11):4173-80.

18. Yang F, Both SK, Yang XC, Walboomers XF, Jansen JA. Development of an electrospun nano-apatite/PCL composite membrane for GTR/GBR application. Acta Biomaterialia. 2009;5 (9):3295-304.

19. Chang CY, Yamada S. Evaluation of the regenerative effect of a 25% doxycycline-loaded biodegradable membrane for guided tissue regeneration. Journal of Periodontology. 2000;71 (7):1086-93.

20. Albuquerque C, Morinha F, Requicha J, Martins T, Dias I, Guedes-Pinto H, *et al*. Canine periodontitis the dog as an important model for periodontal studies. Vet J. 2012;191 (3):299-305.

21. Persson GR, Persson RE. Cardiovascular disease and periodontitis: an update on the associations and risk. Journal of Clinical Periodontology. 2008;35:362-79.

22. Requicha JR, Viegas CA, Muñoz F, Reis RL, Gomes ME. Periodontal tissue engineering strategies based on non-oral stem cells. The Anatomical Record. 2013;invited review:accepted for publication.

23. Dominici M, Le Blanc K, Mueller I, Slaper-Cortenbach I, Marini FC, Krause DS, *et al*. Minimal criteria for defining multipotent mesenchymal stromal cells. The International Society for Cellular Therapy position statement. Cytotherapy. 2006;8 (4):315-7.

24. Requicha J, Viegas C, Albuquerque C, Azevedo J, Reis R, Gomes M. Effect of anatomical origin and cell passage number on the stemness and osteogenic differentiation potential of canine adipose-derived stem cells. Stem Cell Reviews and Reports. 2012;8 (4):1211-22.

25. Leonor IB, Rodrigues MT, Gomes ME, Reis RL. In situ functionalization of wet-spun fibre meshes for bone tissue engineering. J Tissue Eng Regen Med. 2011;5 (2):104-11.

26. Rodrigues AI, Gomes ME, Leonor IB, Reis RL. Bioactive starch based scaffolds and human adipose stem cells are a good combination for bone tissue engineering. Acta Biomaterialia. 2012;8:3765–76.

27. Ni S, Chang J, Chou L, Zhai W. Comparison of osteoblast-like cell responses to calcium silicate and tricalcium phosphate ceramics in vitro. J Biomed Mater Res B Appl Biomater. 2007;80 (1):174-83.

28. Oyane A, Kawashita M, Nakanishi K, Kokubo T, Minoda M, Miyamoto T, *et al*. Bonelike apatite formation on ethylene-vinyl alcohol copolymer modified with silane coupling agent and calcium silicate solutions. Biomaterials. 2003;24 (10):1729-35.

29. Tvedten H. Listing of selected reference values. In: Willard M, Tvedten H, editors. Small Animal Clinical Diagnosis by Laboratory Methods. 5th ed. St. Louis: Elsevier Saunders; 2012. p. 399-402.

30. Livak KJ, Schmittgen TD. Analysis of relative gene expression data using real-time quantitative PCR and the 2 (T) (-Delta Delta C) method. Methods. 2001;25 (4):402-8.

31. Elzein T, Nasser-Eddine M, Delaite C, Bistac S, Dumas P. FTIR study of polycaprolactone chain organization at interfaces. Journal of Colloid and Interface Science. 2004;273 (2):381-7.

32. Pashkuleva I, Azevedo HS, Reis RL. Surface structural investigation of starch-based biomaterials. Macromolecular Bioscience. 2008;8 (2):210-9.

33. Eglin D, Ali SAM, Perry CC. A statistical study of poly (epsilon-caprolactone) crystallinity in poly (epsilon-caprolactone)-silica sol-gel materials and their in vitro calcium phosphate-forming ability. Polymer International. 2003;52 (12):1807-19.

34. Nie KM, Zheng SX, Lu F, Zhu QR. Inorganic-organic hybrids involving poly (epsilon-caprolactone) and silica network: Hydrogen-bonding interactions and isothermal crystallization kinetics. J Polym Sci Pol Phys. 2005;43 (18):2594-603.

35. Puppi D, Piras AM, Chiellini F, Chiellini E, Martins A, Leonor IB, *et al*. Optimized electro- and wet-spinning techniques for the production of polymeric fibrous scaffolds loaded with bisphosphonate and hydroxyapatite. Journal of Tissue Engineering and Regenerative Medicine. 2011;5 (4):253-63.

36. Martins A, Chung S, Pedro AJ, Sousa RA, Marques AP, Reis RL, *et al*. Hierarchical starch-based fibrous scaffold for bone tissue engineering applications. Journal of Tissue Engineering and Regenerative Medicine. 2009;3 (1):37-42.

37. Rodrigues MT, Gomes ME, Viegas CA, Azevedo JT, Dias IR, Guzon FM, *et al*. Tissue-engineered constructs based on SPCL scaffolds cultured with goat marrow cells: functionality in femoral defects. Journal of Tissue Engineering and Regenerative Medicine. 2011;5 (1):41-9.

38. Oliveira AL, Pedro AJ, Arroyo CS, Mano JF, Rodriguez G, San Roman J, *et al*. Biomimetic Ca-P coatings incorporating bisphosphonates produced on starch-based degradable biomaterials. Journal of Biomedical Materials Research Part B-Applied Biomaterials. 2010;92B (1):55-67.

39. Duarte ARC, Mano JF, Reis RL. Supercritical phase inversion of starch-poly (epsilon-caprolactone) for tissue engineering applications. Journal of Materials Science-Materials in Medicine. 2010;21 (2):533-40.

40. Gomes ME, Bossano CM, Johnston CM, Reis RL, Mikos AG. In vitro localization of bone growth factors in constructs of biodegradable scaffolds seeded with marrow stromal cells and cultured in a flow perfusion bioreactor. Tissue Eng. 2006;12 (1):177-88.

41. Santos TC, Marques AP, Horing B, Martins AR, Tuzlakoglu K, Castro AG, *et al*. In vivo short-term and long-term host reaction to starch-based scaffolds. Acta Biomater. 2010;6 (11):4314-26.

42. Azevedo HS, Gama FM, Reis RL. In vitro assessment of the enzymatic degradation of several starch based biomaterials. Biomacromolecules. 2003;4 (6):1703-12.

43. Martins AM, Pham QP, Malafaya PB, Sousa RA, Gomes ME, Raphael RM, *et al*. The role of lipase and alpha-amylase in the degradation of starch/poly (epsilon-caprolactone) fiber meshes and the osteogenic differentiation of cultured marrow stromal cells. Tissue Eng Part A. 2009;15 (2):295-305.

44. Ku Y, Shim IK, Lee JY, Park YJ, Rhee S-H, Nam SH, *et al*. Chitosan/poly (L-lactic acid) multilayered membrane for guided tissue regeneration. Journal of Biomedical Materials Research Part A. 2009;90A (3):766-72.

45. Milella E, Ramires PA, Brescia E, La Sala G, Di Paola L, Bruno V. Physicochemical, mechanical, and biological properties of commercial membranes for GTR. J Biomed Mater Res. 2001;58 (4):427-35.

46. Lee EJ, Teng SH, Jang TS, Wang P, Yook SW, Kim HE, *et al*. Nanostructured poly (epsilon-caprolactone)-silica xerogel fibrous membrane for guided bone regeneration. Acta Biomaterialia. 2010;6 (9):3557-65.

47. Woodruff MA, Hutmacher DW. The return of a forgotten polymer-Polycaprolactone in the 21st century. Progress in Polymer Science. 2010;35 (10):1217-56.

48. Rada T, Reis RL, Gomes ME. Distinct stem cells subpopulations isolated from human adipose tissue exhibit different chondrogenic and osteogenic differentiation potential. Stem Cell Rev. 2011;7 (1):64-76.

49. Zuk PA, Zhu M, Ashjian P, De Ugarte DA, Huang JI, Mizuno H, *et al*. Human adipose tissue is a source of multipotent stem cells. Molecular Biology of the Cell. 2002;13 (12):4279-95.

50. Kato T, Hattori K, Deguchi T, Katsube Y, Matsumoto T, Ohgushi H, *et al*. Osteogenic potential of rat stromal cells derived from periodontal ligament. Journal of Tissue Engineering and Regenerative Medicine. 2011;5 (10):798-805.

51. Pietak AM, Reid JW, Stott MJ, Sayer M. Silicon substitution in the calcium phosphate bioceramics. Biomaterials. 2007;28 (28):4023-32.

52. Reffitt DM, Ogston N, Jugdaohsingh R, Cheung HF, Evans BA, Thompson RP, *et al*. Orthosilicic acid stimulates collagen type 1 synthesis and osteoblastic differentiation in human osteoblast-like cells in vitro. Bone. 2003;32 (2):127-35.

53. Xynos ID, Edgar AJ, Buttery LDK, Hench LL, Polak JM. Gene-expression profiling of human osteoblasts following treatment with the ionic products of Bioglass® 45S5 dissolution. Journal of Biomedical Materials Research. 2001;55 (2):151-7.

54. Zou S, Ireland D, Brooks RA, Rushton N, Best S. The effects of silicate ions on human osteoblast adhesion, proliferation, and differentiation. Journal of Biomedical Materials Research Part B-Applied Biomaterials. 2009;90B (1):123-30.

55. Kokubo T, Matsushita T, Takadama H, Kizuki T. Development of bioactive materials based on surface chemistry. J Eur Ceram Soc. 2009;29 (7):1267-74.

Chapter VI

A tissue engineering approach for periodontal regeneration based on a biodegradable double layer scaffold and adipose-derived stem cells

Abstract

Human and canine periodontium are often affected by an inflammatory pathology called periodontitis, which is associated with severe damages across tissues, namely in the periodontal ligament, cementum and alveolar bone. However, the therapies used in the routine dental practice, often consisting in a combination of different techniques, and do not allow to fully restore the functionality of the periodontium.

Tissue Engineering (TE) appears as a valuable alternative approach to regenerate periodontal defects but for this purpose, it is essential to develop supportive biomaterials and stem cells sourcing/culturing methodologies that address the complexity of the various tissues affected by this condition.

The main aim of this work was to study the *in vitro* functionality of a newly developed double layer scaffold for periodontal Tissue Engineering. The scaffold design was based on a combination of a 3D fiber mesh functionalized with silanol groups and a membrane, both made of a blend of starch and poly (ε-caprolactone) (SPCL). Adipose-derived stem cells (cASCs) were seeded and cultured onto such scaffolds, and the obtained constructs were evaluated in terms of cellular morphology, metabolic activity and proliferation. The osteogenic potential of the fiber mesh layer functionalized with silanol groups was further assessed concerning the osteogenic differentiation of the seeded and cultured ASCs. The obtained results showed that the proposed double layer scaffold supports the proliferation and selectively promotes the osteogenic differentiation of cASCs seeded onto the functionalized mesh. These findings suggest that the 3D structure and asymmetric composition of the scaffold in combination with stem cells may provide the basis for developing alternative therapies to treat periodontal defects more efficiently.

---

*This Chapter is based on the following publication:

Requicha JF, Viegas CA, Leonor IB, Reis RL, Gomes ME. A tissue engineering approach for periodontal regeneration based on a biodegradable double layer scaffold and adipose-derived stem cells. Submitted

1. Introduction

The tooth is involved by a complex organ, called periodontium, which comprises different tissues, namely the alveolar bone, maxilla and mandible, the cementum (which is part of the tooth root), the periodontal ligament (PDL) and the gingiva (1). The above mentioned structures have an important role in the chewing sensibility and, above all, act as a dynamic support apparatus for the tooth structure (2). Periodontitis is the most important periodontal pathology, known to cause tissue destruction that leads to tooth exfoliation, when not treated in due time (3, 4). The main goals of current periodontal therapies are to preserve the natural dentition, as well as the aesthetics and function of the periodontium. However, none of the currently available treatments for treating periodontal defects has shown the ability to restore completely the functionality of all the damaged tissues. A complete regeneration is only achieved when the Sharpey's fibers of the PDL between the bone and the radicular cementum are formed with oblique orientation, and when it is possible to avoid the expansion of the gingival epithelium and connective tissue into the lesion, as well as the occurrence of the ankylosis and radicular resorption (1, 4-6).

In the clinical routine, the periodontologists are forced to combine different techniques in order to achieve better results. However, the outcomes are quite variable and difficult to predict. Tissue Engineering (TE), using supportive biomaterials and cells, might provide new approaches for periodontal regeneration as it suggested in recent scientific reports (7-12). Different strategies have been proposed, including the use of adipose-derived stem cells combined with platelet rich plasma (7), collagen sponges seeded with autologous periodontal ligament (PDL) cells (11), autologous bone marrow stem cells (BMSCs) laden in a collagen gel (10), and a combination of multi-layered PDL cell sheets with a poly (glycolic acid) membrane and with a tricalcium phosphate (9). However, these strategies have not shown a clear potential to enhance, synchronically, the alveolar bone regeneration and the formation of a new functional PDL.

In previous studies, we have developed a scaffold specifically designed for periodontal regeneration, which is composed by two layers combined in a single matrix: a starch plus poly (ε-caprolactone) (SPCL) membrane aiming at acting as physical barrier between the gingival epithelium and the bone and ligament compartment of periodontium, creating a selective space for bone and PDL regeneration; and a SPCL fiber mesh functionalized with osteoconductive silanol groups, which is aimed at promoting new bone formation (13-15). The characterization of these constructs performed so far, namely regarding the morphology/structure, surface chemical composition, mechanical properties and *in vitro* degradability, suggests their suitability for the envisioned application (16).

The present work focused on studying the *in vitro* behaviour of ASCs seeded and cultured onto both layers of the described scaffold, to further assess the potential of this Tissue Engineering scaffold for the proposed application. The potential of such scaffold for the envisioned application can only be fully assessed upon performing *in vivo* studies in relevant animal models. Nevertheless, the *in vitro* studies are expected to demonstrate the ability of the proposed double layer scaffold to promote either cellular proliferation or osteogenic differentiation, onto the membrane and fiber mesh layers, respectively. Adipose-derived stem cells have been extensively described in terms of stemness and osteogenic differentiation capacity and proposed for the treatment of distinct pathological conditions, including in tissue engineered approaches for periodontal regeneration (7, 17, 18). ASCs seeded/cultured onto the membrane layer, were characterized in terms of adhesion, proliferation and metabolic activity and ASCs seeded/cultured onto the fiber mesh layer, were further evaluated concerning their osteogenic differentiation by real time RT-PCR and alkaline phosphatase (ALP) activity analysis.

This versatile double layer material was shown to enhance osteogenic differentiation of ASCs cultured onto the fiber mesh layer functionalized with silanol groups. Additionally, it was observed that the membrane has the potential to allow the adhesion and proliferation of the undifferentiated ASCs.

2. Materials and Methods

2.1. Preparation of the materials

The double layer scaffolds were prepared from a blend of starch and poly (ε-caprolactone) (30:70% w/w) (Novamont, Italy) (SPCL) by combining two different components/layers: a wet-spun fiber mesh and a solvent casting membrane (Fig. 6.1A) as described previously (16). Briefly, to prepare the fiber meshes, the SPCL was dissolved in chloroform (Sigma-Aldrich, Germany) at a concentration of 20% (w/v). This solution was loaded into a 5 mL plastic syringe with a metallic needle (21 G×1.5”), which was connected to a programmable syringe pump (KD Scientific, World Precision Instruments, UK). The solution was injected at a controlled pumping rate of 5 mL/h into the coagulation bath that was randomly moved to allow the formation of the fiber mesh structure. Two different coagulation baths were used: methanol (Vaz Pereira, Portugal) to produce the SPCL wet-spun fiber meshes (SPCL-WS) and a calcium silicate solution produce SPCL wet-spun fiber meshes functionalized with silanol groups (SPCL-WS-Si) as described previously (13, 14, 16). SPCL-WS were then dried at room temperature overnight in order to remove any remaining solvents and the SPCL-WS-Si were dried at 60 ºC for 24 hours.

The membrane was obtained by casting 3 mL of the same polymeric solution onto a 5 cm diameter either patterned/non-patterned Teflon mold, in order to obtain patterned (SPCL-P) or smooth/non-patterned (SPCL-NP) membranes, respectively. The objective was to analyze the effect of topography on the cellular attachment and proliferation. Membranes were dried in a hood and then cut into discs samples of 6 mm of diameter.

Both membranes and fiber meshes were cut into 6mm diameter samples and sterilized by ethylene oxide before the biological assays described below.

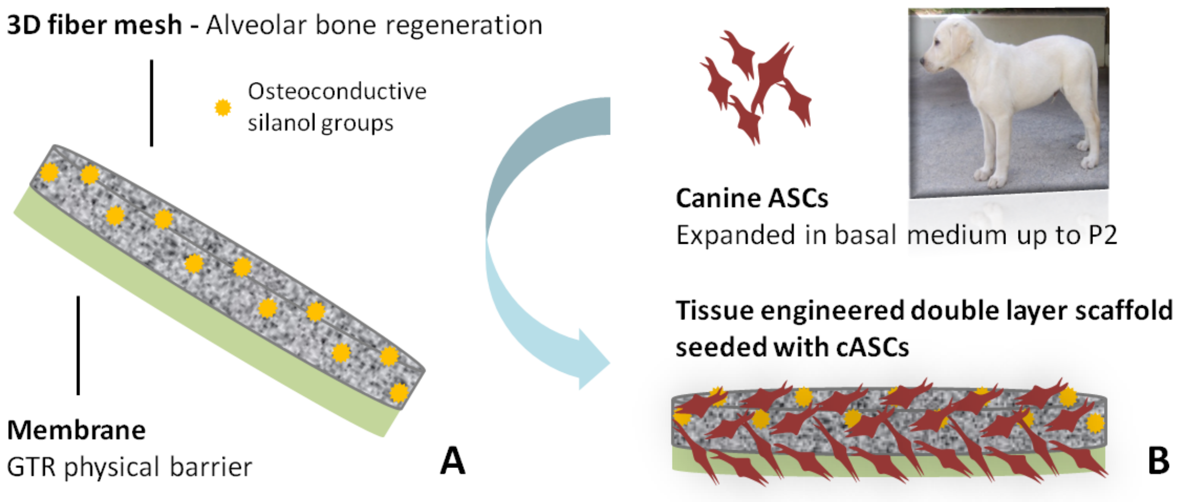
3D fiber mesh - Alveolar bone regeneration
Osteoconductive silanol groups
Membrane
GTR physical barrier
A
Canine ASCs
Expanded in basal medium up to P2
Tissue engineered double layer scaffold seeded with cASCs
B

Layers	Description	Abbreviation	Characterization
SPCL membranes	Non-patterned	SPCL-NP	SEM, DNA, MTS
	Patterned	SPCL-P	
SPCL wet-spun fiber mesh	Non-functionalized with silanol groups	SPCL-WS	SEM, DNA, MTS, ALP, PCR
	Functionalized with silanol groups	SPCL-WS-Si	

C

Figure 6. 1 – Schematic representation of the envisioned tissue engineering strategy based on the use of a double layer scaffold with two different target functionalities (A) to culture the harvested/isolated canine ASCs (B). Description of the different components (C).

2.2. Seeding/culturing of the canine ASCs onto materials

Canine adipose stem cells (cASCs) were isolated from subcutaneous abdominal tissue of adult healthy dogs and expanded in basal medium composed of Dulbecco Modified Eagle

Medium (DMEM) (Sigma Aldrich, Germany) supplemented with 10% fetal bovine serum (FBS; Invitrogen, USA) and 1% antibiotic/antimicotic (Sigma, USA) until passage 2 (P2), as described in a previous work (18) (Fig. 6.1B). The rationale behind the use of canine ASCs resides in the fact that dog is the most suitable animal model used in Periodontology, and thus this could facilitate the future autologous assessment of the proposed Tissue Engineering approach.

The two components of the double layer scaffolds were assessed separately by seeding/culturing them with ASCs, as we intent to analyze their distinct functionalities.

The SPCL-P and SPCL-NP membranes were seeded with 5.0×10^4 cASCs/sample and then maintained in basal medium for 2h to allow cell attachment. Afterwards, 1 mL of medium was added to each culture well and cell-seeded membranes were further cultured for 1, 3, 7 and 14 days.

The SPCL-WS and SPCL-WS-Si fiber meshes were seeded with cASCs at a concentration of 1.0×10^5 cells/sample and then cultured in either basal or osteogenic medium, containing alpha Modification Eagle Medium (α-MEM) (Sigma Aldrich, Germany), 10% FBS, 1% antibiotic/antimicotic supplemented with 50 µg/mL ascorbic acid (Sigma, USA), 10^{-8} M dexamethasone (Sigma, USA) and 10 mM β-glycerophosphate (Sigma, USA) for 7, 14, 21 and 28 days.

2.3. Characterization of the membranes/fiber meshes cultured with canine ASCs

After each selected culturing period of time, the culture medium was aspirated and the cell-membrane/fiber mesh samples were carefully washed with sterile PBS and then, characterized using different techniques, namely, SEM, histology, DNA quantification, MTS assay, ALP activity analysis and PCR analysis, as described in detail bellow.

2.3.1. Cellular morphology

Scanning electron microscopy

For scanning electron microscopy (SEM) evaluation, samples were fixed in 2.5% glutaraldehyde (Merck Milipore, Germany) solution in PBS for one hour at 4 ºC and then dehydrated by immersion in a series of ethanol-water solutions with increasing concentration (30%, 50%, 70%, 90% and 100%, v/v). Afterwards, the samples were dried at room temperature overnight.

SEM was performed using Hitachi SU-70 UHR Schottky (Hitachi, Japan) equipment. Prior to any SEM observations, all the scaffolds were sputter-coated with gold (Polaron SC502, Fisons Instruments, UK). Three samples of each material/condition under study were analyzed.

Histology – Donath technique

The SPCL-WS and SPCL-WS-Si, cultured along 28 days with cASCs in both culturing conditions, were fixed in 4% phosphate-buffered formalin for one hour at 4 ºC for further histological analysis by the Donath technique.

Briefly, the fiber meshes-cells constructs were dehydrated in alcohol solutions of increased concentrations, embedded in glycol methacrylate (Technovit 7200 VLC, Heraeus Kulzer, Germany) and processed for ground sectioning according to the method described by Donath and Breuner (19). The slides with a thickness of approximately 30 µm were prepared by micro-cutting and grinding (Exakt, Norderstedt, Germany), and stained using a modified Lévai Laczkó stain (20).

2.3.2. Cellular metabolic activity

Cell metabolic activity was assessed using the MTS test. For this purpose, the cultured constructs (membranes and fiber meshes seeded/cultured with cASCs), retrieved at different time points, were rinsed with PBS, immersed in a mixture consisting of serum-free cell culture medium and MTS reagent (VWR, USA) in a 5:1 ratio and incubated for 3 hours at 37 °C in a humidified atmosphere containing 5% CO_2. Subsequently, 200 µL of this mixture were transferred to new 96-well plates and finally the optical density (OD) was measured on a microplate reader (BioTek, USA) using an absorbance of 490 nm.

2.3.3. Cellular proliferation

Double strain DNA (dsDNA) quantification was performed to assess the proliferation of the cASCs seeded/cultured onto the membranes and fiber meshes under study. For this purpose, samples removed from culture were rinsed twice in a PBS solution and transferred into 1.5 mL microtubes containing 1 mL ultra-pure water. Afterwards, the samples were incubated for 1 hour at 37 ºC in a water-bath and stored in a -80 ºC freezer, promoting a thermal shock variation and thus inducing cell lysis. Before assessing DNA levels, constructs were thawed and sonicated for 15 min.

A fluorimetric dsDNA quantification kit (PicoGreen, Molecular Probes, USA) was used to determine the cellular proliferation. Samples and standards (0-2 µg/mL) were prepared in triplicate. Briefly, in each well of a 96-well white plate (Costar; Becton-Dickinson, USA), were deposited 28.7 µL of sample or of each standard, 71.3 µL of PicoGreen solution and 100 µL 1X (Life Technologies, USA), then the plate was incubated for 10 min in the dark and the fluorescence was read using a microplate reader (BioTek, USA) at an excitation of 485/20 nm and an emission of 528/20 nm. A standard curve was developed in order to read DNA values of samples from the standard graph.

2.3.4. Osteogenic differentiation of the canine ASCs on the wet-spun fiber meshes

Alkaline phosphatase activity

Alkaline phosphatase (ALP) activity assay was used to assess the osteogenic differentiation of the cASCs cultured onto the wet-spun fiber mesh layers, SPCL-WS and SPCL-WS-Si. For this purpose, in each well of a 96-well plate (Costar; Becton-Dickinson, USA) were added 20 µL of each sample (the same used for DNA assay) plus 60 µL of a substrate solution consisting of 0.2% (wt/v) p-nytrophenyl phosphate (Sigma, Germany) in a substrate buffer with 1M diethanolamine HCl (Merck, Germany), pH 9.8. The plate was then incubated in the dark for 45 min at 37 ºC. After this incubation period, 80 µL stop solution [2 M NaOH (Panreac, Spain) plus 0.2 mM EDTA (Sigma, Germany)] was added to each well. Standards were prepared with p-nytrophenol (Sigma, Germany) in order to achieve final concentrations in the range 0-0.3 µM/mL. Samples and standards were prepared in triplicates. Absorbance was read at 405 nm and sample concentrations were read from the standard.

Gene expression of specific osteogenic markers

Real time RT-PCR analysis was performed to analyse the relative gene expression of specific osteogenic markers, namely, *Collagen type I α1* (*COLIA1*), *Runt-related transcription factor 2* (*RUNX2*) and *Osteocalcin* (Table 6.1) on the SPCL-WS and SPCL-WS-Si cultured with cASCs. For this purpose, the samples retrieved at each time point were kept in 800 µL of TRIzol reagent (Invitrogen, USA). The mRNA was extracted with TRIzol following the procedure provided by the supplier. Briefly, after an incubation of 5 min at 4 ºC, additional 160 µL of chloroform (Sigma Aldrich, Germany) were added; the samples were incubated for 15 min at 4 °C and then centrifuged at 13000 rpm for 15 min at the same temperature. Subsequently, the aqueous part was collected and an equal part of isopropanol (VWR, USA) was added. The samples were further incubated for 2 hours at -20 °C and afterwards washed in ethanol, centrifuged at 4 °C and 9000 rpm for 5 min and resuspended in 12 µL of

RNase/DNase free water (Gibco, UK). The samples were quantified using the NanoDrop ND1000 Spectrophotometer (NanoDrop Technologies, USA). For the cDNA synthesis the samples with a 260/280 ratio between 1.7 and 2.0 were used. The cDNA synthesis was performed in the Mastercycler real time PCR equipment (Eppendorf, USA) using the iScript cDNA Synthesis Kit (Quanta Biosciences, USA) with an initial amount of mRNA of 2 µg in a total volume of 20 µL. RNAse free water (Gibco, UK) was used as a negative control.

Table 6. 1 – Primer sequences for targeted cDNAs.

Primer	**RefSeqID**	**Product length (bp)**	**5′-3′ sequence (F, forward; R, reverse)**
COL1A1	ENSCAFT00000026953	170	F: ATGCCATCAAGGTTTTCTGC R: CTGGCCACCATACTCGAACT
Osteocalcin	ENSCAFT00000026668	166	F: GATCGTGGAAGAAGGCAAAG R: AGCCTCTGCCAGTTGTCTGT
RUNX2	ENSCAFT00000020482	148	F: CAGACCAGCAGCACTCCATA R: CAGCGTCAACACCATCATTC
GAPDH	NM_001003142.1	238	F: CCAGAACATCATCCCTGCTT R: GACCACCTGGTCCTCAGTGT

After the synthesis of the cDNA, real time PCR analysis was performed using in the Mastercycler real time PCR equipment (Eppendorf, USA) using the PerfeCta Sybr-Green FastMix (Quanta Biosciences, USA) to analyze the relative expression of the three studied markers in each sample, using GAPDH as housekeeping gene. The primers were previously designed using the Primer 3 Plus v0.4.0 (MWG Biotech, Germany) (Table 6.1). The Delta Delta Ct method, according to Livak and Schmittgen (2001) (21), was performed using the data obtained for the cell-fiber mesh constructs upon seeding as calibrator.

2.4. Statistical analysis

The obtained results were elaborated using the software JMP v9.0.1 (SAS Institute Inc., USA). The statistical significance was assessed by the ANOVA single factor method. Data was presented as mean ± standard error of the mean (SEM) and differences between data groups were considered to be statistically significant for $p<0.05$ (Student's t-test).

3. Results

3.1. Cellular morphology

SEM micrographs of the membrane layer (Fig. 6.2A) upon 1, 7, 14 and 21 days on culture with cASCs revealed a good attachment of the cells onto both surface types (patterned and non-patterned), exhibiting an elongated shape, typical of the mesenchymal stem cells. It was not possible to observe differences in the attachment or morphology of the cells seeded onto the two different membranes.

Regarding the wet spun fiber meshes (Fig. 6.2B), SEM observation suggest that both functionalized and non-functionalized materials allowed attachment and uniform distribution of the seeded cells, independently of the culturing conditions, either basal or osteogenic medium. The images show a clear increase in the amount of cells along the culturing time and suggest the formation of an extracellular matrix (ECM) that in some cases covered almost the fiber mesh at the latest time point studied.

The histological sections of the SPCL-WS and SPCL-WS-Si stained with Lévai Laczkó (Fig. 6.3) shown that a monolayer of cells was formed along the surface of the fiber meshes. Moreover, these cells did not migrate throughout the material to the opposite layer of the material.

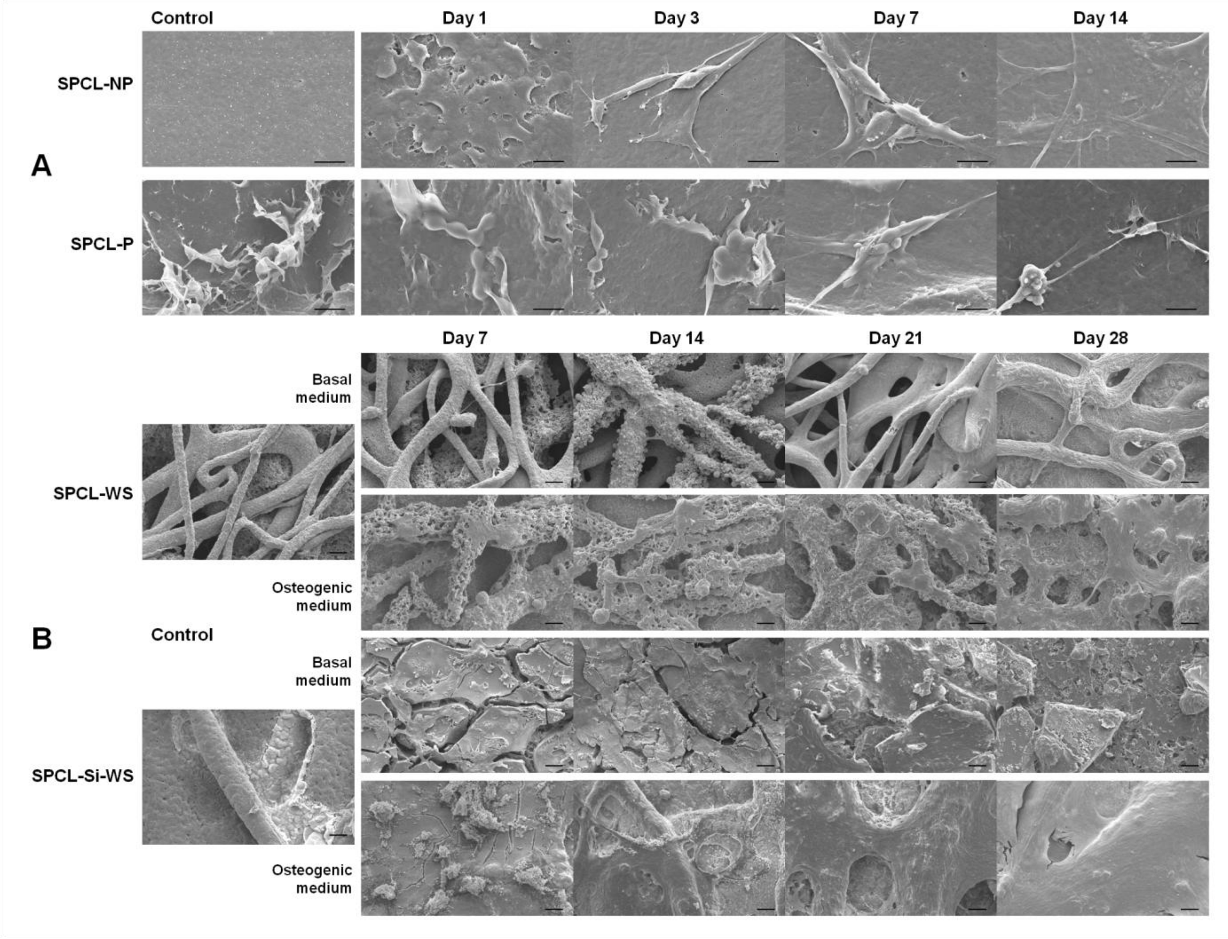
Control
Day 1
Day 3
Day 7
Day 14
SPCL-NP
A
SPCL-P
Day 7
Day 14
Day 21
Day 28
Basal medium
SPCL-WS
Osteogenic medium
B
Control
Basal medium
SPCL-Si-WS
Osteogenic medium

Figure 6. 2 – SEM micrographs of: A) patterned (SPCL-P) and non-patterned (SPCL-NP) membranes cultured with cASCs for 1, 3, 7 and 14 days in basal medium (scale bar = 20 µm). B) SPCL-WS and SPCL-WS-Si cultured with cASCs for 7, 14, 21 and 28 days in both basal medium and in osteogenic medium (scale bar = 100 µm).

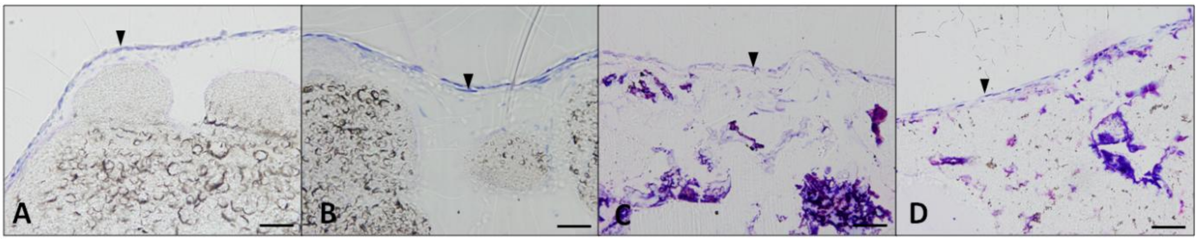

Figure 6. 3 – Optical microscopy images of cASCs (indicated by the arrows) cultured on the SPCL-WS (A, B) and SPCL-WS-Si (C, D) for 28 days both in basal (A, C) and in osteogenic medium (B, D) (Lévai Laczkó staining, scale bar = 100 µm).

3.2. Cellular metabolic activity – MTS assay

In terms of cells metabolic activity, the values were found higher for the cASCs cultured on the patterned (SPCL-P) than for non-patterned (SPCL-NP) membranes (Fig. 6.4A), particularly, in the later culturing times. The metabolic activity of the cells cultured onto the SPCL-WS and SPCL-WS-Si layer (Fig. 6.4B) was generally found higher in the functionalized fiber meshes (SPCL-WS-Si), particularly in the last day of culture. It was also possible to observe that the different culturing medium used did not induce any significant effect in the metabolic activity of cells cultured in the different fiber meshes.

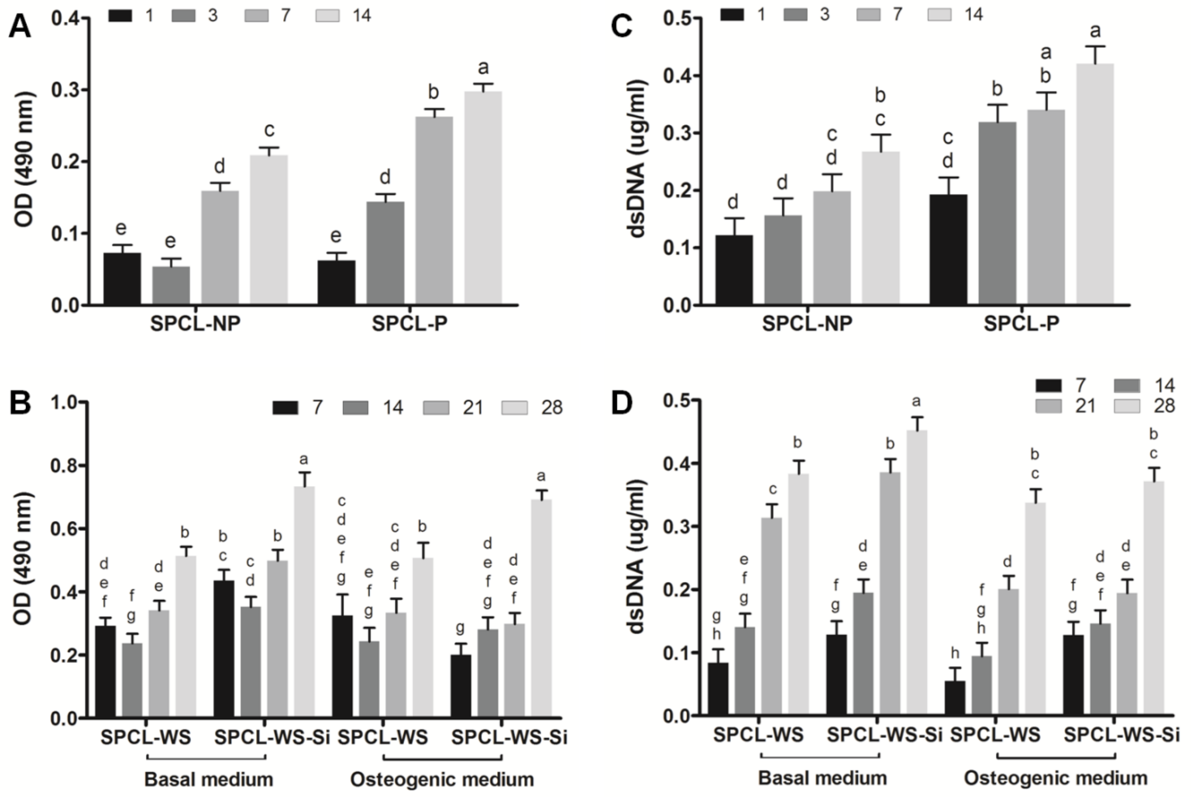

Figure 6. 4 – cASCs metabolic activity (A, B) and proliferation (C, D) upon culturing onto the SPCL-NP and SPCL-P membranes for 1, 3, 7 and 14 days in basal medium (A, C) and culturing onto the SPCL-WS and SPCL-WS-Si for 7, 14, 21 and 28 days in basal and osteogenic medium (B, D). Levels connected by different letters are significantly different (p<0.05, Student's t-test).

3.3. Cellular proliferation – dsDNA assay

In general, the results obtained from the dsDNA assay (Fig. 6.4C) showed increased values along the culturing time for SPCL-P and SPCL-NP, demonstrating that both membranes supported the adhesion and further proliferation of the seeded cASCs. Nevertheless, the cellular content was significantly higher in the SPCL-P as compared to the SPCL-NP, at all the time points.

Similarly, for the fiber meshes (Fig. 6.4D), it was also observed an increase in the cell content with increasing culturing times indicating that cASCs were able to proliferate in both functionalized and non-functionalizes scaffolds cultured either in basal or osteogenic media. However, the first evidence is that, in general, the basal medium promoted a higher cellular proliferation, mainly in the later time points. It is also possible to observe that the functionalization with silanol groups had a positive effect in the cellular proliferation, which is more significant on the cells cultured in basal medium.

3.4. Osteogenic differentiation assessment

The osteogenic differentiation of the cASCs cultured onto the fiber mesh layer was evaluated by alkaline phosphatase (ALP) activity measurement and by real time RT-PCR analysis of the expression profile of three different osteogenic markers, namely *COLIA1, RUNX2* and *Osteocalcin*.

Alkaline phosphatase quantification revealed, in general, a significant increase until the 21th day of culturing followed by a decrease in the last experimental time point (Fig. 6.5). The ALP activity was significantly higher in the cells cultured under osteogenic medium, particularly in the latest time points and for the non-functionalized samples (SPCL-WS).

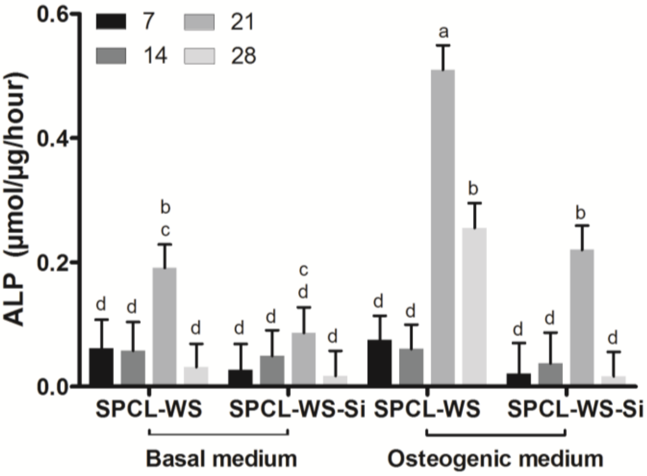

Figure 6. 5 – Alkaline phosphatase activity of the cASCs cultured onto the SPCL-WS and SPCL-WS-Si for 7, 14, 21 and 28 days in basal and osteogenic medium. Levels connected by different letters are significantly different (p<0.05, Student's t-test).

In the Fig. 6.6, it is possible to observe the different expression profiles of the analyzed osteogenic markers.

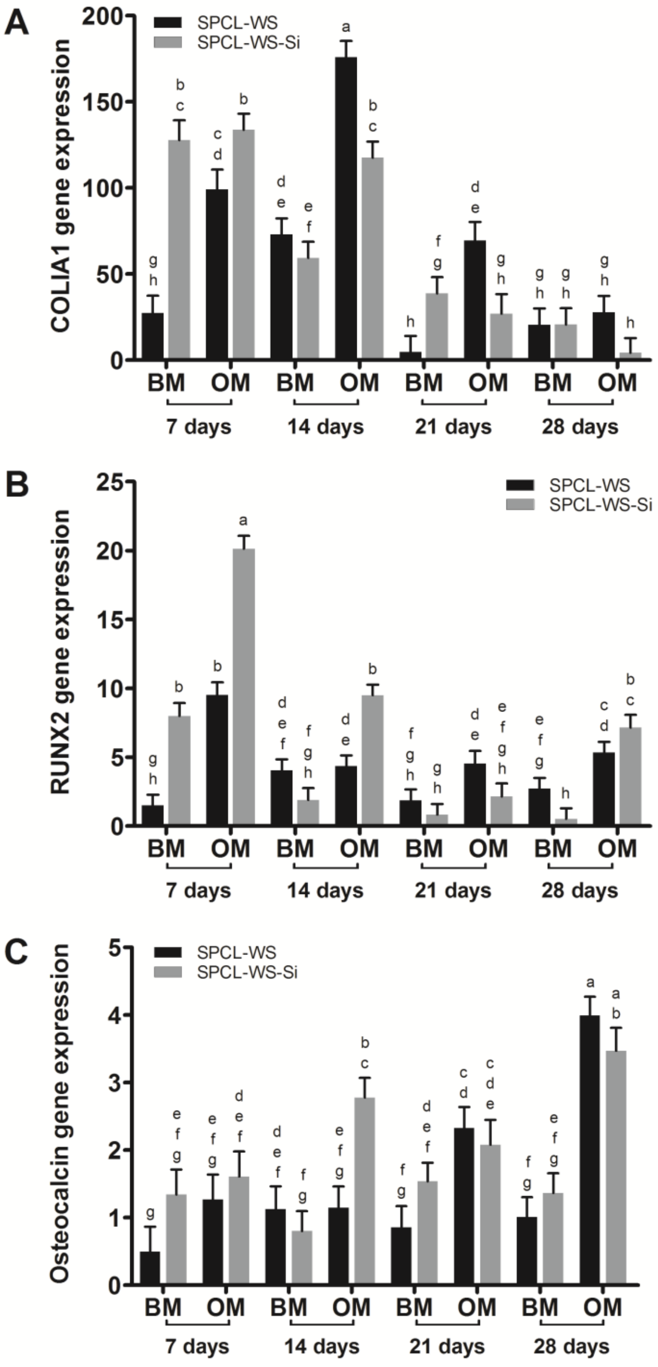

Figure 6. 6 – Real time RT-PCR analysis of osteoblastic genes: COLIA1 (a), RUNX2 (b) and Osteocalcin (c) analyzed in cASCs cultured on the SPCL-WS and SPCL-WS-Si for 7, 14, 21 and 28 days in basal (BM) and osteogenic medium (OM) (mean ± SEM). Considering each marker independently, levels connected by different letters are significantly different (p<0.05, Student's t-test).

The expression of COLIA1 was higher in the beginning of the studied period, followed by a decrease between the 14th and 21th culturing days in all conditions. In the 7th day, the expression of this marker was significantly higher in the SPCL-WS-Si samples in both culturing medium, and for the later time points the expression levels were variable being, in general, higher in the SPCL samples cultured in osteogenic medium. Regarding the expression of the RUNX2 gene, an early marker for osteogenic differentiation, it was found a significant up-regulation in the initial culturing times, particularly in the SPCL-WS-Si scaffolds. This marker was expressed along all the experiment, particularly on the cASCs cultured on osteogenic medium. Concerning the expression of Osteocalcin, a late marker, it was registered increased levels of expression along the time, significantly higher in the samples cultured in osteogenic medium. The SPCL-WS-Si samples promoted, in general, a higher expression of this marker in almost all conditions.

4. Discussion

SPCL has been used in the development of several scaffolds architectures with different physicochemical characteristics aimed at being used in TE applications, having been extensively tested both *in vitro* (14, 22-24) and *in vivo* (25-27). The feasibility of producing an SPCL double layer scaffold specifically designed for periodontal regeneration was demonstrated in a previous work (16).

The good elasticity and mechanical strength, as well as its degradability, allows to hypothesize that, once implanted in a periodontal defect, this scaffold will enable to maintain an occlusive space for some months while the tissue regeneration is accomplished (16).

The canine adipose-derived stem cells used in this wok were previously characterized in terms of stemness and osteogenic potential along culture passages (18). These studies have shown that the cASCs lose their stemness and osteogenic differentiation potential along the passages and, for this reason in the present work they were used at passage 2.

As described above, the proposed scaffold is composed by two layers, an osteoconductive wet-spun fiber mesh and a solvent casting membrane, that can be further enriched with stem cells, envisioning to achieve two main functions upon implantation in a periodontal defect, namely to induce the formation of new alveolar bone and act as a GTR barrier, respectively. Specifically, in order to evaluate the osteogenic potential of the bioactive fiber mesh layer, we have herein assessed the ability of such scaffold to promote the differentiation of cASCs into the osteogenic lineage. As for the membrane, it is thought to avoid the migration of epithelial cells ingrowth to the periodontal defect hindering the anchorage of other cell types essential to the regeneration, but should simultaneously promote an effective integration with the surround smooth gingival tissue. Therefore, it was evaluated the effect of the surface topography (patterned and non-patterned) of the solvent casting membrane layer, in order to select the most adequate to allow cellular adhesion and proliferation.

The SEM images of the membrane and fiber mesh layers revealed that both aspects of the double layer scaffold allowed the adhesion of cells displaying the typical filopodia morphology of the ASCs, independently of the surface topography and presence/absence of silanol groups. The fact that the cASCs grow preferentially on the surface of the fiber meshes, has been typically reported in static cultures that hinder the distribution of cells towards the interior of the scaffolds and prevent their viability within the scaffold due to diffusion limitations (28, 29) and might be overcome by culturing constructs in adequate bioreactors.

In all the studied materials, it was observed an increase of cellular metabolic activity along the culturing period, independently of the conditions or the composition/topography of the scaffolds, further demonstrating the biocompatibility of the materials selected.

Concerning the outcomes of the DNA assays performed on the membrane layer, it was shown a positive effect of the patterning in the membrane layer. This shows that a simple methodology can be used to promote the cells proliferation, but also paves the way for the development of other topographies specifically designed to guide the cellular migration along the surface, either restricting some cellular populations as the epithelial cells or promoting the migration of others, such as the periodontal ligament cells. Regarding the DNA assays results registered for the fiber mesh layers, it was found that the functionalization with silanol groups increased the proliferation of the cASCs on the fiber meshes, which is in good agreement with previous results (16).

The incorporation of a 3D functionalized fiber mesh in the design of the proposed double layer scaffold was aimed at enhancing the osteogenic differentiation of seeded stem cells and/or to promote the ingrowth of alveolar bone tissue into the porous structure of the mesh layer upon implantation in a periodontal defect. This osteogenic potential was evaluated *in vitro* by quantifying the ALP activity, and by assessing the gene expression of specific osteogenic markers along the culturing period in basal and osteogenic medium.

The ALP is an enzyme anchored to membrane inositol-phosphate on the outer surface of osteoblasts (30) that reduces phosphate-containing substances and hydrolyzes pyrophosphate which is known to inhibit hydroxyapatite formation (31), and is considered an early osteogenic differentiation marker (32). In this work it was revealed that the SPCL-WS induced higher levels of ALP activity than the SPCL-WS-Si, as reported in a previous study using human ASCs cultured onto similar materials (14), as well as other studies using various cells types and materials (33). In fact, some osteoconductive calcium and silicon rich-materials have shown a negative effect in ALP activity, such as a bioactive glass based scaffolds cultured with human ASCs when compared with non-bioactive scaffolds (33). The same negative effect of calcium in the ALP activity have also been reported on human osteosarcoma cells (SaOs-2) cultured with Ca-enriched culture medium (30).

Gene expression analysis showed that all the studied osteogenic markers were expressed along the culturing time of cASCs onto the SPCL-WS-Si and SPCL-WS. The highest levels of *Osteocalcin* expression, a late marker of differentiation (34) were registered at the 21th day of culturing, concomitantly with higher activity of the ALP, and after the expression peaks of *RUNX2* and *COLIA1* at the 7th and 14th culturing days, respectively. This result was particularly evident for the samples cultured under osteogenic medium. The expression of these markers has been also reported in canine ASCs cultured in 2D cultures under osteogenic medium, where it was observed a later peak of *COLIA1* expression at the 21th day, also followed by the *Osteocalcin* (18) which suggests that the functionalized scaffolds might be accelerating the onset of the cASCs osteogenic differentiation. Moreover, the expression profile of *COLIA1* in the cASCs-fiber meshes was similar to the observed during the natural healing of the canine mandibular alveolar bone (35).

The positive effect of silicon has been also reported in cells attached to silicon-rich calcium phosphate nanocomposite, which showed higher expression of *COLIA1* and Osteocalcin compared to cells cultured on tissue culture plates (36), as well as reported by Botelho *et al*, who observed that Si-doped HA have improved performance compared to pure HA on human osteoblasts differentiation (37). Silicon and calcium were shown to upregulate osteoblastic markers and accelerate osteogenic differentiation of cultured stem cells (38, 39). The expression of the studied genes on the cultured cASCs on the SPCL-WS-Si, lead us to conclude that silanol groups promote the osteogenic differentiation of the cASCs, despite the lower ALP activity registered for the functionalized fiber meshes. Nevertheless it is recognized the importance of further investigating the role of silicon in the mechanism of osteogenesis.

Overall, the proposed asymmetric double layer scaffold supported the attachment and proliferation of cASCs in both layers, enhancing of the osteogenic differentiation of the cASCs cultured on the osteoconductive fiber mesh layer. These findings, together with physicochemical characteristics previously reported, clearly demonstrate that the proposed scaffold might be used as a matrix for cell-seeding/culturing before implantation in a tissue defect. Nevertheless, to address its suitability to promote the required functionalities, supporting the simultaneous regeneration of different tissue in a periodontal defect, either with or without the pre-culture of stem cells, *in vivo* studies must be performed. These studies should start by assessing the bone regeneration ability in small animal model but ultimately, it should be used the canine circumferential periodontal defect models, which is considered the most adequate model for research in Periodontology.

5. Conclusion

The present study described a new Tissue Engineering approach aimed at being used in periodontal regeneration, based on a recently developed construct composed of a biodegradable double layer scaffolds and mesenchymal stem cells obtained from adipose tissue.

The results obtained in the present work demonstrated that the wet-spun fiber mesh layer functionalized with silanol groups stimulated the osteogenic differentiation of cASCs while the membrane layers enabled a good cell attachment and proliferation. Considering these results together with those obtained previously suggested the potential of this double layer scaffolds to be used in periodontal Tissue Engineering approaches. In such strategies, the double layer scaffold, with or without pre-cultured stem cells, is envisioned to enhance osteogenesis, which is essential for the regeneration of the alveolar bone compartment of the periodontium while simultaneously promote the colonization with a distinct cellular population of the periodontium and to avoid the migration of epithelial cells into the defect, through the specific features of the fiber mesh and the membrane layers, respectively. This approach should be assessed in a suitable animal model in order to be proposed as a viable alternative for treating periodontal defects.

6. Acknowledgments

The research leading to these results has received funding from the European Union's Seventh Framework Programme (FP7/2007-2013) under grant agreement n° REGPOT-CT2012-316331-POLARIS. J.F. Requicha acknowledges the Portuguese Foundation for Science and Technology (FCT) for his PhD scholarship (SFRH/BD/44143/2008).

7. References

1. Polimeni G, Xiropaidis AV, Wikesjo UME. Biology and principles of periodontal wound healing/regeneration. Periodontology 2000. 2006;41:30-47.

2. Chen FM, Jin Y. Periodontal tissue engineering and regeneration: current approaches and expanding opportunities. Tissue Engineering Part B-Reviews. 2010;16 (2):219-55.

3. Kuo L-C, Polson AM, Kang T. Associations between periodontal diseases and systemic diseases: A review of the inter-relationships and interactions with diabetes, respiratory diseases, cardiovascular diseases and osteoporosis. Public Health. 2008;122 (4):417-33.

4. Bosshardt DD, Sculean A. Does periodontal tissue regeneration really work? Periodontology 2000. 2009;51:208-19.

5. Wikesjo UME, Lim WH, Thomson RC, Hardwick WR. Periodontal repair in dogs: gingival tissue occlusion, a critical requirement for GTR? Journal of Clinical Periodontology. 2003;30 (7):655-64.

6. Bartold PM, McCulloch CAG, Narayanan AS, Pitaru S. Tissue engineering: a new paradigm for periodontal regeneration based on molecular and cell biology. Periodontology 2000. 2000;24:253-69.

7. Tobita M, Uysal AC, Ogawa R, Hyakusoku H, Mizuno H. Periodontal tissue regeneration with adipose-derived stem cells. Tissue Engineering Part A. 2008;14 (6):945-53.

8. Dogan A, Ozdemir A, Kubar A, Oygur T. Healing of artificial fenestration defects by seeding of fibroblast-like cells derived from regenerated periodontal ligament in a dog: A preliminary study. Tissue Engineering. 2003;9 (6):1189-96.

9. Iwata T, Yamato M, Tsuchioka H, Takagi R, Mukobata S, Washio K, *et al*. Periodontal regeneration with multi-layered periodontal ligament-derived cell sheets in a canine model. Biomaterials. 2009;30 (14):2716-23.

10. Kawaguchi H, Hirachi A, Hasegawa N, Iwata T, Hamaguchi H, Shiba H, *et al*. Enhancement of periodontal tissue regeneration by transplantation of bone marrow mesenchymal stem cells. Journal of Periodontology. 2004;75 (9):1281-7.

11. Nakahara T, Nakamura T, Kobayashi E, Kuremoto KI, Matsuno T, Tabata Y, *et al*. In situ tissue engineering of periodontal tissues by seeding with periodontal ligament-derived cells. Tissue Engineering. 2004;10 (3-4):537-44.

12. Requicha JR, Viegas CA, Muñoz F, Reis RL, Gomes ME. Periodontal tissue engineering strategies based on non-oral stem cells. The Anatomical Record. 2013;invited review:accepted for publication.

13. Leonor IB, Rodrigues MT, Gomes ME, Reis RL. In situ functionalization of wet-spun fibre meshes for bone tissue engineering. J Tissue Eng Regen Med. 2011;5 (2):104-11.

14. Rodrigues AI, Gomes ME, Leonor IB, Reis RL. Bioactive starch based scaffolds and human adipose stem cells are a good combination for bone tissue engineering. Acta Biomaterialia. 2012;8:3765–76.

15. Ni S, Chang J, Chou L, Zhai W. Comparison of osteoblast-like cell responses to calcium silicate and tricalcium phosphate ceramics in vitro. J Biomed Mater Res B Appl Biomater. 2007;80 (1):174-83.

16. Requicha J, Viegas C, Hede S, Leonor I, Reis R, Gomes M. Design and characterization of a biodegradable double layer scaffold aimed at periodontal tissue engineering applications. Submitted.

17. Vieira N, Brandalise V, Zucconi E, Secco M, Strauss B, Zatz M. Isolation, characterization and differentiation potential of canine adipose-derived stem cells. Cell Transplant. 2010;19 (3):279-89.

18. Requicha J, Viegas C, Albuquerque C, Azevedo J, Reis R, Gomes M. Effect of anatomical origin and cell passage number on the stemness and osteogenic differentiation potential of canine adipose-derived stem cells. Stem Cell Reviews and Reports. 2012;8 (4):1211-22.

19. Donath K, Breuner G. A method for the study of undecalcified bones and teeth with attached soft tissues. J Oral Pathol. 1982;11:318–26.

20. Laczkó J, Lévai G. A simple differential staining method for semi-thin sectionsof ossifying cartilage and bone tissues emhedded in epoxy resin. Mikroskopie. 1975;31:1-4.

21. Livak KJ, Schmittgen TD. Analysis of relative gene expression data using real-time quantitative PCR and the 2 (T) (-Delta Delta C) method. Methods. 2001;25 (4):402-8.

22. Gomes ME, Bossano CM, Johnston CM, Reis RL, Mikos AG. In vitro localization of bone growth factors in constructs of biodegradable scaffolds seeded with marrow stromal cells and cultured in a flow perfusion bioreactor. Tissue Eng. 2006;12 (1):177-88.

23. Puppi D, Piras AM, Chiellini F, Chiellini E, Martins A, Leonor IB, *et al*. Optimized electro- and wet-spinning techniques for the production of polymeric fibrous scaffolds loaded with bisphosphonate and hydroxyapatite. Journal of Tissue Engineering and Regenerative Medicine. 2011;5 (4):253-63.

24. Tuzlakoglu K, Pashkuleva I, Rodrigues MT, Gomes ME, van Lenthe GH, Muller R, *et al*. A new route to produce starch-based fiber mesh scaffolds by wet spinning and subsequent surface modification as a way to improve cell attachment and proliferation. Journal of Biomedical Materials Research Part A. 2010;92A (1):369-77.

25. Rodrigues MT, Gomes ME, Viegas CA, Azevedo JT, Dias IR, Guzon FM, *et al*. Tissue-engineered constructs based on SPCL scaffolds cultured with goat marrow cells: functionality in femoral defects. Journal of Tissue Engineering and Regenerative Medicine. 2011;5 (1):41-9.

26. Santos TC, Marques AP, Horing B, Martins AR, Tuzlakoglu K, Castro AG, *et al*. In vivo short-term and long-term host reaction to starch-based scaffolds. Acta Biomater. 2010;6 (11):4314-26.

27. Link D, Gardel L, Correlo V, Reis R, Gomes M. Osteogenic properties of starch poly (ε-caprolactone) (SPCL) fiber meshes loaded with osteoblast-like cells in a rat critical-sized cranial defect. Journal of Biomedical Materials Research: Part A. 2013. In press.

28. Gomes ME, Sikavitsas VI, Behravesh E, Reis RL, Mikos AG. Effect of flow perfusion on the osteogenic differentiation of bone marrow stromal cells cultured on starch-based three-dimensional scaffolds. Journal of Biomedical Materials Research Part A. 2003;67A (1):87-95.

29. Goncalves A, Costa P, Rodrigues MT, Dias IR, Reis RL, Gomes ME. Effect of flow perfusion conditions in the chondrogenic differentiation of bone marrow stromal cells cultured onto starch based biodegradable scaffolds. Acta Biomater. 2011;7 (4):1644-52.

30. Anh DJ, Dimai HP, Hall SL, Farley JR. Skeletal alkaline phosphatase activity is primarily released from human osteoblasts in an insoluble form, and the net release is inhibited by calcium and skeletal growth factors. Calcified Tissue International. 1998;62 (4):332-40.

31. Balcerzak M, Hamade E, Zhang L, Pikula S, Azzar G, Radisson J, *et al*. The roles of annexins and alkaline phosphatase in mineralization process. Acta Biochim Pol. 2003;50 (4):1019-38.

32. Nandakumar A, Yang L, Habibovic P, van Blitterswijk C. Calcium Phosphate Coated Electrospun Fiber Matrices as Scaffolds for Bone Tissue Engineering. Langmuir. 2010;26 (10):7380-7.

33. Haimi S, Suuriniemi N, Haaparanta AM, Ella V, Lindroos B, Huhtala H, *et al*. Growth and osteogenic differentiation of adipose stem cells on PLA/bioactive glass and PLA/beta-TCP scaffolds. Tissue Eng Part A. 2009;15 (7):1473-80.

34. Rodan GA, Noda M. Gene expression in osteoblastic cells. Crit Rev Eukaryot Gene Expr. 1991;1 (2):85-98.

35. Sun LY, Wu L, Bao CY, Fu CH, Wang XL, Yao JF, *et al*. Gene expressions of Collagen type I, ALP and BMP-4 in osteo-inductive BCP implants show similar pattern to that of natural healing bones. Materials Science & Engineering C-Materials for Biological Applications. 2009;29 (6):1829-34.

36. Gupta G, Kirakodu S, El-Ghannam A. Dissolution kinetics of a Si-rich nanocomposite and its effect on osteoblast gene expression. J Biomed Mater Res A. 2007;80 (2):486-96.

37. Botelho CM, Brooks RA, Best SM, Lopes MA, Santos JD, Rushton N, *et al*. Human osteoblast response to silicon-substituted hydroxyapatite. Journal of Biomedical Materials Research Part A. 2006;79A (3):723-30.

38. El-Ghannam A, Ning CQ. Effect of bioactive ceramic dissolution on the mechanism of bone mineralization and guided tissue growth in vitro. Journal of Biomedical Materials Research Part A. 2006;76A (2):386-97.

39. Beck GR, Jr., Moran E, Knecht N. Inorganic phosphate regulates multiple genes during osteoblast differentiation, including Nrf2. Exp Cell Res. 2003;288 (2):288-300.

Chapter VII

Evaluation of a starch-based double layer scaffold for bone regeneration in a rat model

Abstract

Damages in the maxilofacial bones are frequent in humans after trauma, metabolic diseases, neoplasia or inflammatory processes, but current treatments to regenerate bone are sometimes ineffective.

The goal of this work was to assess the *in vivo* behaviour of an innovative double-layered scaffold based on a blend of starch and poly (ε-caprolactone) (SPCL) that comprises a membrane obtained by solvent casting, which aims to act as a guided tissue regeneration membrane, and a wet-spun fiber mesh (in some cases functionalized with osteoconductive silanol groups) targeting bone regeneration.

The behaviour of the double layer scaffold, functionalized with the silanol groups (SPCL-Si) or without the functional groups (SPCL), was assessed in a mandibular rodent model and compared to a commercial collagen membrane (positive control) and to empty defects (negative control). After 8 weeks of implantation, the histomorphometric analysis revealed that the SPCL-Si scaffolds induced significant higher new bone formation compared to the collagen membrane and to the empty defects, although they had a similar performance when compared to the SPCL scaffolds.

---

*This Chapter is based on the following publication:

Requicha JF, Moura T, Muñoz F, Leonor IB, Martins T, Gomes ME, Reis RL, Viegas CA. Evaluation of a starch-based double layer scaffold for bone regeneration in a rat model. Submitted

1. Introduction

The maxilofacial bones and, in particular, the alveolar bone, which makes part of the periodontium, are often affected by severe damages caused by trauma, metabolic diseases, neoplasia or inflammatory processes, like osteomyelitis or periodontitis (1).

Alveolar bone defects are usually managed by using bone grafts like autografts, allografts, or biomaterials, such as hydroxyapatite (HA) and tricalcium phosphate (TCP) (2). Growth/differentiation factors could be used alone, such as platelet rich plasma which is easy to use in autologous patients (3), or the enamel matrix derivative (EMD) (4). Some vehicles have been combined with the factors, namely, the fibrin glue with basic fibroblast growth factor (bFGF), vascular endothelial growth factor (VEGF) and transforming growth factor-β (TGF-β) (5), a TCP osteoconductive matrix with human platelet derived growth factor (5, 6) and collagen sponges containing recombinant human bone morphogenetic protein-2 (BMP-2) for alveolar bone augmentation (7). In addition, barrier membranes could be placed between the different periodontal compartments, including bone and periodontal ligament, aiming to prevent epithelial and fibrous tissues to grow toward the defects, and allow the recruitment of the local undifferentiated cells and their differentiation into the desired phenotypes (8). This guiding effect can be achieved with various biocompatible materials, including non-resorbables, like expanded-polytetrafluoroethylene (ePTFE) (9), cellulose acetate (10) and titanium (11), and resorbable biomaterials, namely polylactic acid (11), collagen (12) and poly (lactic-co-glycolic acid) (PLGA) (10). Apart from these materials, scaffolds have been studied for the promotion of regeneration of the damaged bone combining polymers with osteoconductive materials like HA (13) or TCP (14).

Many of these biomaterials proposed for bone and periodontal regeneration have been combined with osteoconductive and osteoinductive molecular signals. Among them, silanol groups incorporated in wet-spun fiber meshes made of a blend of starch and poly (ε-caprolactone) (SPCL) have shown great osteoconductive properties *in vitro*, demonstrated by the ability to promote the osteogenic differentiation of the seeded/cultured goat bone marrow stem cells (BMSCs) or human adipose-derived stem cells (ASCs) (15, 16). In a previous work, a double layer scaffold based on the combination of a similar tridimensional fiber mesh with a SPCL solvent casting membrane has been developed and characterized (17).

The main objective of this study was to evaluate the potential of this double layer scaffold, with and without the silanol groups, to enhance bone regeneration in a critical size mandibular defect. Moreover, the performance of the membrane layer to act as physical barrier against cell ingrowth was also evaluated. The mandibular defect has been considered to be a suitable model to study the functionality of either non-resorbable or resorbable membranes in several animal models, such as rats, rabbits, dogs and monkeys (8). The performance of the developed scaffolds was compared with collagen commercial membranes and with empty defects, after 8 weeks of implantation, through histomorphometric analysis of slides prepared by the Donath technique (18).

2. Materials and Methods

2.1. Production of the materials

A polymeric solution was prepared by dissolving the starch and poly (ε-caprolactone) blend (30:70% w/w) (SPCL; Novamont, Italy) in chloroform (Sigma-Aldrich, Germany) (20 wt%). According to a previously optimized methodology, the membrane layer was produced by casting 3 ml of the solution onto a 5 cm diameter Teflon patterned mould. The same solution was used to produce a SPCL fiber mesh by wet-spinning, which was then combined with the solvent casting membrane in order to obtain a double layer scaffold. The same technique was used to obtain the functionalized fiber meshes with osteoconductive silanol groups (SPCL-Si) (15, 16). A commercial collagen membrane (Resodont, Resorba, Germany) was used as positive control of the experiment. The SPCL and SPCL-Si double layer scaffolds were previously sterilized by ethylene oxide and all the materials, including the collagen membrane, were cut in 5 mm diameter discs prior to implantation.

2.2. Animals

Twelve male, 10-weeks old Wistar rats (strain code 003; Charles River, United Kingdom) were used in this protocol with a mean body weight of 433.87 ± 21.69 g. The housing care and experimental protocol was performed according to national guidelines, after approval by the National Ethical Committee for Laboratory Animals and conducted in accordance with Portuguese legislation (Portaria 1005/92) and international standards on animal welfare as defined by the European Directive 2010/63/EU. The animals were housed in pairs, fed with a maintenance diet for rats (A04/A04C/R04 diet; Safe, France) and autoclaved water, both *ad libitum*, and bedded in wood shavings (Scobis Uno; Mucedola, Italy) with suitable environment enrichment and with a day/night cycle of 14/10 hours.

2.3. Surgical procedure

The rats were premedicated with dexmedetomidine (Dexdomitor; Pfizer, Finland) 0.5 mg/kg intraperitoneal and anesthetized with ketamine (Imalgene 1000; Merial, Portugal) 75 mg/kg intraperitoneal. The heads were pre-operative radiographed to confirm normal anatomy and to determine if the bony surface was suitable to encompass a 5 mm circular defect.

The defects were randomly assigned in the following four experimental groups (six defects per group): (i) empty defects (negative control), (ii) defects implanted with collagen membranes (positive control), (iii) defect implanted with SPCL double layer scaffolds and (iv) defect implanted with SPCL-Si double layer scaffolds. Each rat was subject of two bilateral defects which were then filled with different materials/empty defect.

The mandibular area was shaved and aseptically prepared with iodopovidone. Then, a skin incision was made, exposing the masseter muscle and then the mandible. In the mandibular ramus, a bicortical 5 mm circular defect was drilled using a 5 mm outer diameter trephine (ACE Surgical Supply, USA) under irrigation, and then the materials were placed and fitted in the defects. The surgical wound was closed in two layers using a 4-0 glyconate resorbable suture (Monosyn; BBraun, Portugal) for muscle and 4-0 silk non-resorbable suture (Silkan; BBraun, Portugal) for skin.

The anaesthesia was reversed using atipamezol (Antisedan; Pfizer, Germany) 1 mg/kg intraperitoneal. Analgesia was given by a single dose of butorphanol (Butador; Richterpharma, Austria) 0.4 mg/kg intraperitoneal three hours postoperatively, and maintained with meloxicam (Movalis; Boehringer Ingelheim, Germany) 1.5 mg/kg subcutaneous, once a day, during five consecutive days. For post-operative antibiotherapy, enrofloxacin (Baytril 5%; Bayer, Germany) was given in drink water (0.1 mg/mL) for six consecutive days.

After 8 weeks of implantation, the animals were anaesthetized and then euthanized by an intraperitoneal injection of sodium pentobarbital (Eutasil; CEVA, Portugal) and the mandibles explanted and fixed in 4% phosphate-buffered formalin (Inopat, Portugal) solution for 1 week.

2.4. Histology

The same samples were dehydrated in alcohol solutions of increased concentrations, embedded in glycol methacrylate (Technovit 7200 VLC, Heraeus Kulzer, Germany) and processed for ground sectioning according to the method described by Donath and Breuner (18). From each tissue block one transversal section, comprising the center of the created defect was prepared to a thickness of approximately 30 µm for histological assessment by micro-cutting and grinding (Exakt; Norderstedt, Germany) and stained using a modified Lévai Laczkó staining (19) which stains allows to differentiate between local and newly formed bone and also to maintain the matrix-cellular bone architecture essential for the subsequent histomorphometric evaluation.

Histomorphometric analysis was performed using a light microscope and a computer-based image analysis system (Microimage 4.0; Media Cybernetics, USA) evaluating the percentage of bone ingrowth into the defect in a defined region of interest of 5 mm of length by 1 mm of width.

2.5. Statistical analysis

Statistical comparison of the percentage of new bone formation was performed using two-way analysis of variance (ANOVA) and Tukey post-hoc test. P-values<0.05 were considered to be statistically significant.

3. Results

During the implantation, collagen membranes were found more difficult to fit in the same position inside the defect due to their higher flexibility, and, upon implantation, higher blood infiltration into the SPCL scaffolds was observed. At the end of the experiment, all the animals revealed good body condition and no macroscopic signs of inflammation.

3.1. Histology

The histological analysis (Fig. 7.1) of the defects with collagen revealed a very low number of inflammatory cells, as neutrophils, lymphocytes, macrophages, giant cells, as well as a low amount of necrotic debris. Some new vessels, fibrosis and adipose infiltration were also observed. In the majority of the cases, the collagen membrane was not very easily distinguished from the surrounding tissues. In these cases, the defect was invaded by the adjacent muscular tissue.

SPCL and SPCL-Si scaffolds were still present after 8 weeks of implantation and surrounded, in some cases, by a granulation tissue and an infiltrate of inflammatory cells. The inflammatory infiltrate was mainly composed of lymphocytes, macrophages and giant cells around the implant indicating cellular activity of degraded material removal. In addition, these scaffolds allowed osteoconduction of bone tissue from the edge of the defect but did not allow its growth into the membrane layer of the material.

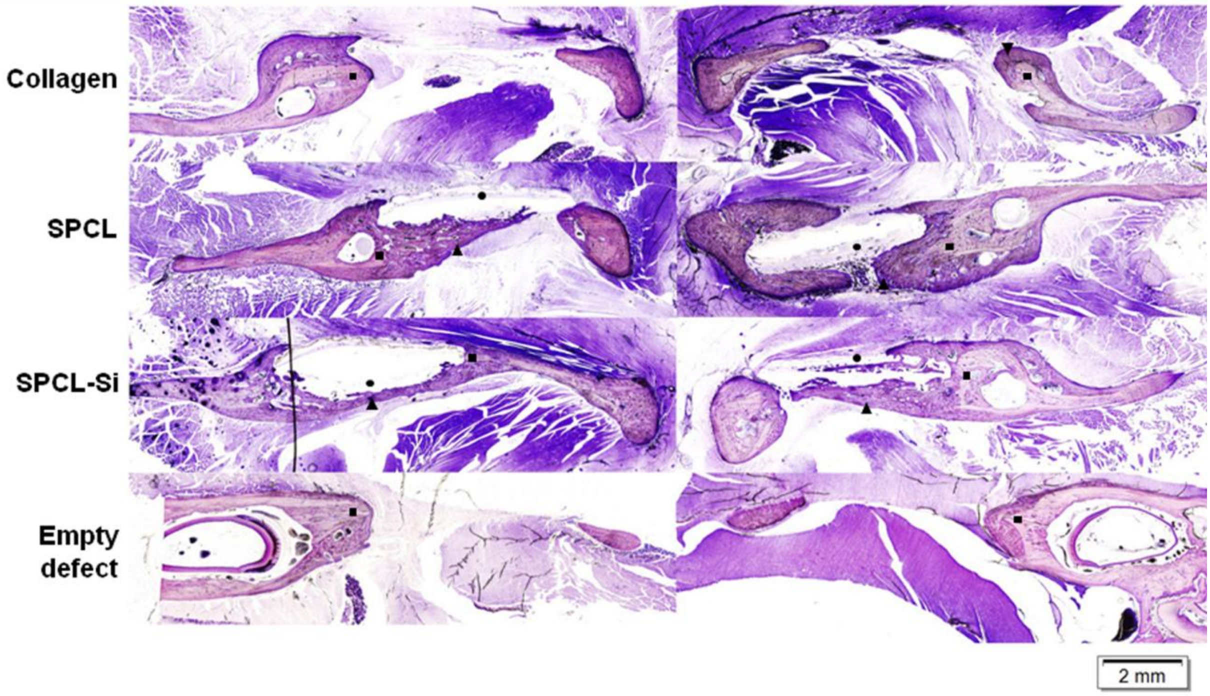

Figure 7. 1 – Representative images of the mandibular defect without scaffold (empty) and filled with collagen, SPCL and SPCL-Si scaffolds (Lévai Laczkó staining). In these histological images, it can be observed the old bone tissue (square), the new formed bone (triangle) and the implanted material (circle) (scale bar = 2 mm).

3.2. Bone histomorphometry

As observed in Fig. 7.2, the percentage of new bone in the defined region of interest was 0.45 ± 0.40% in the empty defects, 13.46 ± 5.51% with collagen, 23.49 ± 10.88% for SPCL scaffolds and 28.23 ± 13.24% after SPCL-Si implantation for 8 weeks. The SPCL-Si group median (24.26%) was higher than the collagen group (13.27%) which in turn was higher than in empty defects (0.40%). Comparing the extreme observations in collagen and SPCL-Si samples, it was found that the maximum collagen observation (20.33%) exceeded the minimum SPCL-Si observation (13.85%).

Statistical analysis showed that there were differences in new bone formation comparing the experimental SPCL and SPCL-Si groups to the negative control. When compared to the positive control, both experimental groups revealed higher bone formation, although statistical significance was found only between collagen and SPCL-Si.

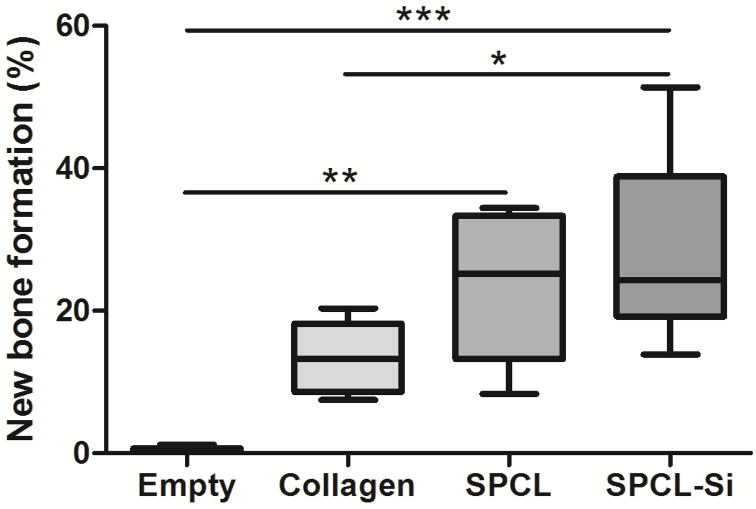

Figure 7. 2 – Box plot of the percentage of new bone formation in empty defects, collagen, SPCL and SPCL-Si in the defined region of interest after 8 weeks of implantation. * indicates a significant difference with $p<0.05$, (**) $p<0.01$ and (***) $p<0.001$.

4. Discussion

The double layer scaffold evaluated in this study has already been characterized *in vitro*, using canine adipose-derived stem cells (cASCs), showing ability to act as an osteoconductive matrix, supported by the expression of osteoblastic markers on the cultured cASCs (17). The osteogenic potential of the functionalized fiber mesh layer has also been assessed *in vitro*, using goat BMSCs (15) and human ASCs (16), leading to similar outcomes. Moreover, the SPCL fiber meshes are known to have good biocompatibility under subcutaneous and intramuscular implantation in rat (20).

Although both experimental scaffolds enhanced bone formation when compared to the negative and positive controls, they presented similar performance between them, meaning that the functionalization with silanol groups did not have the expected effect in osteogenesis, as expected based in previous *in vitro* outcomes (16, 17). Results variability could be attributed to the lack of stability of the implant in the mandible defect and inadequate contact between bone and biomaterial (21). In the mandible, the area of implantation is subject to constant forces, such as those resulting from mastication. It is essential to develop a scaffold so that its edges are in strict contact with the bone edges in order to avoid fracture of the newly formed bone, which is naturally less dense, leading to its resorption.

The mandible model has been proposed for the evaluation of several membranes and scaffolds aiming to enhance and guide bone regeneration. Zellin *et al*. (1995) revealed that e-PTFE, PGLA and cellulose were suitable membranes for osteopromotion (10). Later, Schliephake *et al*. (2009) concluded that porous TCP induces more new bone formation than porous CaCO3-collagen scaffolds. The referred TCP induced a similar new bone formation (21.6%) comparing to our SPCL-Si (28.3%) and the results obtained for the porous CaCO3 (15.1%) was similar to our positive control (13.46%) (12).

Two different works on poly (DL-lactide-e-caprolactone) membranes reported higher bone formation in comparison with empty defects, but no advantages with respect to collagen (22). van Leeuwen *et al*. (2012) observed no statistical significant differences between the tested poly (trimethylene carbonate) membrane and the collagen or e-PTFE (positive controls) (23). Other scaffolds combined with growth/differentiation factors and cells have also been assessed in this model, such as autologous dermal fibroblasts transduced with adenoviral vector carrying LIM mineralization protein-3 adsorbed on hydroxyapatite/collagen (24) and premineralized silk fibroin protein scaffold combined with BMP-2 gene modified BMSCs (25). In the near future, additional Tissue Engineering strategies will open a way for new biomedical devices, mimicking the molecular and cellular mechanism of bone regeneration and also increasing the biocompatibility of the materials with the surrounding tissues.

In the histological slides it was not possible to observe traces of the implanted equine collagen membrane, which can confirm its good biocompatibility and biodegradability. On the other hand, the high degradation rate can be a drawback because it leads to the loss of mechanical properties and consequently barrier function. The degradation of resorbable membranes based on polyesters such as the one used in this work can cause foreign body reaction due to the production of acidic compounds (1). SPCL-Si also revealed higher neovascularisation, which can be associated to a certain local irritation and need of continuous arrival of cells and molecules to the injured site. The presence of SPCL and SPCL-Si scaffold after 8 weeks could be considered an advantage comparing to collagen, because bone tissue requires more than 8 weeks to regenerate. No bone ingrowth through the membrane layer was a suitable finding for the purpose of our scaffold as a physical barrier as well. On the contrary, collagen membranes have already disappeared as mentioned above and did not sustain a complete regeneration. Polyglactin 910 membranes showed a pronounced collapse inside the bone defect; however, micro-movements were proposed to cause inflammation around the implants, which activated growth factors and thus enhance osteogenesis (10).

SPCL-based scaffolds have already been assessed in rat and mice calvarial bone defects, namely, SPCL melt-spun fiber meshes (26) and wet-spun fiber meshes (data not published by Carvalho *et al.*), respectively, after 4 and 8 weeks of implantation. Link *et al*. (2013) observed that SPCL scaffolds seeded with BMSCs pre-differentiated into osteoblasts enhance more bone formation in comparison to SPCL scaffolds alone. Moreover, the new bone formation in the center of the implant and not only in the edges suggested that the material is osteoinductive (26). In the second work, SPCL wet-spun fiber meshes, similar to the ones used in this study, were seeded/cultured with human ASCs and found to achieve higher bone formation compared to scaffolds alone.

With the findings of the current study and also from previous *in vivo* studies mentioned above, it is reasonable to propose the SPCL double layer scaffold as potential scaffolds for bone regeneration strategies, either alone or tissue-engineered with stem cells in order to increase bone regeneration potential. Nevertheless, this double layer scaffold needs to be further assessed in other animal model, namely periodontal defect models, in order to evaluate in detail the potential of the membrane layer when facing to distinct tissue damages in the periodontium.

5. Conclusion

This work was focused on the *in vivo* performance of a new starch-based scaffold, based on a membrane combined with a 3D fiber mesh, as well as the effect of its functionalization with osteoconductive silanol groups.

The obtained results revealed that, after 8 weeks of implantation both SPCL and SPCL-Si scaffold induced significant higher new bone formation when compared to collagen-filled defects and empty defects. In addition, the membrane layer of the scaffolds did not allow the proliferation of bone tissue throughout the material.

In conclusion, these results provide new information on the potential of the developed SPCL-based scaffolds for maxillofacial bone regeneration.

6. Acknowledgments

The research leading to these results has received funding from the European Union's Seventh Framework Programme (FP7/2007-2013) under grant agreement n° REGPOT-CT2012-316331-POLARIS and from the Portuguese Foundation for Science and Technology

(FCT) under the project (ref. MIT/ECE/0047/2009). J.F. Requicha acknowledges the FCT for his PhD scholarship (SFRH/BD/44143/2008).

7. References

1. Petrovic V, Zivkovic P, Petrovic D, Stefanovic V. Craniofacial bone tissue engineering. Oral Surg Oral Med Oral Pathol Oral Radiol. 2012;114 (3):e1-9.

2. Lin NH, Gronthos S, Bartold PM. Stem cells and periodontal regeneration. Australian Dental Journal. 2008;53 (2):108-21.

3. Tobita M, Uysal AC, Ogawa R, Hyakusoku H, Mizuno H. Periodontal tissue regeneration with adipose-derived stem cells. Tissue Engineering Part A. 2008;14 (6):945-53.

4. Mrozik KM, Gronthos S, Menicanin D, Marino V, Bartold PM. Effect of coating Straumann Bone Ceramic with Emdogain on mesenchymal stromal cell hard tissue formation. Clin Oral Investig. 2012;16 (3):867-78.

5. Chen FM, An Y, Zhang R, Zhang M. New insights into and novel applications of release technology for periodontal reconstructive therapies. Journal of Controlled Release. 2011;149 (2):92-110.

6. Nevins M, Giannobile WV, McGuire MK, Kao RT, Mellonig JT, Hinrichs JE, *et al*. Platelet-Derived Growth Factor Stimulates Bone Fill and Rate of Attachment Level Gain: Results of a Large Multicenter Randomized Controlled Trial. Journal of Periodontology. 2005;76 (12):2205-15.

7. Govender S, Csimma C, Genant HK, Valentin-Opran A, Amit Y, Arbel R, *et al*. Recombinant human bone morphogenetic protein-2 for treatment of open tibial fractures: a prospective, controlled, randomized study of four hundred and fifty patients. J Bone Joint Surg Am. 2002;84-A (12):2123-34.

8. Dahlin C, Linde A, Gottlow J, Nyman S. Healing of bone defects by guided tissue regeneration. Plast Reconstr Surg. 1988;81 (5):672-6.

9. Sandberg E, Dahlin C, Linde A. Bone regeneration by the osteopromotion technique using bioabsorbable membranes: an experimental study in rats. Journal of Oral and Maxillofacial Surgery. 1993;51 (10):1106-14.

10. Zellin G, Gritli-Linde A, Linde A. Healing of mandibular defects with different biodegradable and non-biodegradable membranes: an experimental study in rats. Biomaterials. 1995;16 (8):601-9.

11. Deppe H, Stemberger A. Effects of laser-modified versus osteopromotively coated titanium membranes on bone healing: a pilot study in rat mandibular defects. Lasers in Medical Science. 2004;18 (4):190-5.

12. Schliephake H, Zghoul N, Jäger V, van Griensven M, Zeichen J, Gelinsky M, *et al*. Bone formation in trabecular bone cell seeded scaffolds used for reconstruction of the rat mandible. International Journal of Oral and Maxillofacial Surgery. 2009;38 (2):166-72.

13. Liao S, Wang W, Uo M, Ohkawa S, Akasaka T, Tamura K, *et al*. A three-layered nano-carbonated hydroxyapatite/collagen/PLGA composite membrane for guided tissue regeneration. Biomaterials. 2005;26 (36):7564-71.

14. Kikuchi M, Koyama Y, Yamada T, Imamura Y, Okada T, Shirahama N, *et al*. Development of guided bone regeneration membrane composed of beta-tricalcium phosphate and poly (L-lactide-co-glycolide-epsilon-caprolactone) composites. Biomaterials. 2004;25 (28):5979-86.

15. Leonor IB, Rodrigues MT, Gomes ME, Reis RL. In situ functionalization of wet-spun fibre meshes for bone tissue engineering. J Tissue Eng Regen Med. 2011;5 (2):104-11.

16. Rodrigues AI, Gomes ME, Leonor IB, Reis RL. Bioactive starch based scaffolds and human adipose stem cells are a good combination for bone tissue engineering. Acta Biomaterialia. 2012;8:3765–76.

17. Requicha J, Viegas C, Hede S, Leonor I, Reis R, Gomes M. Design and characterization of a biodegradable double layer scaffold aimed at periodontal tissue engineering applications. Submitted.

18. Donath K, Breuner G. A method for the study of undecalcified bones and teeth with attached soft tissues. J Oral Pathol. 1982;11:318–26.

19. Laczkó J, Lévai G. A simple differential staining method for semi-thin sectionsof ossifying cartilage and bone tissues emhedded in epoxy resin. Mikroskopie. 1975;31:1-4.

20. Santos TC, Marques AP, Horing B, Martins AR, Tuzlakoglu K, Castro AG, *et al*. In vivo short-term and long-term host reaction to starch-based scaffolds. Acta Biomaterialia. 2010;6 (11):4314-26.

21. Stamatialis DF, Papenburg BJ, Girones M, Saiful S, Bettahalli SNM, Schmitmeier S, *et al*. Medical applications of membranes: Drug delivery, artificial organs and tissue engineering. J Membrane Sci. 2008;308 (1-2):1-34.

22. Hoogeveen EJ, Gielkens PFM, Schortinghuis J, Ruben JL, Huysmans MCDNJM, Stegenga B. Vivosorb® as a barrier membrane in rat mandibular defects. An evaluation with transversal microradiography. International Journal of Oral and Maxillofacial Surgery. 2009;38 (8):870-5.

23. van Leeuwen AC, Huddleston Slater JJR, Gielkens PFM, de Jong JR, Grijpma DW, Bos RRM. Guided bone regeneration in rat mandibular defects using resorbable poly (trimethylene carbonate) barrier membranes. Acta Biomaterialia. 2012;8 (4):1422-9.

24. Parrilla C, Lattanzi W, Rita Fetoni A, Bussu F, Pola E, Paludetti G. Ex vivo gene therapy using autologous dermal fibroblasts expressing hLMP3 for rat mandibular bone regeneration. Head Neck. 2010;32 (3):310-8.

25. Jiang X, Zhao J, Wang S, Sun X, Zhang X, Chen J, *et al*. Mandibular repair in rats with premineralized silk scaffolds and BMP-2-modified bMSCs. Biomaterials. 2009;30 (27):4522-32.

26. Link D, Gardel L, Correlo V, Reis R, Gomes M. Osteogenic properties of starch poly (ε-caprolactone) (SPCL) fiber meshes loaded with osteoblast-like cells in a rat critical-sized cranial defect. Journal of Biomedical Materials Research: Part A. 2013. In press.

Section IV

Final Conclusions

Chapter VIII

Final Conclusions

In both veterinary and human medicine, the periodontal disease is a high prevalent pathology. This condition is primarily induced by the bacteria plaque on the tooth crown surface and is characterized by an initial inflammation of the gingiva, called gingivitis. When left untreated, it progresses to periodontitis which is associated to the destruction of the periodontal ligament, the alveolar bone and the cementum that may ultimately lead to tooth loss. Apart of the local effects in the oral health and the implications in the oral esthetic, this pathology is also associated to life-threatening implications in the systemic health of the individual.

Usually, the patients affected by periodontitis present several damages in more than one periodontal tissue which concurs to increase the difficulty in the treatment of some periodontal defects. Thus, the periodontal regeneration and the reestablishment of the functionality are often challenging in the clinical routine practice.

The work accomplished on the scope of this Thesis provided new insights concerning the development of new strategies to treat periodontal defects, envisioning the regeneration of the alveolar bone around the tooth and the reestablishment of a functional periodontal ligament between the bone and the root cementum.

In this work, the specific characteristics of the periodontium, both cellular and structural, were considered in the design of an innovative tissue-engineered matrix combining canine adipose-derived stem cells and a biodegradable scaffolds thought to accommodate these cells and to promote the regeneration of the distinct compartments of the periodontium.

The referred scaffolds were obtained from a polymeric blend of starch and poly-ε-caprolactone that was selected with basis on previous studies that have demonstrated the promising properties and processing versatility of this material envisioning other applications in the tissue engineering and regenerative medicine field. This biomaterial was processed by two different methods (solvent casting and wet-spinning) in order to obtain a double (or bi)-layered construct composed of a membrane aiming to act as a barrier against the migration of the gingival epithelium combined with a fiber mesh functionalized with osteoconductive cues aimed at promoting bone regeneration. The processing of each of these components and their further combination into a double layer scaffold were optimized and then these constructs were extensively characterized *in vitro* with respect to their physicochemical properties, mechanical properties, degradation and biological behavior and by culturing the scaffolds with cASCs and assessed *in vivo* by implanting the constructs in a rodent model in order to evaluate their potential to regenerate bone.

Envisioning the use of these double layer scaffolds in Tissue Engineering applications, as well as their assessment in a canine autologous/allogenic periodontal model prior to clinical translation to human or veterinary medicine, we have focused on the use of canine ASCs and subsequently cultured the developed scaffolds with these cells. For this purpose, in a first stage, it was optimized the harvesting, isolation and culture of ASCs from canine origin and their stemness and osteogenic differentiation potential were assessed along culturing passages. Furthermore, these cASCs were implanted in mice tissue in order to allow evaluating the response of the host against the cells and optimizing their detection in the xenogenic tissue.

In summary, the work developed allowed to accomplish the following conclusions concerning the proposed objectives:

i) Characterization of the canine ASCs: effect of anatomical origin and passaging in the stemness and osteogenic potential

It was shown that cASCs are positive for the characteristic markers of MSCs and exhibit the capacity to differentiate into both osteogenic and chondrogenic lineage. It was demonstrated that the passaging of the cells is associated with a decrease in the level of expression of the typical MSCs markers as well as their osteogenic potential. The anatomical origin of the adipose tissue was also found to have influence both in the stemness and in the osteogenic differentiation potential. Despite of the subcutaneous origin seemed to have higher osteogenic potential, these finding were not consistent. Nevertheless, considering that the subcutaneous tissue is easier to collect and is associated to lower site morbidity, this anatomical origin is of higher interest envisioning future regenerative medicine approaches.

ii) Evaluation of the response to the implantation of canine ASCs in a healthy mice subcutaneous model

The canine ASCs implanted subcutaneously in a mouse were detected through the positive expression of vimentin and CD44 markers and the negative expression of keratin; however methods to label and track these cells in the living tissues should be optimized aiming at evaluate the dispersion of this cells in the host organism and the effects at distance. The reported mild inflammatory response, mainly comprising macrophages and lymphocytes, against the implanted cASCs paves the way for the future use of the subcutaneous mouse model in the study of Tissue Engineering strategies based on cASCs.

The evaluation of the allogenic canine host response against the cASCs should be explored, in the future, in order to allow the use of cASCs between different individuals of this species. Thus this work contributed to increase the knowledge on an alternative and promising stem cells source not only for tissue engineering applications but also for use in other regenerative medicine approaches with application in human and in veterinary medicine. In fact, the use of ASCs avoid the use of the undifferentiated cells that exist in small niches in the dental and oral tissues that are difficult to obtain in large quantities, take longer to expand and are associated to high morbidity during the harvesting.

iii) Development of the a new scaffolds for periodontal regeneration

In this work it was possible to combine two distinct structures into a single construct aimed at addressing different functionalities required for the full regeneration of periodontal defects. The developed constructs showed an adequate biodegradation profile under the effect of α-amylase and lipase as well as tensile strength and elasticity fulfilling the main requisites to be used as a supportive matrix in the periodontium. Moreover, it was demonstrated the effective functionalization of the fiber mesh layer with silanol osteoconductive groups, conferring to this layer of the scaffold the potential to induce osteogenic differentiation of the cultured stem cells obtained from the adipose tissue.

iv) Evaluation the potential of the developed double layer scaffold for Tissue Engineering by seeding/culturing it with canine ASCs

The biological assessment of the developed scaffolds that was carried out by culturing the newly developed constructs with the previously studied cASCs showed that both layers promote cellular adhesion and proliferation, an essential requisite to propose this construct for use in Tissue Engineering. The functionalized wet-spun fibre mesh enhanced higher osteogenic differentiation as compared to the non-functionalized material. This outcome confers to the double layer scaffold the potential to promote the regeneration of the alveolar bone compartment of the periodontium. In addition, the impermeable structure of the membrane layer also confer to this asymmetric matrix the potential to serve as physical barrier for guided tissue regeneration, being expected to avoid the migration and ingrowth of epithelial tissue into the defects, which is the main drawback with which the clinicians have to deal in the treatment of periodontal damages. Therefore, it might be envisioned the use of the proposed construct in a tissue engineering approach, i.e., combined with cells or in acellular approaches, i.e., by direct implantation of the construct in to the defect.

v) Assessing of the in vivo functionality of the scaffolds for bone regeneration, using a rat mandibular defect model

The implantation of this biomaterial in induced mandibular bone defects allowed to observe that the double layer scaffold with a fiber mesh functionalized with silanol groups enhanced new bone formation as compared to collagen commercial membrane and empty defects. The matrix also avoided the migration of cells through the material which is a mandatory requirement for a future use aiming at be used for guided tissue regeneration. In order to better extrapolate these findings for a future periodontal application, the developed constructs should be further assessed in periodontal defects induced in small mammals, for example, in the rat fenestration defect model and ultimately in the canine model.

The regeneration of the periodontium is known to be challenging to the clinicians due to the complexity of the damaged tissues and the specific interactions between them. However, the increasing knowledge on the pathophysiology of the periodontal disease and the molecular and cellular mechanisms of the periodontal regeneration is contributing to the developing of new approaches for periodontal regeneration.

In conclusion, the work presented under the scope of this Thesis demonstrated the potential of using a recently discovered source of stem cells that presents several advantages in combination with and a suitable supportive biodegradable material to create a new tissue-engineered construct for use in the treatment of periodontal defects.

Tissue Engineering is an area of knowledge with a promising future that opens wide possibilities of applications in Regenerative Medicine. The understanding of how the tissues regenerate upon damage and how it is possible to artificially mimic and promote that phenomenon is a slow but a gradual and solid process in this research field. The growing interest of the general society for this new therapeutic strategies obligate the researchers to gather efforts within multidisciplinary teams aiming at applying the basic knowledge in biological and material sciences for the improvement of human and animal healthcare.